European Commission

JRC TECHNICAL REPORT

EU HARMONISED PROTOCOLS FOR Testing of LOW TEMPERATURE WATER Electrolysers

G. Tsotridis, A. Pilenga

Temporary Image

Contact information [optional element]
Name:
Address:
Email:
Tel.:

EU Science Hub
https://ec.europa.eu/jrc

JRCXXXXXX

EUR XXXXX XX

PDF	ISBN XXX-XX-XX-XXXXX-X	ISSN XXXX-XXXX	doi:XX.XXXX/XXXXXX
Print	ISBN XXX-XX-XX-XXXXX-X	ISSN XXXX-XXXX	doi:XX.XXXX/XXXXXX

Luxembourg: Publications Office of the European Union, 20XX [if no identifiers, please use Brussels: European Commission, 20XX or Ispra: European Commission, 20XX or Geel: European Commission, 20XX or Karlsruhe: European Commission, 20XX or Petten: European Commission, 20XX or Seville: European Commission, 20XX depending on your unit]

How to cite this report: Author(s), *Title*, EUR (where available), Publisher, Publisher City, Year of Publication, ISBN 978-92-79-XXXXX-X (where available), doi:10.2760/XXXXX (where available), JRCXXXXXX

TABLE OF CONTENTS

ACKNOWLEDGEMENTS

The protocols presented in this report are the result of a collaborative effort between industry partners and research organisations participating in a number of Fuel Cell and Hydrogen Joint Undertaking funded projects dealing with low-temperature electrolysis research and applications.

We are very grateful to S. A. Ansar, A. Aricò, R. Backhouse, B. Bensmann, J. Brauns, A. Gago, D. Greenhalgh, C. Harms, V. G. Hernandez, C. Lamy, F. Marchal, P. Millet, I. Radev, R.H. Rauschernbach, F. Razmjooei, R. Reissner, S. Stypka, M. Suermann, I.G. Torregrosa, T. Turek, P. Wagner for their feedback on the previous version of this document.

The authors would like to express their sincere gratitude to all participants and their respective organisations for their contributions in developing the harmonised testing protocols in this report (cited in organization's alphabetical order in the next section).

They would also like to thank the Fuel Cell and Hydrogen Joint Undertaking Programme Office for the continuous support and encouragement received throughout the different stages of this activity.

The authors would like to thank our colleagues at the Directorate for Energy, Transport and Climate of the Joint Research Centre for their continuous support throughout the different stages of this effort.

Last but not least we would like to acknowledge Marc Steen for his prolific contribution for the revision of the document.

LIST OF CONTRIBUTORS

Name	Organisation
David Frimat	AirLiquide
Jessie Ponce	AirLiquide
Laurent Ferenczi	AirLiquide
Louis Sentis	AirLiquide
Nicolas Richet	AirLiquide
Esther Albertin	Aragon Hydrogen Foundation
Pablo Marcuello Fernández	Aragon Hydrogen Foundation
Vanesa Gil Hernandez	Aragon Hydrogen Foundation
Fabien Auprêtre	AREVA H2Gen, Les Ulis
Frederic Fouda-Onana	CEA, Grenoble
Aricò Antonino Salvatore	CNR-ITAE, Messina

Alexander Dyck	DLR, Oldenburg
Aldo Saul Gago Rodriguez	DLR, Stuttgart
Indro Biswas	DLR, Stuttgart
Regine Reißner	DLR, Stuttgart
Aziz Nechache	Engie
Madeleine Odgaard	EWII Fuel Cells A/S
Marcello Carmo	Forschungszentrum Jülich GmbH
Dominik Härle	Fraunhofer IMWS, Halle (Saale)
Tom Smolinka	Fraunhofer ISE, Freiburg
Bernd Bauer	FUMATECH BWT GmbH, Bietigheim-Bissingen
Tomas Klicpera	FUMATECH BWT GmbH, Bietigheim-Bissingen
Africa Castro	H2B2 Electrolysis Technologies, S.L., Sevilla
Denis Thomas	Hydrogenics Europe
Wouter Schutyser	Hydrogenics Europe
Richard Hanke-Rauschenbach	IfES, Leibniz Universität Hannover, Hannover
Manuel Romero	IMDEA
Franco Nodari	Industrie Haute Technologie S. A., Monthey
Andre Weber	Institut für Angewandte Materialien – Werkstoffe der Elektrotechnik (IAM-WET), KIT, Karlsruhe
Stelios G. Neophytides	Institute of Chemical Engineering Sciences (ICE-HT), Forth, Patras
Laila Grahl-Madsen	IRD Fuel Cells A/S
Frederic A. L. Marchal	ITM Power plc
Marcus Newborough	ITM Power plc
Marius Bornstein	NEL
Anders Søreng	NEL, Notodden
Graham Smith	NPL, Middlesex UK

Paolo Marocco	Politecnico Torino / Sintef
Nick van Dijk	PV3 Technologies, Launceston
Richard R. W. Wagner	Siemens
Alejandro Oyarce Barnett'	Sintef Industry, Oslo
Magnus Skinlo Thomassen	Sintef Industry, Oslo
A.P. Shirvanian	TNO (ECN)
Arend De Groot	TNO (ECN)
Claude Lamy	Université de Montpellier
Deborah Jones	Université de Montpellier
Pierre Millet	Université Paris-Sud
Ivan Radev	ZBT GmbH, Duisburg
Sebastian Stypka	ZBT GmbH, Duisburg
Ludwig Jörissen	ZSW, Ulm

EXECUTIVE SUMMARY

The policy frame

Green hydrogen is expected to play a critical role in the transition to a future low carbon energy system characterised by high shares of variable renewables. Hydrogen has the potential to decarbonise those sectors that cannot be easily electrified, such as heavy transport and a range of industrial processes. Green hydrogen may also play a role in energy storage, contributing to ensuring availability and/or flexibility to energy services independently from external factors (weather, time or season, consumer behaviour, etc.). The critical component for any green hydrogen value chain is water electrolysis for the production of hydrogen from renewable electricity sources.

The needs

There is an acknowledged need for objective assessment of the performance and durability of electrolysers under conditions representative of current and future applications. Such assessment should be based on performance tests mimicking the conditions encountered in real life as closely as possible. For a successful adoption of these tests among research centres and industry, it is critical that they are jointly developed and agreed by all stakeholders. This implies reaching consensus on operating conditions, on testing protocols and procedures, as well as on load profiles: this is particularly challenging when simulating dynamic operating conditions for electrolysers connected to intermittent power sources such as wind or solar for off-grid applications, or subject to partial load operation for electricity grid balancing.

Also the way how testing results are reported should be harmonised, to allow for their direct and unambiguous comparison. To facilitate this task, the FCH 2 JU has developed and maintains the results database TRUST (Technology Reporting Using Structured Templates), where projects are required to report progress according to a common repository structure. The TRUST database consists of 'template questionnaires' dedicated to the various technologies and their technology readiness level [1]. Each questionnaire is divided into descriptive parameters and quantitative performance data, which, for low-temperature electrolysers, are the scope of this report.

The goal

The availability and the adoption of tests performed to agreed specifications contributes to the following goals:

- improving the repeatability and reproducibility of the generated test results, thereby enhancing their comparability,
- enhancing the representativeness of laboratory test results in simulating real-world applications,
- achieving coherency of data originating from different projects, and enabling a measurement of the progress towards meeting targets,
- assessing Key Performance Indicators (KPIs) for low temperature electrolysers and proposing improved or new indicators for their performance and durability.

The goal of the report *(Why was the work undertaken?)*

To address the needs identified above, the Fuel Cells and Hydrogen Joint Undertaking (FCH 2 JU) has set up a Working Group on Low Temperature Electrolysers Testing Harmonisation (LTWE), composed of European stakeholders from research and industry, including Original Equipment Manufacturers, (OEMs), electrolysis cell material manufacturers and various establishments active in Electrolysis Research & Development. The activities of the LTWE Working Group have been coordinated by the Joint Research Centre (JRC) of the European Commission and have profited of the results of several FCH JU projects.

The goal of this group is not to replace currently existing testing practices used in various industries and research establishments, but rather to propose commonly agreed, '*harmonised*' testing protocols and procedures. This will enable an objective comparison between different projects and products and an evaluation of the progress achieved towards agreed technology performance targets.

The LTWE work followed a previous harmonisation effort on testing of low temperature PEM fuel cells [1] and used the harmonised terminology available in [2]. Three reports dedicated to specific harmonised test methods for electrolysers were already published in 2018: one on polarisation curves [7], one on cyclic voltammetry [8] and one on electrochemical impedance spectroscopy [9].

The scope and contents of this report

This report is the outcome of this work. It considers all three technologies of low temperature water electrolysis: proton and anion exchange membrane and alkaline water electrolysers. It consists of a set of harmonised operating conditions, testing protocols and procedures for assessing both performance and durability of low temperature water electrolysis devices at every level of aggregation, from materials to stacks, up to grid-coupled systems. For the operating conditions, a number of agreed reference settings are presented, covering a.o. temperature, pressure, gas flow rate and gas composition. System boundaries are defined for these conditions, within which the electrolyser cell or stack is expected to operate. The report also presents an approach for assessing the effect on electrolyser performance and degradation of the exposure to more challenging conditions, known as "stressor conditions". The grid balancing harmonised testing profiles are the result of the QualyGridS project N. 735485 and presented here as described in the deliverable 2.4 [10].

What more is to be done?

This report is based on a state-of-the-art knowledge and on results available today. Along with the development of water electrolysis technologies, we expect a need for updating and improving some of the protocols presented. Particularly in the area of accelerated testing and the grid-electrolyser coupling mode, ongoing FCH2 JU projects and the installation in Europe of high-power electrolyser systems will produce new evidences and identify new testing requirements. The LTWE Working Group will then work on an update of the report.

How will the findings be applied?

The testing protocols provided in this report can be adopted by R&I funding agencies, and in particular by the FCH 2 JU, to assess quantitatively the progress reached towards their programme objectives and targets. To achieve this, it is necessary that the related projects are committed to apply the harmonised test protocols and to report in a consistent way the results. The adoption of the protocols by FCH 2 JU projects could also enable their utilisation in a broader scientific community by offering a methodological approach suitable for use in peer-reviewed scientific publications. Finally, the approaches and outcomes of this report are believed to offer a workable basis for future European and international standardisation.

1 INTRODUCTION

1.1 Background and purpose

There is an acknowledged need for objective comparative assessment of the behaviour of electrolyser components and devices under conditions foreseen in future applications. For such assessment to be reliable and trustworthy, a number of requirements has to be met.

First, the assessment should be based on tests according to specifications agreed by a broad range of stakeholders, covering both performance and durability aspects. Testing according to these agreed specifications will contribute to improving the repeatability and reproducibility of the generated test results, thereby enhancing their comparability.

Second, agreement on the operating conditions imposed during testing for assessing performance and durability under representative application conditions is needed. This applies in particular for simulation of the dynamic operating conditions for electrolysers connected to fluctuating power sources such as wind or solar for off-grid applications, or subject to partial load operation for electricity grid balancing, or for supplying hydrogen to the gas grid or directly for power-to-gas applications, see Figure 1. This also requires agreement on the definition of appropriate electrolyser system boundaries.

Meeting the above set of requirements will improve the consistency between test results originating from different sources and enhance the representativeness of laboratory test results in simulating real-world applications.

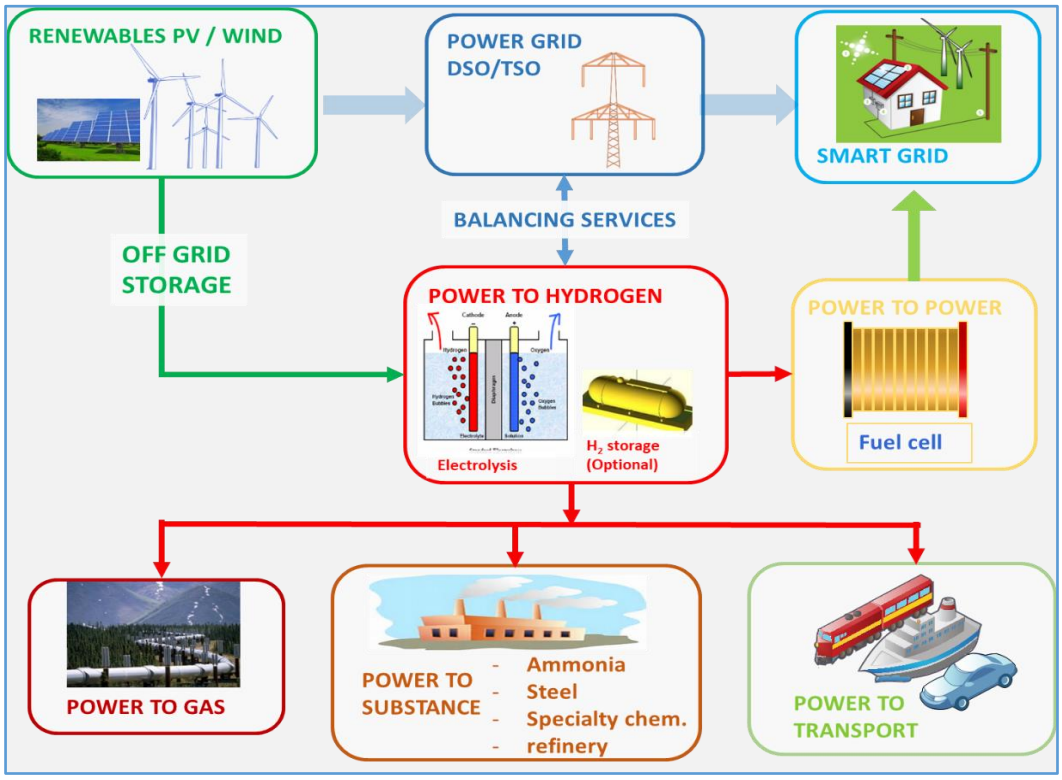

Figure 1. Electrolyser system grid integration

This report addresses the above needs by presenting an agreed set of operating conditions and of testing protocols for assessing both performance and durability of low temperature water electrolysers. It also suggests ways of graphically presenting the test results from performance and durability testing, comparing them to the results obtained under the reference operating conditions[1]. It does not intend to replace testing practices currently used in various industries and research establishments.

In addition to their primary use for enabling comparison, the results of the "harmonised" performance and durability tests presented in this report are expected to assist FCH2JU through enhanced coherency of data originating from various FCH2JU funded projects. The results obtained from harmonised tests can serve in assessing Key Performance Indicators (KPIs) for low temperature electrolysers and for proposing improved and/or new indicators for their performance and durability.

1.2 content

The report first presents a set of protocols for determining the functional properties of materials used in electrolyser components. Additionally it specifies testing conditions and protocols for assessing and evaluating performance of electrolyser cells/short stacks at the Beginning of Life (BoL) or Test (BoT)[2]. It also describes loading profiles and protocols for durability assessment through intermittent performance evaluation before reaching the End of Life (EoL) or Test (EoT). This is followed by a description of accelerated testing at cell/short stack level to assess the capability of cell materials and components to withstand service loads and for evaluating the effect of improvement of materials and or componenets on performance and durability. The report concludes by describing system-level testing as defined by QualyGridS in the project deliverable 2.4.

1.3 methodology

The methodology adopted in this document reflects the successive stages in the efforts aimed at improving performance and durability of electrolysers in a number of applications. The development sequence usually consists of four distinct steps, namely: Development of Materials, of Single Cells and short stacks and of Systems as depicted in the following figure.

[1] The graphical representation of test results is complementary to the mandatory reporting in TRUST

[2]Throughout this report the terms Beginning of Test (BoT) and End of Test (EoT) refer to laboratory practices i.e. Single Cell and Short Stack Testing, whereas Beginning of Life (BoL) and End of Life (EoL) refer to System Testing.

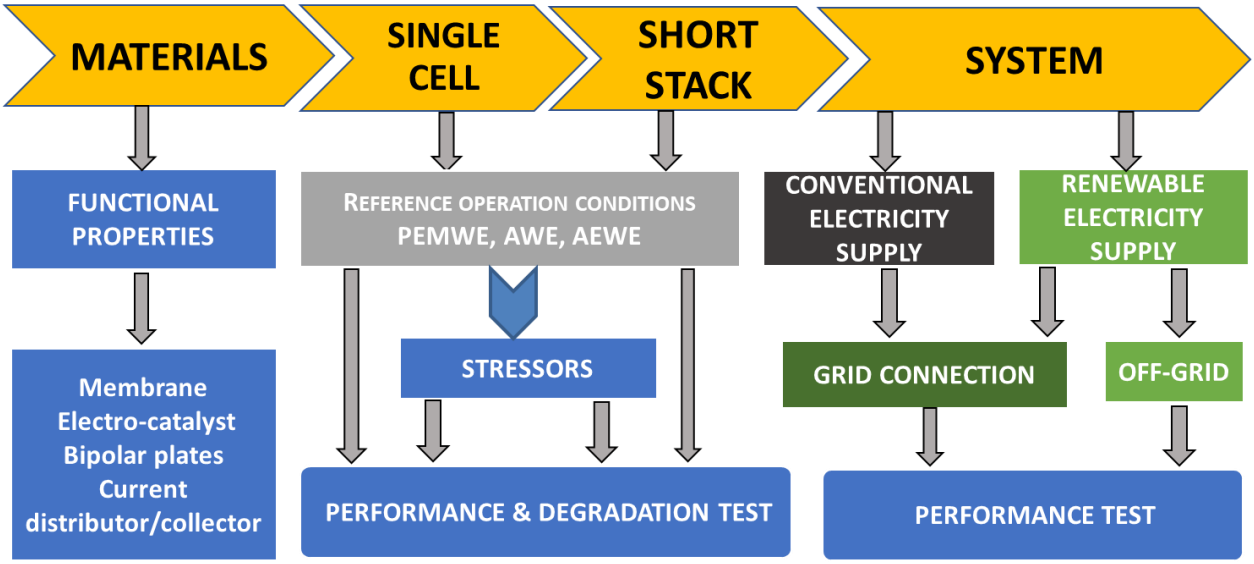

Figure 2. Schematic of the process chain for electrolyser development

The development of materials entails R&D for a range of components such as membranes and catalysts, using innovative methods, processes and manufacturing techniques. Once these new materials and components have been developed, they are "screened" *ex-situ* for their potential use as candidate materials for water electrolysis. When the *ex-situ* results meet the expectations, the materials are subsequently used for preparation of components such as Catalyst Coated Membranes (CCMs, when the catalyst layer is coated on the membranes) or in Membrane Electrode Assemblies (MEAs, when the catalyst layer is coated on a Porous Transport Layer, PTL[3]), bipolar plates, diaphragms, etc. These components are subsequently tested *in-situ,* in single cell configuration. Single cells with successful in-situ performance are considered as candidates for direct use or after scaling up to the required electrode geometric area for inclusion in short stacks and then the stacks are integrated with appropriate Balance of Plants (BOPs) to systems level.

This report is the result of a joint effort by several mainly European interested parties, including Original Equipment Manufacturers, (OEMs), electrolysis cell material manufacturers and various research establishments active in Electrolysis Research & Development who, on a voluntary basis, agreed on a set of operating conditions and testing protocols for characterization of Low Temperature Water Electrolysers at Single Cell, Stack and System levels.

[3] The term MEA may also include CCMs with integrated anode and cathode PTLs

2 OVERVIEW OF LOW-TEMPERATURE WATER ELECTROLYSIS TECHNOLOGIES

2.1 Underlying electrochemistry

In water electrolysis, two main parameters dictate technology differences namely:

(i) the operating conditions: temperature and pressure (Figure 3a)

(ii) the pH of the electrolyte (Figure 3b).

2.1.1 operating temperature

As shown in Figure 3a, electrolytic water dissociation is endothermic, i.e. it requires heat input in addition to electricity over the zero to 1,000 °C temperature range. The step change in the required amount of heat and hence in the total energy need (electricity + heat) at 100 °C is due to the water phase transition from liquid to gas. The heat required ($T \cdot \Delta S$) linearly increases with temperature T because the entropy change ΔS is assumed constant. Consequently, the Gibbs free energy change (ΔG) or electricity input required decreases with temperature, whereas the total energy need corresponding to the enthalpy change $\Delta H = \Delta G + T \cdot \Delta S$ only weakly depends on temperature both below and above 100 °C.

According to Faraday's law, the change in Gibbs free energy for an electrochemical system in equilibrium is expressed as

$$\Delta G = n F U_{rev}$$

with Faraday constant F = 96,485 coulombs $mole^{-1}$ and n the number of electrons involved in the electrochemical reaction. U_{rev} represents the reversible cell voltage, which is the minimum voltage needed to drive the reaction. For water electrolysis, U_{rev} is the minimum voltage needed for water splitting. At lower cell voltage water electrolysis is not possible, whereas at higher cell voltage electrolysis is possible and heat is consumed in the reaction. Isothermal cell operation (i.e. reactant and reaction products at the same temperature) hence requires additional heat input from the environment.

However, cell operation generates heat by internal resistance as electric and ionic currents flow through the cell (Joule heating). This internally generated heat reduces the amount of heat to be supplied from the environment to the cell for maintaining thermal equilibrium. With increasing cell voltage, the internal heat generation by the Joule effect increases and at the thermoneutral voltage the internally generated heat equals the amount of heat $T \cdot \Delta S$ required for maintaining the reaction in thermal equilibrium. According to the above, the thermoneutral cell voltage U_{tn} given by

$$\Delta H = n F U_{tn}$$

is the voltage required for electrolysis without withdrawing heat from the surroundings. In this case, ΔH represents the amount of *electric* energy required for electrolysis in the absence of external heat supply.

When the cell is operated at higher voltage than U_{tn}, the reaction becomes exothermic and heat needs to be removed for maintaining thermal equilibrium. In practice excess heat is generated because electrolysers are operated above the thermoneutral voltage to overcome losses incurred by inefficiencies of the electrochemical reactions and by electrical and ionic resistance as the current flows through the cell.

Because of the phase transition of water upon heating, two different regimes need to be considered for electrolysis of liquid water and for electrolysis of water in the gas phase (water vapour), respectively.

1) liquid water electrolysis

When water is supplied to the electrolyser in the liquid phase, as applies for low-temperature electrolysis, the hydrogen production reaction reads:

$$\mathbf{2\,H_2O_{(l)} + \Delta G_{H2O(l)} + T\Delta S \rightarrow 2H_{2(g)} + O_{2(g)}} \qquad \text{[eq. 2.1]}$$

The reaction enthalpy $\Delta H_{H2O(l)} = \Delta G_{H2O(l)} + T\Delta S = 237.16 + 48.68 = 285.84$ kJ.mol^{-1} The energy content of the produced hydrogen corresponds to the higher heating value of hydrogen (HHV).

The indicated values for ΔG, $T\Delta S$ and ΔH apply for a perfect cell operating in a thermodynamically reversible manner at standard conditions of temperature (25C) and pressure (1 bar). Under these conditions (n=2 for hydrogen)

$$U_{rev,\,HHV} = \Delta G_{H2O(l)} / (n \cdot F) = \mathbf{1.229\ V} \qquad \text{[eq. 2.2]}$$

$$U^{tn,\,HHV} = \Delta H_{H2O(l)} / (n \cdot F) = \mathbf{1.481\ V} \qquad \text{[eq. 2.3]}$$

2) water vapour electrolysis

When water to the electrolyser is supplied in the gas phase, the heat energy needed for water vaporization does not need to be provided and the reaction reads:

$$\mathbf{2\,H_2O_{(g)} + \Delta G_{H2O(g)} + T\Delta S \rightarrow 2H_{2(g)} + O_{2(g)}} \qquad \text{[eq. 2.4]}$$

In this case, the reaction enthalpy $\Delta H_{H2O(g)} = \Delta G_{H2O(g)} + T\Delta S = 228.60 + 13.23 = 241.83$ kJ.mol^{-1} and the energy content of the produced hydrogen corresponds to its lower heating value (LHV). The difference between HHV and LHV originates from the latent heat of water evaporation. The thermoneutral and reversible cell voltages for water vapour electrolysis are:

$$U_{rev,\,LHV} = \Delta G_{H2O(g)} / (n \cdot F) = \mathbf{1.185\ V} \qquad \text{[eq. 2.5]}$$

$$U^{tn,\,LHV} = \Delta H_{H2O(g)} / (n \cdot F) = \mathbf{1.253\ V} \qquad \text{[eq. 2.6]}$$

For electrolysers operating at temperatures above the 100C boiling point of water, the use of LHV rather than HHV is relevant for the produced hydrogen and temperature dependences of ΔH, ΔG and $T\Delta S$ shown in Figure 3a need to be considered.

3) pressure and temperature effects on cell voltage

The effect of the pressure arises from the change in Gibbs free energy. For ideal gases the variation of the cell voltage as a function of pressure is expressed by the equation:

$$\Delta U_{cell} = U_{rev}(T,p) - U_{rev}(T,p^{\theta}) = \frac{RT}{2F} ln\left[\left(\frac{p_{O2}}{p^{\theta}}\right)^{\frac{1}{2}}\left(\frac{p_{H2}}{p^{\theta}}\right) / \left(\frac{p_{H2O}}{p^{\theta}}\right)\right] \quad \text{[eq. 2.7]}$$

The overall expression for the cell voltage, U_{cell}, as a function of temperature and pressure is:

$$U_{cell} = U^{0}_{rev} + \frac{RT}{2F} ln\left[(p_{O2})^{\frac{1}{2}}(p_{H2})/(p_{H2O})\right] \quad \text{[eq. 2.8]}$$

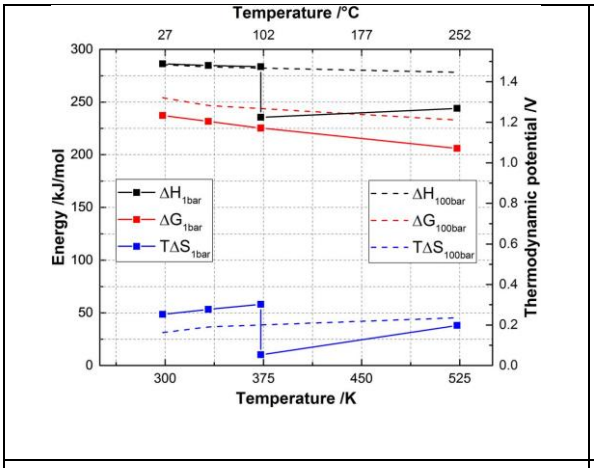

Figure 3a. The energy required to split water over a range of temperatures at 1 bar and 100 bar.

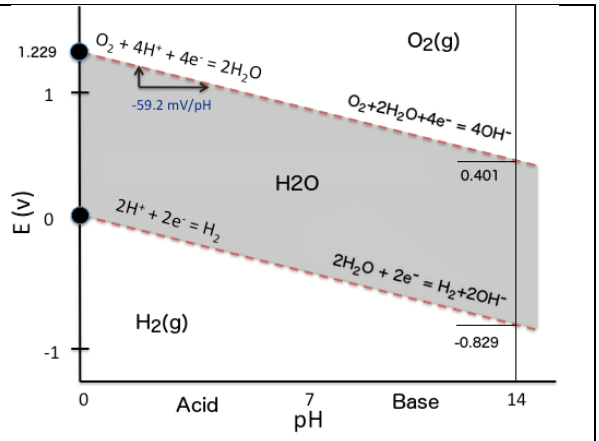

Figure 3b: Water electrolysis electrode potentials with pH at standard conditions ()

 https://doi.org/10.1149/2.1441704jes

*Source:*https://commons.wikimedia.org/wiki/File:H2OPourbaix.png

Figure 3. Water splitting characteristics

2.1.2 electrolyte pH

The values for Urev and Utn quoted in the previous section apply for electrolysis of pure water. Because of its low electric conductivity, electrolysis of pure water proceeds very slowly. By adding a water-soluble electrolyte, the conductivity of water rises considerably. The Pourbaix-diagram in Figure 3b shows that by increasing pH of the electrolyte, the half cell (water/hydrogen and water/oxygen) redox potentials shift downwards to a voltage range where conventional metals are usually passivated. This explains why water electrolysers have traditionally been using an alkaline aqueous solution as electrolyte. This has changed recently with acidic ionomer membranes becoming commercially available, while research on alkaline membranes has started.

These three types of electrolyte lie at the basis of the three low-temperature electrolysis technologies included in this report, namely AWE, PEMWE and AEMWE respectively.

2.2 Low-temperature electrolysis technologies

Three different low temperature electrolysis technologies are currently available as commercial products or under development, namely Proton Exchange Membrane (PEM) that uses an acidic polymer membrane sheet as solid electrolyte, Alkaline Water Electrolysis (AWE) that uses a liquid electrolyte (usually an aqueous solution of an alkaline product, e.g. potassium hydroxide) and a diaphragm and more recently Anion Exchange Membrane (AEM) that uses a hydroxyl-ion conducting polymer membrane sheet as solid electrolyte. Relevant state-of-the-art data for these three technologies are summarized in **Error! Reference source not found.**. A succinct description of these low temperature liquid water electrolysis technologies is given in the sections below. Note that high temperature electrolysis (700–1000 °C), such as Solid Oxide Water Electrolysis is not considered in this report.

Table 1. State of the art low temperature water electrolysis technologies

ELECTROLYSIS TYPE	PEMWE Proton Exchange Membrane	AWE Alkaline	AEMWE Anion Exchange Membrane
Charge carrier	H^+	OH^-	OH^-
Reactant	Liquid Water	Liquid Water	Liquid Water
Electrolyte	Proton exchange membrane	NaOH or KOH 20-40 wt.% /water	Anion exchange membrane
Anode Electrode	IrO_2 IrO_2/Ti_4O_7 $Ir_xRu_yTa_zO_2$, Ir black	Co_3O_4, Fe, Co, Mn Mo, P, S, $NiFe(OH)_2$, Fe(Ni)OOH, oxides, hydroxides, borides, nitrides, carbides based catalyst	IrOx $Pb_2Ru_2O_{6.5}$, $Bi_{2.4}Ru_{1.6}O_7$ NiOx, $LixCo_{3-x}O_4$, $Cu_{0.6}Mn_{0.3}Co_{0.21}O_4$, CuCoOx
Cathode electrode	Pt/C	Raney Ni, Co, Cu, NiCu, NiCuCo, Ni-Co-W, Ni-Cu-Zn-B, Ni-Co, Ni-Fe, Ni-Co-Mo, NiCoZn, Raney Co, Ni-Mo, Ni-S, Ni-rare earth alloys	Raney Ni, NiO, Co based catalystNi/(CeO_2-La_2O_3)/C
Current density	0.2-8.0 A/cm^2	0.2-2.5 A/cm^2	0.2-0.8 A/cm^2
Temperature	20-80 °C [4]	40-90 °C	40-60 ^{0}C

[4] Research efforts are targeting temperatures up to 150°C and 200°C with water vapour

Pressure H_2 out[5]	10^5 –$30 \cdot 10^5$ Pa	10^5 – $30 \cdot 10^5$ Pa	10^5 – $30 \cdot 10^5$ Pa
Cathode reaction (H_2 evolution reaction HER)[6]	$2H^+(aq) + 2e^- \rightarrow H_2(g)$	$2H_2O(l) + 2e^- \rightarrow H_2(g) + 2\,HO^-(l)$	$2H_2O(l) + 2e^- \rightarrow H_2(g) + 2\,HO^-(aq)$
Anode reaction (O_2 evolution reaction OER)	$H_2O(l) \rightarrow 1/2\,O_2(g) + 2H^+(aq) + 2e^-$	$2\,HO^-(aq) \rightarrow H_2O(l) + 1/2\,O_2(g) + 2e^-$	$2\,HO^-(aq) \rightarrow H_2O(l) + 1/2\,O_2(g) + 2e^-$

2.3 PROTON EXCHANGE MEMBRANE WATER ELECTROLYSIS (PEMWE)

A PEM water electrolysis cell is a zero-gap cell, i.e. the electrodes are directly sandwiched or coated onto the membrane. Reaction gases (H_2 and O_2) are evolved at the rear of the catalytic layers, and not in the inter-polar gap. This compact design allows for high (in the several $A \cdot cm^{-2}$ range) current density operation. Figure 4 shows the cross-section of a PEM electrolysis cell. The elementary cell is delimited by two end plates usually made of titanium or of coated stainless steel, see Figure 5. The total cell thickness is typically 5-7 mm.

The central cell component is the proton conducting membrane {region 1} made of Perfluorosulfonic Acid (PFSA) or containing other chemical groups with similar behaviour. The membrane needs hydration to maintain conductivity, which limits the operating temperature, and is surface coated by two catalytic layers. Unsupported or carbon supported Pt nanoparticles are usually used at the cathode for the Hydrogen Evolution Reaction (HER) and supported or unsupported iridium dioxide (IrO_2) or alternative catalyst based particles are used mostly at the anode for the Oxygen Evolution Reaction (OER) {regions 2 and 2'}. Both catalytic layers are microscopically porous to allow gas evolution and contain a mixture of catalyst particles, support particles and ionomer which acts as a binder and provides a high ionic contact with the membrane.

The membrane and its two catalytic layers form a so-called Catalyst Coated Membrane or CCM. The CCM is clamped between two Porous Transport Layers (PTL) {regions 4 and 4'} which are used for water distribution as well as for gas collection and removal. In some cases, the catalyst layer is coated directly on the PTLs and not on the membrane. Whereas sintered titanium disks are usually used at the anode {region 3'}, carbonaceous PTLs are at the cathode {region 3}. PTLs can be subject to physicochemical degradation due to temperature gradients and hotspots, the presence of an acid environment [3], as well as to mechanical degradation caused by compression effects.

Cell spacers, meshes or grids can be placed between the end plates and porous transport layers. They offer an open space allowing water flux through the cell and gas removal from the cell. De-ionised liquid water is pumped through the anodic compartment to feed the electrolysis reaction and to remove heat (when the cell operates above the

[5] Higher hydrogen output pressure reduces the compression needs for storage or transport of hydrogen,

[6] (aq), (l) & (g) refers to aqueous, liquid and gaseous state

thermoneutral potential). To assist in heat removal and maintaining temperature constant, in some cases water is also provided to the cathode compartment. The gaseous reaction products H_2 and O_2 need to be de-humidified and the captured water is recirculated to the water inlet.

During operation, protons migrate from the anode (where they form) through the membrane to the cathode (where they reduce to hydrogen gas). During their migration, protons transport a number of water molecules from the anode to the cathode, a process known as electro-osmotic drag. The magnitude of this water flux depends on the type of proton conducting polymer, temperature, pressure and electric current density used in the electrolysis process.

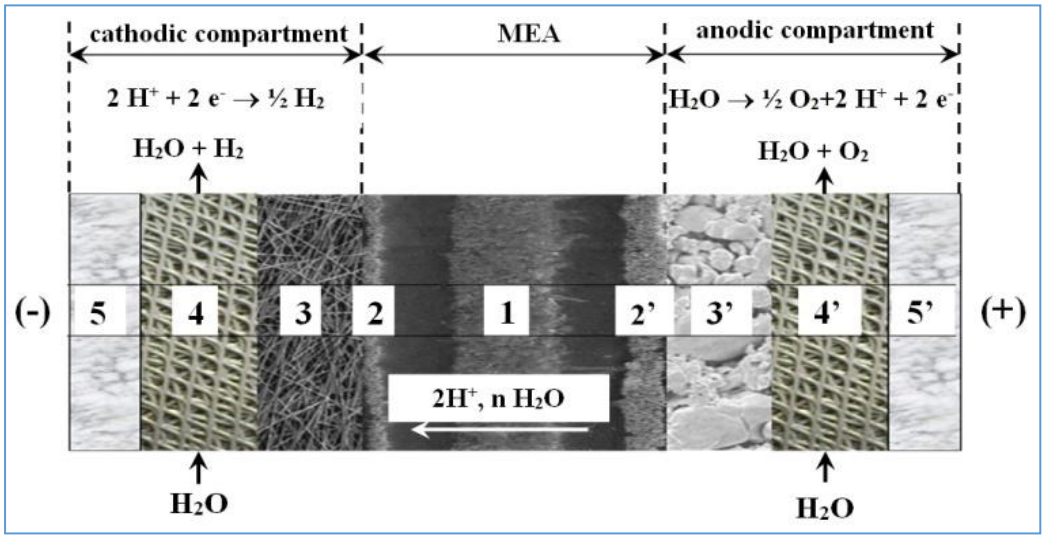

Figure 4. Cross section of a PEMWE cell.

***Source*: C. Rozain, P. Millet, Electrochimica Acta 131 (2014) 160-167**

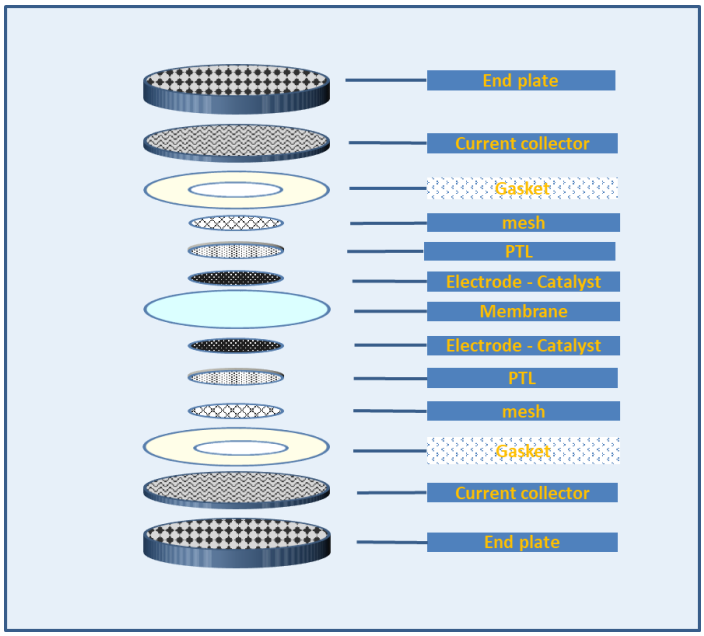

Figure 5. Typical PEM water electrolysis cell components (highlights identify those components for which functional testing is discussed in this report)

To yield higher hydrogen production rates, several single cells, a set of components as shown in Figure 5, are connected electrically in series and hydraulically in parallel as a stack. A metallic plate separates two adjacent cells and simultaneously acts as anode of one cell and cathode of the adjacent cell, hence the term bipolar plate (BPP). Pressure plates fix the components of the cells and provide the clamping force by threaded bolts and nuts.

Industrial PEM electrolysers have a typical hydrogen discharge pressure of 10-30 bar. High pressure operation is possible in two modes: either with anode and cathode at the

same pressure ("equibar"), or in differential mode with the hydrogen compartment at higher pressure. In the latter case, the BoP of the oxygen compartment is simpler, but with the drawback of the additional stress on the MEA.

Compared to the main other low temperature electrolyser technology, alkaline electrolysis, a concentrated electrolytic solution is not required and the advantages include high current density, high energy efficiencies, and ease of gas separation. These advantages enable high performance and excellent load-following at a low safety risk and make PEM electrolysers the most suited technology for coupling with RES. However, the acidic environment of PEM limits the materials of bipolar plates and current collectors, and in particular the catalysts to expensive platinum-group metals (PGMs). Also durability related to catalyst loss and membrane lifetime is an issue.

Hydrogen and oxygen produced with this technique have a very low level of contaminants. In the hydrogen gas, the main other compounds are water that can be easily removed and oxygen due to gas crossover that also can easily be removed (e.g. with catalytic conversion). The final hydrogen purity can reach 99.99%.

The power of PEM electrolysers ranges from a few kilowatts to several megawatts. The system power, for equal cell area and current density depends on the number of stacks contained in the system.

Water purification treatment at 1 MΩ·cm level is recommended to minimize negative impact of impurities on membrane operation.

2.4 ALKALINE WATER ELECTROLYSIS (AWE)

Alkaline water electrolysis is a mature technology industrialised since the nineteenth century. In an alkaline water electrolyser (AWE), water molecules are decomposed electrochemically at the cathode to hydrogen molecules and hydroxide ions; the latter diffuse through the alkaline electrolyte and a diaphragm, and discharge at the anode releasing oxygen molecules.

The major components of an AWE single cell are the diaphragm and the two electrodes. The diaphragm has a microporous structure, allowing the alkaline electrolyte to seep through for sufficient ion-conductance. The electrolyte is an aqueous solution containing either sodium hydroxide (NaOH) or potassium hydroxide (KOH). The latter is usually preferred for its higher OH^- conductivity for the same molarities. The typical concentration of 20-40 wt.% corresponds to the highest conductivity; at higher concentrations the conductivity decreases due to Coulombic force interactions.

The KOH concentration can be expressed in % or in molar unit, hereafter a table and formulas for the conversion.

KOH [M]	KOH [wt.%]
1	5,45
2	10,61
3	15,50
4	20,13
5	24,54
6	28,72
7	32,71
8	36,51
9	40,14
10	43,61
11	46,92
12	50,10

M – molar mass of KOH = 56.10564 $g \cdot mol^{-1}$

ρ - density of dry KOH = 2.044 $g \cdot cm^{-3}$

n – molarity of the KOH solution in water [M] ≡ $[mol \cdot l^{-1}]$

c – KOH concentration [wt.%]

m – mass of dry KOH for 1l KOH solution in water = M·n

$V_{KOH\ solution}$ = volume of KOH solution = M n / ρ

Formula for conversion from $mol \cdot l^{-1}$ to wt.%:

$$c\ [wt.\%] = (M \cdot n) / (M \cdot n + (1000 - (M \cdot n / \rho)) \quad [eq.\ 2.9]$$

Formula for conversion from wt.% to $mol.l^{-1}$:

$$M\ [mol \cdot l^{-1}] = c\ (M \cdot n + (1000 - (M \cdot n / \rho)) / n \quad [eq.\ 2.10]$$

Anode and cathode are separated into two compartments by the diaphragm. Two configurations exist: Figure 6a depicts the cross-section of a gap-cell, in which a void between electrodes and diaphragm is filled with electrolyte. Gases evolve on both sides of each electrode, especially in the inter-polar domain, which results in ohmic losses. Figure 6b shows the cross-section of a zero-gap cell. Electrodes with latticed or porous structures (grids, meshes, fibre felts, porous sinters or foamed metals) are pressed against the central diaphragm. Gases evolve at the rear of both electrodes; leading to a reduction of ohmic losses caused by the gaps and gaseous films. The zero-gap design is widely used in modern alkaline water electrolysers. The thickness of commercial diaphragms (e.g. Zirfon®, Supor-200®), which is equal to the distance between two electrodes, is typically 0.5 mm for the former and 0.14 mm for the latter. Some manufacturers integrate the electrodes and the diaphragm into a single component to achieve a true zero gap.

The cathode catalyst typically is a high-area nickel foam or nickel supported on stainless steel. Alternatives are Ni-Mo on a ZiO_2-TiO_2 support. The anode catalyst is usually made of Ni_2CoO_4, La-Sr-CoO_3 or Co_3O_4. Current distributors are typically nickel (the electrodes are directly pressed or welded onto the bipolar plates) with the main containment material being Ni-coated steel.

Alkaline electrolysers like PEM ones have a very wide range of rated power, from a few kilowatts to several megawatts. The system power is a function on the number of stacks

present in the system. Operation temperatures are in the range of 60 - 80 °C to ensure electrolyte conductivity and to promote reaction kinetics. Typical electrolysis pressure is 10-30 bar. The current density is typically 200 to 400 mA·cm^{-2}. In the latest technology development, replacement of diaphragms by membranes with lower ohmic resistance has resulted in current density increases up to 1.5 A cm^{-2} and even to 2.5 A cm^{-2} by increasing the surface area of the Ni mesh electrode.

For AWE, water needs to be purified before use and the product gases must be dried before release. The purity level of hydrogen and oxygen can reach 99.9 and 99.7 vol. %, respectively, without auxiliary purification equipment.

Advantages of alkaline electrolysis are that it does not use expensive noble metal catalysts and that it is stable over a long lifetime, often in excess of 100,000 hours. One drawback is that alkaline electrolysers experience high ohmic losses across the electrolyte and separator and hence operate at relatively low current densities compared to PEM electrolysers. Historically alkaline electrolysis systems have shown poor dynamic behaviour, with limited load flexibility. This occurs because separator materials are not very effective at preventing cross-diffusion of gases. Specifically, oxygen crossing to the cathode leads to a lowering in efficiency (as it can be converted back to water) and to potential safety issues, particularly in low load scenarios. These challenges need to be overcome when using alkaline electrolysers with RES such as wind or solar PV.

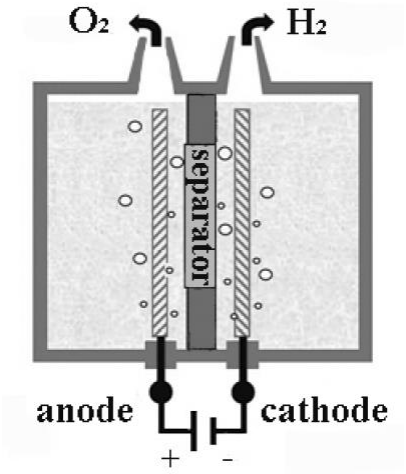

Figure 6a: Alkaline water electrolysis gap-cell.

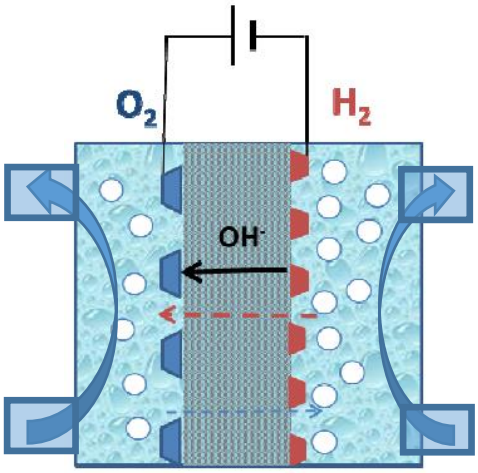

Figure 6b: Alkaline water electrolysis zero-gap-cell.

Figure 6. Alkaline electrolysis cell

2.5 ANION EXCHANGE MEMBRANE WATER ELETROLYSIS (AEMWE)

AEM (anion exchange membrane) electrolysis is a technology still under development. The main difference with alkaline electrolysis is the replacement of the diaphragm with a solid AEM, which allows the use of distilled water or of a low concentration alkaline solution as electrolyte instead of concentrated KOH or NaOH. The membrane serves as solid electrolyte for conducting OH^- ions and as separator for hydrogen and oxygen gasses. Compared to PEM electrolysis, switching the working condition from acidic to alkaline, relaxes the material restriction for the cell components. In particular, bipolar plates can be made from a cheaper material such as stainless steel, significantly reducing cost. In addition, alkaline conditions can enable the use of a lower amount of PGM catalyst, or even their substitution with catalysts based on lower cost transition metals, such as Ni, Co, Fe, Cu.

Figure 7 shows the schematic diagram of an anion exchange membrane (AEM) water electrolysis cell.

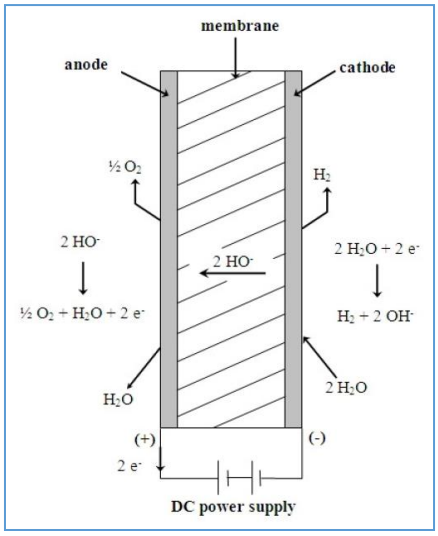

Figure 7. Schematic diagram of an AEM water electrolysis cell

Water quality requirements for AEMWE are similar to those for PEM WE. As for PEM electrolysis, the produced hydrogen can be easily pressurized. Because mechanical properties of the membrane and other components are almost the same for both PEM and AEM electrolysers, safe pressurized operation of an AEM electrolyser is expected to be possible. However, for pressurized operation, the increase in hydrogen cross-permeation through the membrane needs to be addressed.

With a view to achieving commercially viable hydrogen production, AEM electrolysis requires further improvements, specifically regarding efficiency, membrane stability, robustness, and cost reduction [reference:]

3 MATERIALS TESTING for electrolyser applications

Improvement of properties of materials and of components for electrolyser application is based on a number of innovative methods, processes and manufacturing techniques. In a first step, *"screening"* the functional properties of newly developed or improved materials making up the different cell components is needed. Such *"screening"* is performed by two testing approaches, namely *"ex-situ"* and *"in-situ",* as depicted in Figure 8. When performing screening tests, either ex-situ or in-situ, care must be taken that the test outcomes are not affected by experimental artefacts or biased measurements resulting from testing in different environments, from damages during preparation (cutting, crushing, etc.), storing and handling, or from unintended damages induced by the testing technique itself ((i.e. rotating disk electrode measurements [4]).

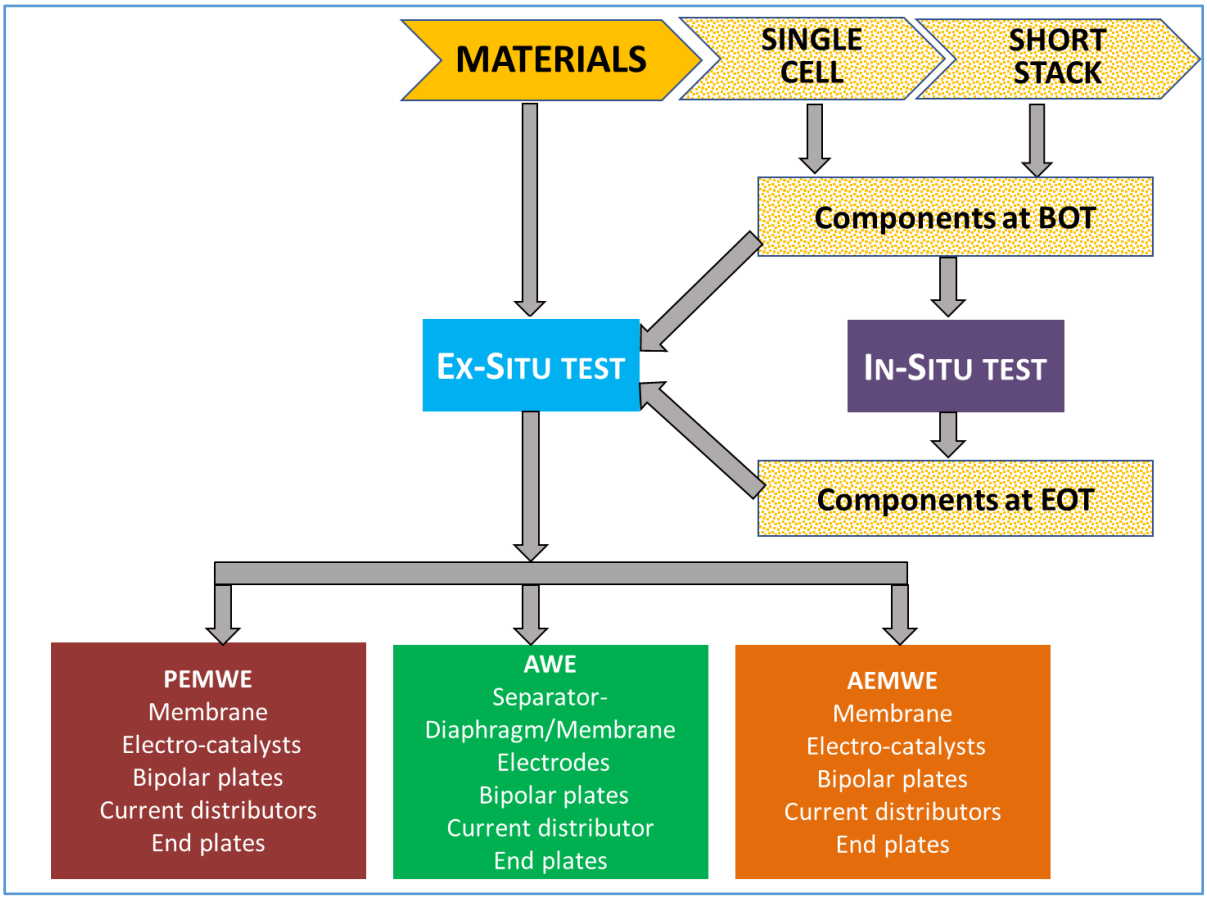

Figure 8. flow chart for functional materials testing according to the two approaches

"*Ex-situ*" tests discussed in this chapter support the development or improvement of materials to better meet the requirements for use in electrolysis cell components such as e.g. Catalyst Coated Membranes, CCMs, or Membrane Electrode Assemblies, MEAs. Such tests in which materials under test are not integrated in an electrochemical cell, may also be performed on materials that have been previously assembled in a cell structure for in-situ testing (which will be treated in chapter 4). In this case, ex-situ testing aims

at evaluating the effect of material modifications that may result from electrolyser operation.

Ex-situ testing covers a wide range of analyses, aimed at assessing materials used in PEMWE, AWE and AEMWE components. The material properties to be characterised are those that affect cell performance. **Error! Reference source not found.** provides a list of such relevant functional properties and identifies associated test methods.

Table 2. Ex-situ test methods

Property Classification	PROPERTY	EX-SITU TEST METHOD OR MEASUREMENT TOOL
PHYSICAL	Thickness	micrometer screw gauge
	Ultimate tensile strength	Tensile Test
	Elongation at break	Tensile Test
	Young's Modulus	Tensile Test
	Permeability	Mercury intrusion method, Mercury porosimeter
		Potential sweep (H2 crossover test)
	Hydrogen uptake and permeation	Potentiodynamic polarization test - ASTM G148 -97(2018)
	Porosity	Bubble point pressure test cell
		Mercury intrusion method, Mercury porosimeter
	Tortuosity	Mercury intrusion method, Mercury porosimeter
	Pore size distribution	Mercury intrusion method, Mercury porosimeter
	Mass loss in water (dissolution)	Hydrolytic stability test
	Water content	Water absorption test (ASTM D570)
	Water uptake	Water absorption (ASTM D570)
	volumetric expansion (swelling)	Water absorption test
	Hydrophobicity/hydrophilicity	Water contact angle test

	Surface Roughness	Profilometer; interferometer
PHYSICO-CHEMICAL	Bulk / surface chemical composition Material microstructure • Grain size • Crystallographic phases • Crystal Orientation	Cyclic voltammetry (CV)
		Atomic emission spectroscopy (AES)
		Atomic force microscopy (AFM)
		Brunauer-Emmett-Teller (BET) surface area measurement
		Energy dispersive X-ray spectroscopy (EDX)
		Field emission gun-scanning electron microscopes energy dispersive X-Ray analysis (FEG SEM-EDX)
		Fourier transformed infrared analysis (FTIR)
		Neutron tomography
		Scanning electron microscopy (SEM)
		Secondary ion mass spectroscopy (SIMS)
		Transmission Electron Microscopy (TEM)
		Extended X-ray absorption fine structure (EXAFS)
		X-ray absorption near-edge structure (XANES)
		X-ray diffraction (XRD)
		X-ray fluorescence (XRF)
		X-ray micro computed tomography (μ-CT)
		X-ray photoelectron spectroscopy (XPS)
	Electrical Conductivity	In-plane/through-plane conductivity test

ELECTRICAL	Contact Resistance	4-wire Kelvin method
	Ionic Conductivity	In-Plane/through plane conductivity test
CHEMICAL	Reaction Kinetics	Rotating disk electrode (RDE) test
	Oxidative Stability (mass loss)	Fenton's reagent test
	Ion exchange capacity (IEC)	Chemical Titration
	Equivalent weight (EW)	Chemical Titration
	Metal dissolution	Inductively coupled plasma mass spectrometry (ICP-MS)
THERMAL	Thermal conductivity	thermal conductivity measurement
	Glass Transition Temperature	Dynamic mechanical analysis DMA(Tg)
	Thermal decomposition	Thermogravimetric Analyser/Differential Scanning Calorimeter (TGA-DSC)

Additional information on physico-chemical methods are presented in appendix A.

The cell components and functional property tests from the above table relevant for the individual low temperature electrolysis technologies are discussed in the following sections of this chapter.

Inputs to the test methods which are treated successively in the following sections have been gathered from literature or provided by the FCH-JU funded project ELECTROHYPEM, HPEM2GAS, NEPTUNE, NOVEL for PEMWE; ELYGRID, ELYNTEGRATION for AWE, ANIONE, CHANNEL and NEWELY for AEMWE.

3.1 PEMWE functional property testing

For PEMWE components ex-situ testing aims at establishing the functional properties of materials used in

- Membranes
- Electrodes and electrocatalysts layer
- Porous Transport Layers (PTLs)
- Current collectors, meshes, bipolar plates and separator plates
- End plates

3.1.1 PEMWE MEMBRANE MATERIALS

Key requirements for the membrane relate to its barrier effect to transfer electrons and gases between the anode and cathode compartments and its capacity of acting as electrolyte for ionic species. For the barrier effect gas transport properties are the most relevant, whereas the ionic resistance serves as a metric for electrolyte properties. The ionic resistance depends on:

- Ion exchange capacity (IEC, mmol ion·g^{-1} polymer) or equivalent weight (EW, g polymer per mol, IEC = 1000 / EW).
- amount of water uptake
- cross-permeation of gasses, which is affected by permeability and depends on the applied current density
- Thickness
- Geometrical area

The ionic resistance can be characterised by two parameters: area resistance [$\Omega.cm^2$], i.e. measured resistance [Ω] multiplied by the geometric area [cm^2], or resistivity [$\Omega.cm^2/cm$], i.e. area resistance divided by thickness.

A list of functional properties of membrane materials is presented in **Error! Reference source not found.**. The protocols agreed for performing the associated ex-situ tests are identified in the table and described in detail in Appendix B. Because functional properties may depend on temperature and on pressure, assessment of PEMWE membrane materials may require performing ex-situ tests over a range of temperatures or pressures.

Table 3. PEMWE membrane material ex-situ tests

MEMBRANE			
Property Classification	**PROPERTY**	**EX-SITU TEST METHOD OR MEASUREMENT TOOL**	**Ref.**
PHYSICAL	Thickness	micrometer screw gauge	B5
	Ultimate tensile strength	Tensile Test (ASTM D882-09, ASTM D638)	
	Elongation at break	Tensile Test	B9
	Young's Modulus	Tensile Test (ASTM D638 type V)	
	Permeability	Potential sweep (H2 crossover test)	B7
	Mass loss in water	Hydrolytic stability test	B2

	(dissolution)		
	Water content	Water absorption test (ASTM D570)	
	Water uptake	Water absorption (ASTM D570)	
	volumetric expansion (swelling)	Water absorption test (ASTM D 756) ➢ Thickness increase Δz in H2O at specific T ➢ Machine Direction (MD) thickness increase Δx in H2O at specific T ➢ Transverse Direction (TD) thickness increase Δy in H2O at specific T	B6
	Surface Roughness	Profilometer; interferometer	
ELECTRICAL	Electrical Conductivity	In-plane/through-plane conductivity test (Four-electrode chronopotentiometry)	
	Contact Resistance	4-wire Kelvin method	
	Ionic Conductivity	In-Plane/through plane conductivity test	B4
CHEMICAL	Reaction Kinetics	Rotating disk electrode (RDE) test	
	Oxidative Stability (mass loss)	Fenton's reagent test	B3
	Ion exchange capacity (IEC)	Chemical Titration	B1
	Equivalent weight (EW)	Chemical Titration	B1
THERMAL	Thermal conductivity	thermal conductivity measurement	
	Glass Transition Temperature	Dynamic mechanical analysis DMA(Tg)	B8
	Thermal decomposition	Thermogravimetric Analyser/Differential Scanning Calorimeter (TGA-DSC)	B8

3.1.2 PEMWE ELECTRODE AND ELECTROCATALYSTS

The function of an electrocatalyst is to increase the electrochemical reaction rate, in this case of water splitting, by reducing the activation energy. When precious materials are used such as Platinum or Iridium are used as catalysts, it is important to maximise their use by increasing the surface area. For this reason, some porous supporting medium like porous Titanium, Magneli phase is used for the anode electrode. Carbon fibres are suitable for the cathode only, because their corrosion resistance is too low in the anodic environment.

For functional property evaluation of electrocatalyst materials, ex-situ tests include determination of morphology, particle size and dispersion of the catalysts (see **Table 4. PEMWE electrode and electrocatalyst ex-situ tests**Table 4). For electrode materials, surface homogeneity, hydrophobicity/hydrophilicity, chemical resistance and electrical properties are the most relevant to be investigated.

Table 4. PEMWE electrode and electrocatalyst ex-situ tests

ELECTRODE AND ELECTROCATALYST		
Property Classification	**PROPERTY**	**EX-SITU TEST METHOD OR MEASUREMENT TOOL**
PHYSICAL	Thickness	micrometer screw gauge
	Hydrophobicity/hydrophilicity	Water contact angle test
	Surface Roughness	Profilometer; interferometer
PHYSICO-CHEMICAL	Bulk / surface chemical composition Material microstructure • Grain size • Crystallographic phases • Crystal Orientation	Cyclic voltammetry (CV)
		Atomic emission spectroscopy (AES)
		Atomic force microscopy (AFM)
		Brunauer-Emmett-Teller (BET) surface area measurement
		Energy dispersive X-ray spectroscopy (EDX)
		Field emission gun-scanning electron microscopes energy dispersive X-Ray analysis (FEG SEM-EDX)
		Fourier transformed infrared analysis (FTIR)

		Neutron tomography
		Scanning electron microscopy (SEM)
		Secondary ion mass spectroscopy (SIMS)
		Transmission Electron Microscopy (TEM)
		Extended X-ray absorption fine structure (EXAFS)
		X-ray absorption near-edge structure (XANES)
		X-ray diffraction (XRD)
		X-ray fluorescence (XRF)
		X-ray micro computed tomography (μ-CT)
		X-ray photoelectron spectroscopy (XPS)
ELECTRICAL	Electrical Conductivity	In-plane/through-plane conductivity test
	Contact Resistance	4-wire Kelvin method
	Ionic Conductivity	In-Plane/through plane conductivity test
CHEMICAL	Reaction Kinetics	Rotating disk electrode (RDE) test
	Metal dissolution	Inductively coupled plasma mass spectrometry (ICP-MS)
THERMAL	Thermal conductivity	through-plane thermal conductivity measurement

3.1.3 PEMWE POROUS TRANSPORT LAYER MATERIALS

The porous transport layer acts as electroconductive diffusion layer facilitating mass transport of reactants and removal of reaction products between electrode and BPP. It is

made of a porous medium or a combination of different porous media forming adjacent layers or a composite layer.

PTLs can be subject to electrochemical degradation due the combination of thermal variation and presence of an acid environment [3], as well as some mechanical degradation due to the compression effects. When differential pressure is applied, the PTL has to provide also mechanical support for the membrane.

The properties of PTLs are measured with tests similar to those used for the bipolar plate materials (see 3.1.4). Additional characterization methods are: gas/water permeation, mechanical tests, X-ray micro computed tomography, and neutron tomography for assessing water/gas presence

A list of ex-situ tests used for PTL materials is provided in Table 5.

Table 5. PEMWE PTL ex-situ tests

POROUS TRANPORT LAYER		
Property Classification	**PROPERTY**	**EX-SITU TEST METHOD OR MEASUREMENT TOOL**
PHYSICAL	Thickness	micrometer screw gauge
	Ultimate tensile strength	Tensile Test
	Elongation at break	Tensile Test
	Young's Modulus	Tensile Test
	Permeability	Mercury intrusion method, Mercury porosimeter
	Hydrogen uptake and permeation	Potentiodynamic polarization test - ASTM G148 -97(2018)
	Porosity	Mercury intrusion method, Mercury porosimeter
	Tortuosity	Mercury intrusion method, Mercury porosimeter
	Pore size distribution	Mercury intrusion method, Mercury porosimeter
	Hydrophobicity/hydrophilicity	Water contact angle test
	Surface Roughness	Profilometer; interferometer
PHYSICO-CHEMICAL	Bulk / surface chemical composition Material microstructure • Grain size • Crystallographic phases Crystal Orientation	Neutron tomography Scanning electron microscopy (SEM) X-ray micro computed tomography (μ-CT)
ELECTRICAL	Electrical Conductivity	In-plane/through-plane conductivity test
	Contact Resistance	4-wire Kelvin method
CHEMICAL	Metal dissolution	Inductively coupled plasma mass spectrometry (ICP-MS)
THERMAL	Thermal conductivity	thermal conductivity measurement

3.1.4 PEMWE BIPOLAR PLATES AND CURRENT DISTRIBUTOR materials

A BPP is an electrically conductive gastight plate separating individual cells in a stack. It distributes current and reagents flows and provides mechanical support for the electrodes or membrane electrode assembly (MEA). For BPP materials the relevant functional properties include electrical/thermal conductivity, corrosion resistance and characterization of applied coating materials. A list of ex-situ tests used for bipolar plates and current distributor materials is reported in Table 6.

BPPs should have sufficient electrical and thermal conductivity. Often a flow field based on a channel structure, typically in the mm-range, is used to distribute the reactant water evenly over the active area and remove product gases and waste heat.

Table 6. PEMWE BPPs and current distributor ex-situ tests

Property Classification	PROPERTY	EX-SITU TEST METHOD OR MEASUREMENT TOOL
PHYSICAL	Thickness	micrometer screw gauge
	Ultimate tensile strength	Tensile Test
	Elongation at break	Tensile Test
	Young's Modulus	Tensile Test
	Hydrogen uptake and permeation	Potentiodynamic polarization test - ASTM G148 -97(2018)
	Hydrophobicity/hydrophilicity	Water contact angle test
	Surface Roughness	Profilometer; interferometer
PHYSICO-CHEMICAL	Bulk / surface chemical composition	Atomic force microscopy (AFM)
		Field emission gun-scanning electron microscopes energy dispersive X-Ray analysis (FEG SEM-EDX)
		Neutron tomography
		Scanning electron microscopy (SEM)
		X-ray diffraction (XRD)
		X-ray micro computed tomography (μ-CT)

		X-ray photoelectron spectroscopy (XPS)
ELECTRICAL	Electrical Conductivity	In-plane/through-plane conductivity test
	Contact Resistance	4-wire Kelvin method
CHEMICAL	Metal dissolution	Inductively coupled plasma mass spectrometry (ICP-MS)
THERMAL	Thermal conductivity	thermal conductivity measurement

3.1.5 PEMWE END PLATE materials

End plates are components located on either end of the electrolyser cell/stack serving to transmit the required compression to the stacked cells. The end plates may comprise ports, ducts and manifolds for transporting fluids (reactants, coolant) to and from the stack.

For end plates components the mechanical and thermal properties are relevant. A list of ex-situ tests used for end plate material assessment is given in Table 7.

Table 7. PEMWE end plate ex-situ tests

Property Classification	PROPERTY	EX-SITU TEST METHOD OR MEASUREMENT TOOL
PHYSICAL	Thickness	micrometer screw gauge
	Ultimate tensile strength	Tensile Test
	Elongation at break	Tensile Test
	Young's Modulus	Tensile Test
	Surface Roughness	Profilometer
THERMAL	Thermal conductivity	thermal conductivity measurement

3.2 AWE FUNCTIONAL PROPERTIES

For AWE systems, materials of the following components require functional testing:

- Diaphragm
- Membranes (for newer AWE technology)
- Electrodes
- Support plates

3.2.1 AWE DIAPHRAGM MATERIALS

The main requirements for the diaphragm are ionic conductivity and gas separation capability. Ionic conductivity should be high to minimise ohmic losses, and it depends on material composition, porosity and wettability, as well as on thickness and assembly. Gas separation capability should also be high to withstand the anode-cathode differential pressure measurable with bubble point pressure (BPP) test cell. Measures to increase gas separation normally negatively affect ionic conductivity.

Other relevant properties are mechanical form stability, flexibility and chemical resistance.

Table 8. AWE Diaphragm ex-situ tests

DIAPHRAGM		
Property Classification	**PROPERTY**	**EX-SITU TEST METHOD OR MEASUREMENT TOOL**
PHYSICAL	Thickness	micrometer screw gauge
	Ultimate tensile strength	Tensile Test (ASTM D882-09, ASTM D638)
	Young's Modulus	Tensile Test (ASTM D638 type V)
	Porosity	Bubble point pressure test cell
	Tortuosity	Mercury intrusion method, Mercury porosimeter
	Pore size distribution	Mercury intrusion method, Mercury porosimeter
	Surface Roughness	Profilometer; interferometer
ELECTRICAL	Electrical Conductivity	In-plane/through-plane conductivity test (Four-electrode chronopotentiometry)
	Contact Resistance	4-wire Kelvin method
	Ionic Conductivity	In-Plane/through plane conductivity test

3.2.2 AWE MEMBRANE MATERIALS

With the latest technology developments polymeric membranes have been introduced in alkaline electrolysers to improve their efficiency. The lower thickness of Nafion® or m-PBI (poly(2,2-(m-phenylene)-5,5-bibenzimidazole) membranes (30-180 μm compared to 500 μm or more of diaphragms) provides acceptable mechanical resistance, whilst it increases ionic conductivity.

For the applicable ex-situ tests see table 3.

3.2.3 AWE ELECTRODE MATERIALS

Electrodes are in contact with the electrolyte for the supply of electrical energy for the electrochemical reaction. Electrode materials normally consist of metal porous structures that exhibit high electrical conductivity, high surface area and high corrosion resistance in the electrolyte caustic environment.

Table 9- AWE Electrode ex-situ tests

ELECTRODE		
Property Classification	**PROPERTY**	**EX-SITU TEST METHOD OR MEASUREMENT TOOL**
PHYSICAL	Thickness	micrometer screw gauge
	Ultimate tensile strength	Tensile Test (ASTM D882-09, ASTM D638)
	Young's Modulus	Tensile Test (ASTM D638 type V)
	Porosity	Bubble point pressure test cell
	Tortuosity	Mercury intrusion method, Mercury porosimeter
	Hydrophobicity/hydrophilicity	Water contact angle test
	Surface Roughness	Profilometer; interferometer
PHYSICO-CHEMICAL	Bulk / surface chemical composition	Atomic emission spectroscopy (AES)
	Material microstructure • Grain size • Crystallographic phases • Crystal Orientation	Atomic force microscopy (AFM)
		Energy dispersive X-ray spectroscopy (EDX)
		Neutron tomography

		Scanning electron microscopy (SEM)
		X-ray diffraction (XRD)
		X-ray fluorescence (XRF)
		X-ray micro computed tomography (μ-CT)
		X-ray photoelectron spectroscopy (XPS)
ELECTRICAL	Electrical Conductivity	In-plane/through-plane conductivity test
	Contact Resistance	4-wire Kelvin method
	Ionic Conductivity	In-Plane/through plane conductivity test
CHEMICAL	Metal dissolution	Inductively coupled plasma mass spectrometry (ICP-MS)
THERMAL	Thermal conductivity	thermal conductivity measurement

3.2.4 AEM SUPPORT PLATE MATERIALS

Support plates or end plates have mainly a mechanical support function and are made from metals. For bipolar plates, considering that their electric conductivity is four orders of magnitude, or more, higher than that of the electrolyte, the electrical properties are not critical. Normally nickel is used as it is cheap, stable and has low contact resistance However use of passivating layers to protect against corrosion can significantly increase contact resistances which may become an important contribution to the total cell resistance. For the applicable ex-situ tests see Table 6.

3.3 AEMWE FUNCTIONAL PROPERTIES

Notwithstanding the difference between PEMWE and AEMWE related to the use of an acidic, resp. alkaline solid electrolyte, the cells and stacks of both technologies contain similar components assembled in a similar way. Hence, the materials of interest as well as the applicable ex-situ tests to establish their functional properties, are the same as for PEMWE (see 3.1).

4 IN-SITU TESTS

In *"in-situ"* tests the performance of materials is assessed by using measurement devices and sample connectors which are compatible with the operational environment that the materials are expected to experience in actual applications. These tests aim at evaluating performance under operating conditions in single cell or short stack arrangement, by measuring the electro-chemical properties in terms of voltage, current and time. Test campaigns should only start after appropriate Cell/Stack Activation and Conditioning according to the manufacturer's instructions has been performed.

In-situ testing can be performed over a wide range of testing conditions and at different moments in time, as indicated schematically in figure 9 below:

Testing conditions include static and dynamic operating conditions (the latter according to a given load-versus-time profile) imposed by the test hardware on the single cell or short stack. To be exhaustive, such conditions should cover normal and out-of-normal or "stressor" operation for the cell or stack components. Hence, four dimensions apply for in-situ test conditions: static/dynamic/normal/stressor.

The time dimension enters because the performance determined from results of in-situ tests constitutes an instantaneous measure that depends on the material properties of the components making up the single cell or short stack at a given time, as affected by their actual exposure history corresponding to a given load-versus-time profile. Interrupting the above-mentioned dynamic loading and subjecting a single cell or short stack to in-situ tests allows assessing the change of performance induced by a change in material properties[7]. Execution of in-situ tests upon repeated interruption thus allows monitoring performance degradation or, in other words, assessing durability.

To reduce testing effort and time required for assessing durability through performance degradation monitoring, the imposed load profiles may require adaptation to accelerate the induced degradation. This approach, known as accelerated in-situ testing, is based on the assumption of an increase in the rate of degradation, with the mechanism(s) causing degradation in the accelerated tests remaining the same as in actual service.

[7] Performing ex-situ tests (as described in chapter 3) allows measuring the functional material properties at any moment during their exposure history.

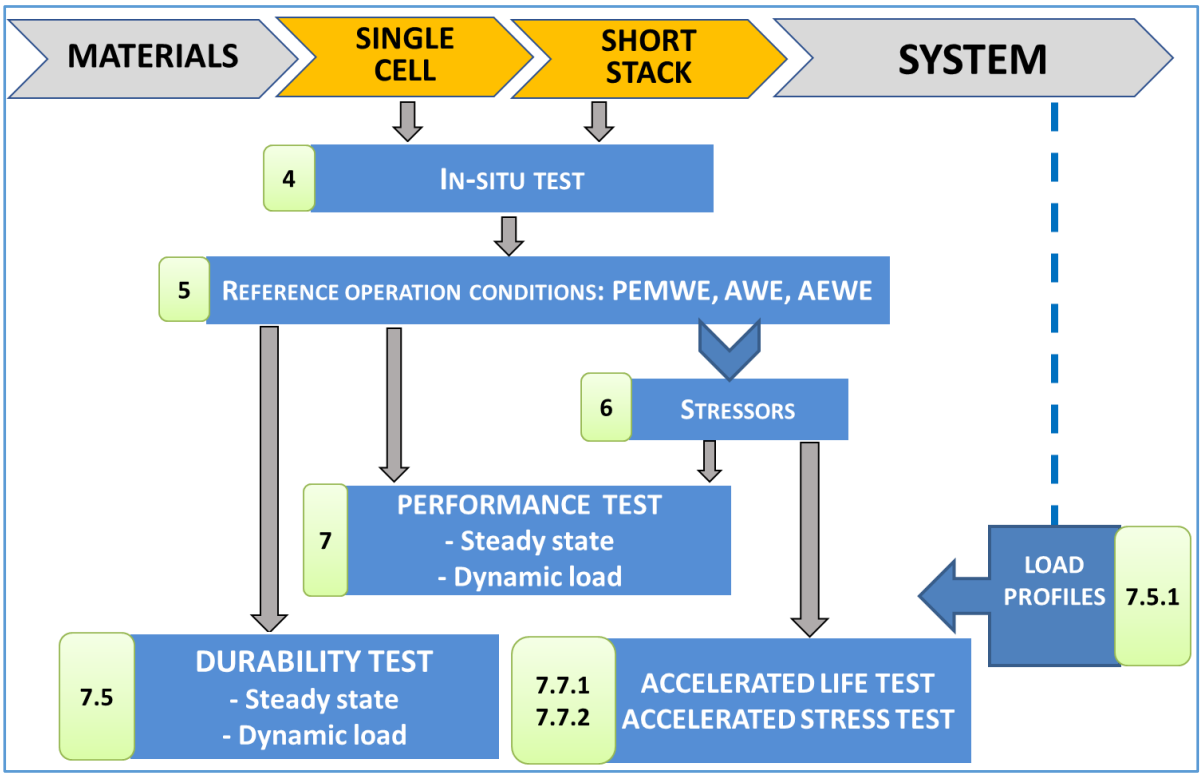

Figure 9. scheme for in-situ single cell and short stack testing. Number labels to boxes refer to chapters in this report

In-situ cell or short stack tests enable evaluating performance in terms of a number of indicators derived from the test outcomes, either as a direct experimental result, or indirectly from an analysis of the test outcomes. The most frequently used in-situ tests are:

- **Polarization curve (I-V Curve)** for overall electrochemical performance evaluation
- **Cyclic Voltammetry (CV)** to measure reaction kinetics for determination of electro-chemical active surface area
- **Electrochemical Impedance spectroscopy (EIS)** for separating ohmic, activation and concentration losses for evaluation of reaction rates, diffusion coefficients, charge transfer resistance and double layer capacity values

A detailed description of the associated test protocols is presented in JRC test reports for Polarisation Curve Measurements [7]; Cyclic Voltammetry [8] and Electrochemical Impedance Spectroscopy [9].

An orientation for the in-situ test approach is presented in the following table, where the last column shows the section of the present report in which this aspect is addressed.

Table 10: in-situ testing orientation table

In-situ Test level	Subject of the assessment	Topic	Section
Single cell/ short stack	performance	Set of reference operating conditions	5
		Type and intensity of stressors	6
		Identification of performance indicators	7.1, table 22
		Definitions for efficiency	7.2
		Performance assessment	7.3
	Durability (through monitoring of performance degradation)	Identification of durability indicators	7.4.1-3, table 25
		Formulation of durability test protocol for steady state loading	7.5.1-2
		Formulation of durability test protocol for dynamic loading	7.5.3-4
	Accelerated testing	Formulation of protocol for accelerated life testing	7.7.1
		Formulation of protocol for accelerated stress testing	7.7.2
System	Performance	Identification of performance indicator	8.7, table 48
		Formulation of grid-balancing fit-for-purpose test	8.4
		Formulation of harmonised grid services protocols	8.5
		Definitions for efficiency	8.6

5 REFERENCE OPERATING CONDITIONS FOR TESTING OF SINGLE CELLS AND OF SHORT STACKS

Electrolyser materials are subjected to a variety of operating conditions. The aim of establishing a set of Reference Operating Conditions is to be able to test and evaluate the Reference Performance of different materials in-situ in single cell or short stack configuration and to provide a means for objective comparison of test results. The reference operating conditions should be representative as far as possible of current and future electrolyser applications.

The operating conditions selected as reference should ideally represent the centre of the window of normal operating conditions. However, in some cases electrolysers are bound to operate under conditions outside of the normal operation window. Some of these conditions could be severe and act as stress factors to cell and short stack materials. These stressor conditions are elaborated upon in chapter 6.

Operating Conditions consist of two sets of parameters:

First, test parameters with a set-point value that can be controlled using a feedback loop within the test hardware are defined as **Test Input Parameters (TIP)**.

Second, non-adjustable parameters whose measured value depends on the values imposed by the TIPs are defined as **Test Output Parameters (TOP**).

Whereas the instrumentation for experimental measurement of TIPs (measurement and control) and TOPs (measurement only) should in principle be located as close as possible to the relevant position of interest in the cell, this is not always feasible in practice. Therefore, in the following sections TIPs and TOPs are identified for properties that are experimentally accessible at the level of the test bench and of the anode and cathode compartments[8]. For test results to be valid, the values assumed by the TIPs have to fall within specific tolerances, independently or in combination with specific TOPs (see Table 14).

The following sections of this chapter list the agreed reference operating conditions (TIPs and TOPs) for the three considered low temperature electrolysis technologies.

[8] In addition, electrical parameters current (density) and cell voltage serve as TIP and TOP, respectively.

5.1 REFERENCE OPERATING CONDITIONS for PEMWE CELL/SHORT STACK TESTING

5.1.1 CELL TEMPERATURE *(TIP)*

Because cell temperature is one of the most important parameters affecting performance, it should be controlled as accurately as possible. Hence, to minimize temperature variations from the intended setting, cell temperature is controlled by a temperature control system incorporated in the recirculating water loop which is adequately insulated to minimize thermal losses to the environment.

The TIP cell temperature should be representative of the temperature of the MEA where the water electrolysis reaction occurs. The temperature sensor for monitoring and controlling cell temperature should hence be located as close as possible to the MEA. Depending on test bench configuration, a number of cases can be differentiated for the location of the temperature sensor:

i. Temperature sensor located inside the anode and cathode bipolar plate close to the MEA
   - The cell temperature is that indicated by the sensor at the anode side

For a temperature sensor placed in the water recirculation loop, two cases should be considered:

ii. The liquid water is fed to the anode compartment only:
   - The cell temperature is equal to the temperature of the water measured as close as possible to the cell inlet.

iii. The liquid water is fed to both anode and cathode compartments.
   - The cell temperature is equal to the average water temperature of the water measured at anode and cathode inlets.

For the latter two cases, the uniformity of the water temperature between inlet and outlet of the cell is important and the water temperature difference between outlet and inlet should be minimised.

5.1.2 WATER QUALITY *(TIP)*

The indicator used for the quality of the de-ionised water is its electrical conductivity measured at the cell inlet. Recirculation of the water may deteriorate the water quality because of possible accumulation of ions or impurities such as organic carbonaceous and non-conducting pollutants. Whereas the presence of such impurities may not show up in the results of electric conductivity measurements, cell performance/durability may nevertheless be affected. It is therefore recommended to fit a purification stage in the recirculation loop upstream of the cell inlet, and to measure water conductivity downstream of the purification system.

The water reacted is replenished in the recirculation loop through a deionisation water treatment system ("water make up" unit).

5.1.3 ANODE CONDITIONS

These are split in two classes: TIPs and TOPs which are discussed consecutively.

Anode Test Input Parameters

i. Anode water quality

- See 5.1.2

ii. Anode water inlet temperature

The anode water inlet temperature serves as TIP when the cell temperature cannot be measured in the cell bipolar plate close to the MEA. The temperature in this case should be measured as close as possible at the inlet of the cell/stack (case ii, 5.1.1).

iii. Water inlet pressure

Pressure is normally controlled indirectly with a feed-back control loop based on the gas outlet pressure that is adjusted from ambient to the maximum design pressure with a backpressure regulation valve.

iv. Water inlet Flow rate

The water inlet flow rate should in principle be set based on the cell or short stack active area perpendicular to the direction of the current, corresponding to the geometrical electrode area in contact with the membrane.

However, next to serving as feedstock for the electrolysis reaction, water also contributes to heat management of the cell/short stack by removing or minimising heat produced by the electrolysis reaction, thereby maintaining the correct temperature at the reaction site of the MEA. The water flow rate is related to the temperature difference between cell input and output through the dimensionless Lambda factor λ_{H_2O} [5] defined as:

$$\lambda_{H_2O} = \frac{2F}{M_{H_2O}\, C^{p}_{H_2O} \Delta T}\left(U^{cell} - U^{tn}\right) \qquad \text{[eq. 5.1]}$$

Where

- λ_{H_2O} is the dimensionless and time independent ratio of the actual water flow rate to that of the electrolysed water;
- F = Faraday constant;
- M_{H_2O} = molar weight of water;
- $C^{p}_{H_2O}$ = heat capacity of liquid water at constant pressure;
- ΔT = water temperature difference between cell outlet and inlet;
- U^{cell} = cell voltage at operational T,p;
- U^{tn} = thermoneutral cell voltage at operational T,p.

  The unit to be used for each of the parameters is that indicated in Table 49, Symbols.

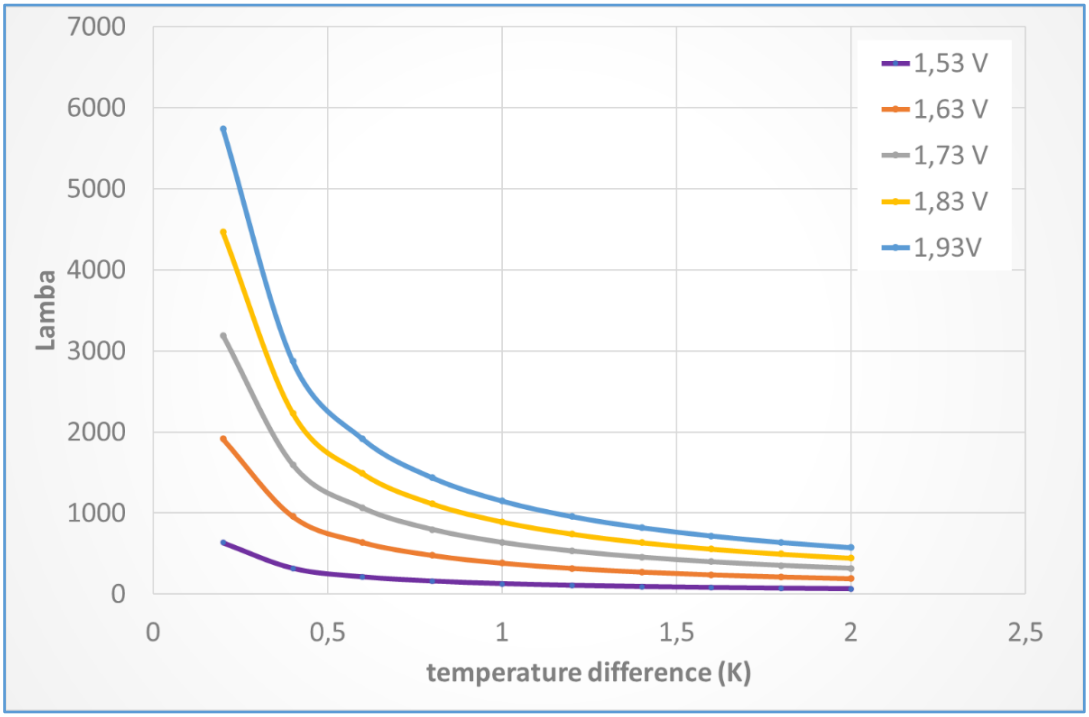

Figure 10. lambda plot for various cell voltages and temperature differences

As shown in Figure 10 lambda increases with decreasing temperature difference and increasing operating voltage, indicating the need for higher water flow rates to maintain thermal equilibrium under these conditions.

Another parameter that can be used for determining an appropriate water inlet flow rate to minimise the temperature difference between inlet and outlet is the water utilization factor (UF_w). It is defined as the ratio of the water reacted at a given current and the corresponding water flow fed to the anode and calculated as follows:

The relationship between water reacted and total current is

$$\dot{n}_{h2O,reacted} = \frac{i \times A \times N}{2F} \quad \text{[eq. 5.2]}$$

Therefore with the specific feed water flowrate expressed in $ml \cdot min^{-1} \cdot cm^{-2}$ of active area, UF_w can be calculated as

$$UF_w = \left(\frac{i \times A \times N}{2F} \times M_{H2O} \times 60\right) / (specific\ feed\ water\ flow\ rate \times A \times N) \quad \text{[eq. 5.3]}$$

$$UF_w = \left(\frac{i}{96485{,}33} \times 18{,}015 \times 30\right) / (Feed\ water\ flow\ rate) \quad \text{[eq. 5.4]}$$

$$UF_w = (i \times 0.0056) / (Feed\ water\ flow\ rate) \quad \text{[eq. 5.5]}$$

For typical water electrolysis operation, UFw is commonly set at 0.5%. As shown in Figure 11, this corresponds to flow rates higher than 2 ml/min for a typical current density of 2 A cm-2. For operation at higher current density, a higher water utilization

factor is required for minimizing temperature difference while maintaining the reaction rate.

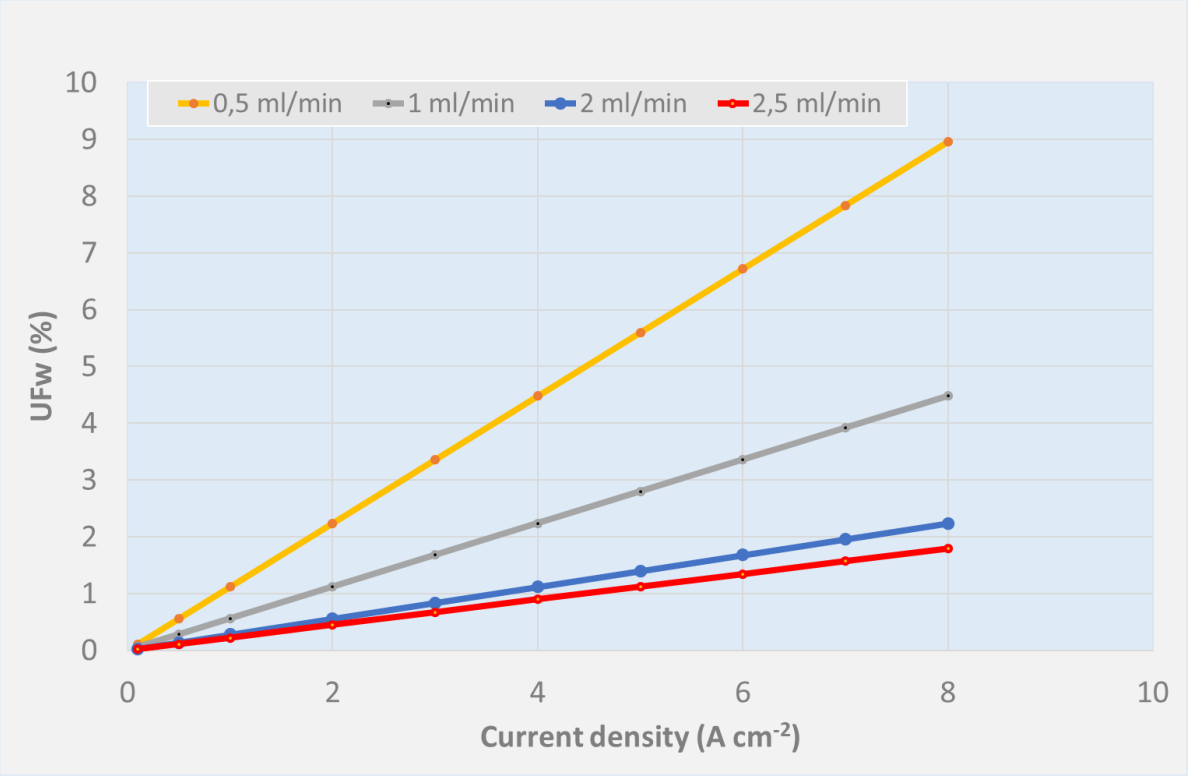

Figure 11. Water utilization factor (UFw) evolution Vs current density and water inlet flowrate

In addition to the water flowrate requirements corresponding to the use of water as reagent and its contribution to heat management, water flow rate also affects gas bubble evolution and removal at the electrodes, with higher flow rates having a beneficial effect on cell performance.

For the two above reasons, the water inlet flowrate is usually set considerably higher than that required for converting it into hydrogen and oxygen for a given active cell area and current density. Accordingly, the minimum specific feed flowrate in the water recirculation loop is set to 2 $ml \cdot min^{-1} \cdot cm^{-2}$ of active area.

v. Oxygen outlet pressure

Depending on the anticipated use of the produced oxygen, its pressure may serve as a TIP. In this case, oxygen pressure should be measured at the outlet of the electrolysis cell/short stack, after the water removal components, and before the backpressure regulation valve. The measured oxygen pressure is then fed as a feedback control signal to the anodic water circulation pressure control loop.

In pressurized test hardware, anode and cathode semi-cells can be designed to operate at the same or at different pressure; in the first case differential pressure effects on the MEA are minimized, while in the second case the oxygen line can be kept at lower (ambient) pressure, thereby reducing possible safety issues and simplifying BoP.

Anode Test Output Parameters

i. Water outlet temperature

The water outlet temperature depends on the water inlet temperature, flowrates of water and of oxygen, heat transfer resulting from ohmic losses in the MEA, conductive heat losses from piping and from hardware surfaces.

The temperature difference between water outlet and inlet serves as a test validity criterion and should not exceed +/- 2K (see Table 14).

ii. Oxygen Quality

When the produced oxygen is to be used as feedstock, its quality should be measured in real time at the cell or stack exit after water removal, according to the specifications for its use.

Due to the high diffusion coefficient of hydrogen, a certain amount of it is expected to be present in the oxygen gas stream. Experimental data shows that anodic hydrogen contamination decreases with increasing applied current density because the associated increase of oxygen evolution rate dilutes the permeating hydrogen, the amount of which is considered rather constant. The operating pressure is another important parameter affecting hydrogen concentration in the anodic compartment, and is limited to approximately 30 bar.

In the absence of a real-time quality control system, for safety reason it is recommended to monitor at least the presence of hydrogen in the oxygen outlet stream using a safety sensor to ensure that the hydrogen concentration does not reach the Lower Explosion Limit (LEL) of a hydrogen-oxygen gas mixture. LEL decreases with temperature and increases with pressure as shown in Table 11 and Figure 12, indicating that higher temperatures and lower pressures merit more attention [6]. In practice, when the hydrogen concentration exceeds 50% of LEL, appropriate safety measures should be triggered.

Table 11. Influence of pressure on explosion limits of H_2-O_2 mixtures at room temperature,25 °C, and 80 °C

[*Source*: Schroeder, V.,Sicherheitstechnische Untersuchungen fur die Hochdruck-wasserelektrolyse zur Speicherung regenerative Energie, Report No. VH2226, BAM Berlin, 2002]

Pressure in bar	LEL in mol% H_2		UEL in mol% H_2	
	25°C	80°C	25°C	80°C
1	4.0	3.8	95.2	95.4

5	4.6	4.4	94.6	95.0
10	5.0	4.8	94.2	94.6
20	5.4	5.2	94.2	94.6
50	5.5	5.3	94.6	95.0
100	5.7	5.7	94.9	95.3
150	5.7	5.3	95.1	95.5
200	5.9	5.7	95.1	95.5

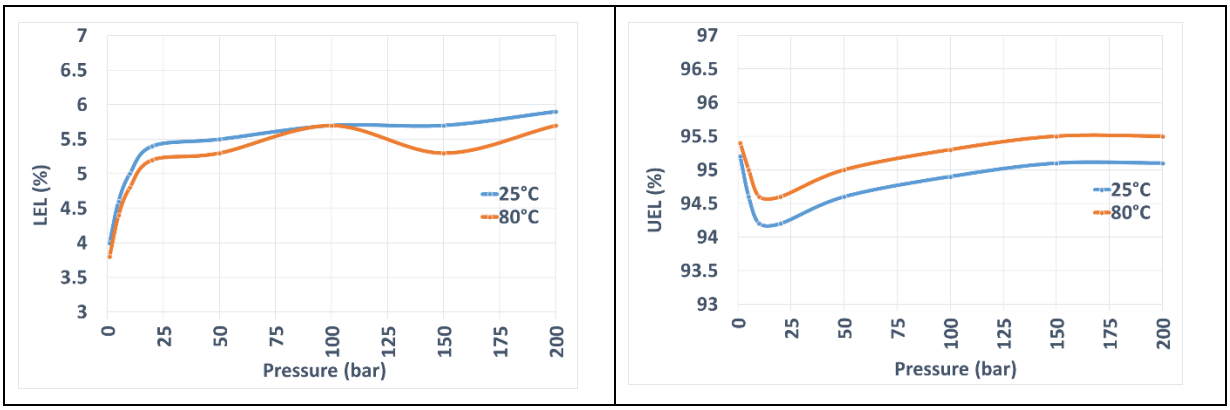

Figure 12. Pressure and temperature effect on LEL and UEL mixture H_2-O_2

iii. Oxygen production rate

The oxygen production rate is a direct consequence of the current applied with some loss depending by the overall system efficiency. Considering 100% faradaic efficiency the oxygen production rate is:

$$\dot{n}_{O2,out} = \frac{I}{4F} \qquad \text{[eq. 5.6]}$$

5.1.4. CATHODE CONDITIONS

These are split in two classes: TIPs and TOPs which are discussed consecutively.

Cathode Test Input Parameters
For heat management purposes, liquid de-ionised water can also be fed to the cathode compartment, in parallel to the anode water feed. The related TIPs are identical to those for the anode water inlet (temperature, quality, pressure) discussed before. An additional TIP at cathode side is

i. Hydrogen outlet pressure

The hydrogen pressure is measured at the outlet of the electrolysis cell/stack after the water mist and vapour removal components and before the backpressure regulation valve. The measured hydrogen pressure is fed as a feedback control signal to the water circulation pressure control loops for tests with the same pressure at anode and cathode side. For differential operation mode, the hydrogen outlet pressure is the relevant TIP, because for safety reason oxygen outlet pressure is set at ambient or lower pressure.

Cathode Test Output Parameters

When optional cathode water feed is used for heat management purposes, the same TOPs apply as for the anode water feed. Additional TOPs at cathode side are:

i. Hydrogen purity

The hydrogen purity should be measured in real time at the exit of the cell or stack, after water removal (when the cathode operates under water flow) by techniques such as Gas Chromatography (GC), Mass Spectrometry (MS), Thermal Conductivity (TC) detector, or Galvanic Electrochemical Cell. The time interval between measurements is determined by the selected technique and the response characteristics of the method used. For research and characterization purposes, the composition of the hydrogen stream should be checked at least every 30 minutes.

Hydrogen purity levels not achievable directly by electrolysis can be increased by additional purification step(s). The main purification technologies available are Pressure Swing Absorption (PSA), cryogenic condensation, getter/palladium membrane adsorption.

The required hydrogen purity for commercial electrolyser systems depends on its subsequent use. For example, for use in fuel cells, hydrogen purity should comply with the Fuel Quality Standards ISO 14687-2:2012 for fuel cell automotive applications and ISO 14687-3:2014 for fuel cell stationary applications. For all other industrial applications, the hydrogen purity level achieved by the electrolysis cell / stack should be mentioned.

In the absence of a real-time quality control system, for safety reason it is recommended to monitor the presence of oxygen in the hydrogen outlet stream using a safety sensor to ensure that the oxygen concentration does not drop below the Upper Explosion Limit (UEL) of hydrogen in a hydrogen-oxygen gas mixture. UEL increases with temperature and changes non-linearly with pressure as shown in Table 11. In practice, when the detected oxygen concentration exceeds 50% of the (100-UEL)% difference appropriate safety measures should be triggered.

ii. Hydrogen production rate

The hydrogen production rate is a direct consequence of the current applied with some loss depending by the overall system efficiency. With 100% faradaic efficiency the hydrogen production rate is:

$$\dot{n}_{h2,out} = \frac{I}{2F} = \dot{n}_{h2O,reacted} \qquad \text{[eq. 5.7]}$$

5.1.5 SETTINGS of TIPS for PEMWE REFERENCE OPERATING CONDITIONS

The settings of the TIPs for the Reference Operating Conditions ("reference settings") for PEM Water Electrolysis for single cell and short stack are agreed as:

Table 12. Agreed reference settings for TIPs for PEMWE single cell and short stack testing

	Test Input Parameters	Unit	Reference Settings
Cell/short stack	Cell / Stack temperature	°C	60
	Water quality (conductivity) at recirculation loop *inlet*	$\mu S \cdot cm^{-1}$	≤1.0 ISO 3696 Grade 2 @ 25 ^{0}C
ANODE	Water inlet temperature	°C	60
	Water inlet pressure (absolute)	kPa	100
	Water quality (conductivity) *within recirculation loop*	$\mu S \cdot cm^{-1}$	≤1.0 ISO 3696 Grade 2 @ 25 ^{0}C
	Minimum Water inlet flowrate	$ml \cdot min^{-1} \cdot cm^{-2}$	2.0
	Oxygen outlet pressure (absolute)	kPa	100
CATHODE	Water inlet temperature	°C	60
	Minimum Water inlet flowrate (if applied)	$ml \cdot min^{-1} \cdot cm^{-2}$	2.0
	Hydrogen outlet pressure (abs)	kPa	100

5.1.6. TEST HARDWARE CONFIGURATION AND REQUIREMENTS FOR MEASUREMENT DEVICES OF TIPS AND TOPS for PEMWE CELL/STACK TESTING

To enable accurate control of the experimental conditions during cell and stack testing, the characteristics and location of the required instrumentation should be carefully considered. A general overall hardware configuration with location of TIPs and TOPs to be measured is schematically shown in

Figure 13.

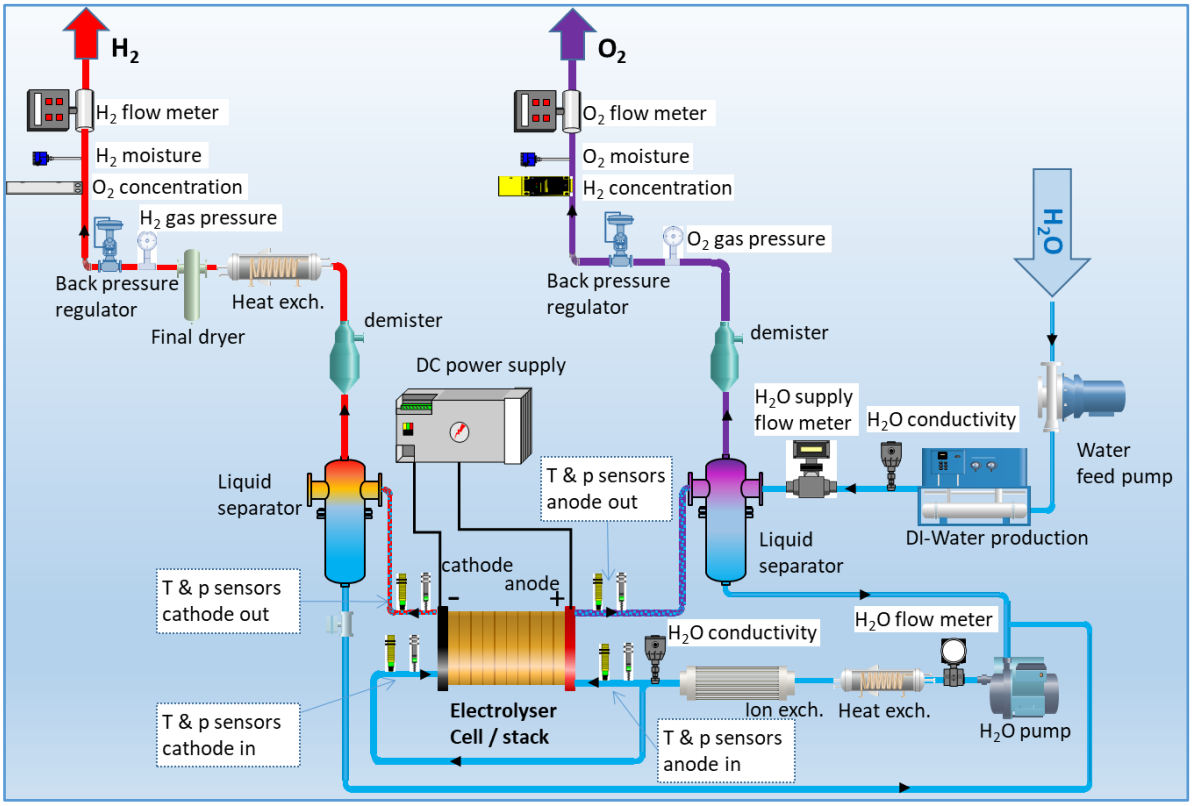

Figure 13: Scheme of PEM single cell/stack testing apparatus including position of the monitoring devices

Table 13 summarises the location of sensors or measuring devices (as in the figure above).

Table 13. Sensor type/location for PEMWE cell/stack testing

INPUT / OUTPUT PARAMETER	TIP/TOP	POSITION OF SENSORS
Current (or current density)	TIP	Power supply module
Cell/Stack voltage	TOP	Cell Hardware, Current collectors, Voltage terminals
Temperatures		
Cell	TIP	anode (TIP), and cathode BPPs, as close as possible to MEA
Water, anode inlet	TIP	as close as possible to cell/stack hardware inlet
Water, anode outlet	TOP	as close as possible to cell/stack hardware outlet
Water, cathode inlet (optional)	TIP	as close as possible to cell/stack hardware inlet
Water, cathode outlet (optional)	TOP	as close as possible to cell/stack hardware outlet
Pressures		
Water, anode inlet	TIP	as close as possible to cell/stack hardware inlet
Water, anode outlet	TOP	as close as possible to cell/stack hardware outlet
Water, cathode inlet (optional)	TIP	as close as possible to cell/stack hardware inlet, if in use
Water, cathode outlet (optional)	TOP	as close as possible to cell/stack hardware outlet
H_2, outlet	TIP	after liquid and vapour separation
O_2, outlet	TIP	after liquid and vapour separation
Flow rates		
Water feed to cell/stack	TIP	deionised water (DIW) cell inlet
Water make-up	TOP	outlet deionised water (DIW) production
Hydrogen	TOP	after water knockout
Oxygen	TOP	after water knockout
Water quality		
Water conductivity	TIP	outlet DIW production & recirculation loop
Gas safety sensors		
Hydrogen concentration	TOP	H_2 gas sensor in O_2 outlet
Oxygen concentration	TOP	O_2 gas sensor in H_2 outlet

The type of measurement devices for the TIPs and TOPs should be selected based on the required range, accuracy, and sampling rate as indicated in Table 14. Measuring equipment should be regularly calibrated.

Table 14. Required measurement accuracy and sampling rate

Parameter to be measured	Unit	Required Measurement accuracy	Sampling rate Performance test	Sampling rate Durability test
Current	A	0.001A	≥1 Hz	≥0,0166 Hz
Temperature	°C	± 2 K	≥1 Hz	≥0,0166 Hz
voltage	*V*	± 0.5%[5]	≥1 Hz	≥0,0166 Hz
Pressure	kPa	± 2%	≥1 Hz	≥0,0166 Hz
Water Flow rate	$l \cdot min^{-1}$	± 2%	≥1 Hz	≥0,0166 Hz
Gas Flow rate	$l \cdot min^{-1}$	± 2%	≥1 Hz	≥0,0166 Hz
Gas concentration	%	± 1%	≥1 Hz	≥0,0166 Hz

For the generation of valid results from in-situ tests the following conditions have to be met during the full test duration:

- As a minimum all the TIPs and TOPs listed in Table 13 shall be measured
- The measurement accuracy and sampling rate shall meet the specifications listed in Table 14
- The temperature difference between water outlet and water inlet shall not exceed +/- 2K.
- Any deviation from the suggested hardware configuration and/or from the location of measuring devices shall be reported

The incorporation of additional temperature sensors at appropriate locations in the test rig layout of Figure 13 can provide supplementary information on performance in terms of efficiency of the cell/short stack (see chapter 7). Next to depending on the functional performance of its components and of the cell/short stack itself, efficiency may be affected e.g. by recuperating heat by the introduction of exchangers at different locations, as shown in Figure 13).

5.2 REFERENCE OPERATING CONDITIONS for AWE CELL/SHORT STACK TESTING

This subsection discusses TIPs and TOPs for in-situ testing of alkaline water electrolysis single cells and short stacks. Where possible and relevant, it refers back to those for PEMWE, while differences with PEMWE are elaborated specifically.

5.2.1 CELL TEMPERATURE (TIP)

Depending on test bench configuration, a number of cases can be differentiated for the location of the temperature sensor:

i. Temperature sensor located close to the electrodes:
   - The cell temperature is that indicated by the sensor in the anode side.

ii. Temperature sensor located in the electrolyte circuit:
   - The cell temperature is equal to the average temperature of the electrolyte measured at anode and cathode inlets.

For the second case, the uniformity of the electrolyte temperature between inlet and outlet of the cell is important and the temperature difference between outlet and inlet should be minimised.

5.2.2 Water Quality (TIP)

Considering the high alkalinity of the electrolyte it is important to reduce impurities in the replenishing water by a demineralisation treatment (or possibly de-ionization for higher purity levels) to minimize the concentration of magnesium and calcium in the feed water to avoid precipitation of their hydroxides, which may cause a performance reduction over time. The solvation of CO2 (from the ambient air) should also be minimized. Requirements at system level are given by the manufacturer (e.g. concentration for Ca/Mg/Fe, Cl^-, CO_3^{2-}, SO_4^{2-}, Si, etc.); for laboratory testing de-ionised water with 1μS·cm^{-1} conductivity has been agreed as the reference to be used.

5.2.3 Electrolyte TIPs

The circulation of the electrolyte can be implemented in two different ways, (i) mixed circuit and (ii) separated circuit:

i- mixed circuit: after separation of product gas from the electrolyte exiting each semi-cell, both electrolyte streams are mixed and the concentration is adjusted by water replenishment. As both electrolyte streams still contain remaining product gases soluble in the electrolyte solution, their mixing causes losses and higher gas impurities.

ii- separated circuit: the electrolyte streams are kept separated. Water formation on the anode side results in a decreased concentration, while water consumption on the cathode side increases the concentration. Occasional mixing of the two electrolyte streams is needed to re-establish the optimal concentration.

The TIPs below relate to the presence of an aqueous alkaline solution acting as liquid electrolyte and contributing to heat management.

i. Inlet temperature

The electrolyte temperature at anode inlet serves as TIP when the cell temperature cannot be measured in the bipolar plate. The temperature in this case should be measured as close as possible at the inlet of the cell/stack.

ii. inlet pressure

Typically test benches have controlled back pressure valves positioned in the exhaust gas stream close to the cell outlet. Therefore, the pressure regulation is normally performed at cell outlet. Alkaline electrolysers are operated with the same pressure (balanced pressure) on both compartments, or with a small differential pressure to limit cross-permeation of the electrolyte with its dissolved gases through the porous separator.

iii. inlet concentration

The concentration of the aqueous solution electrolyte is measured at the inlet of the cell and adjusted to the set value with fresh demineralised water replenishment to maintain the correct specific conductivity of the electrolyte. Examples of the specific conductivity change with electrolyte concentration for NaOH and KOH are given in **Error! Reference source not found.**. The ionic conductivity increases with electrolyte concentration up to a value beyond which interactions by Coulombic force interactions between ions result in a reduction of the conductivity.

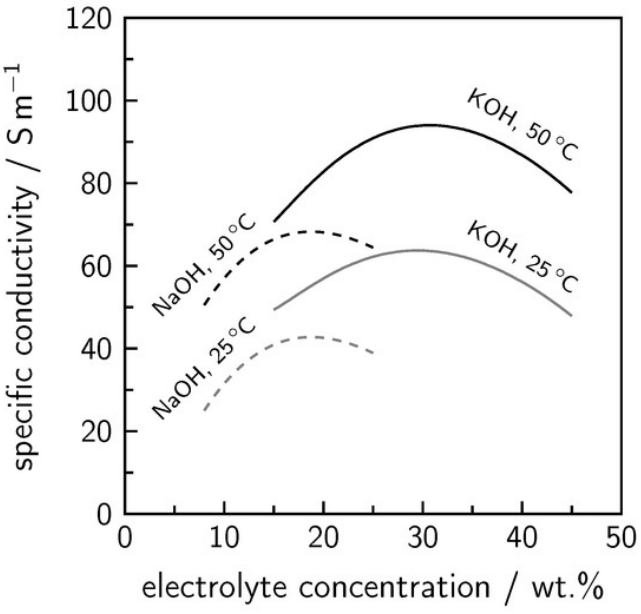

Figure 14. calculated specific electrolyte conductivity as a function of the electrolyte concentrations and temperature

 Processes 2020, 8(2), 248; https://doi.org/10.3390/pr8020248

iv. inlet Flow rate

Electrolyte flow operation can be done without pump aid through natural convection. The associated savings of the reduced BOPs are counterbalanced by the risk of increasing the gas coverage of electrodes, hence requiring a higher operation cell voltage. Nevertheless, for optimal process control the electrolyte is constantly pumped through the cell to maintain the electrolysis reaction and contribute to heat management. The circulation flowrate is hence set to minimise both the concentration difference and the temperature difference between inlet and outlet.

5.2.4 ANODE CONDITIONS

i. Oxygen outlet pressure *(TIP)*

In pressure balanced operation mode, the oxygen outlet pressure equals the hydrogen outlet pressure TIP. High outlet pressures increase the concentration of H2 in O2 at anode outlet and O2 in H2 at and cathode outlet and thereby the risk of explosion, as shown in Figure 15 for the anode side.

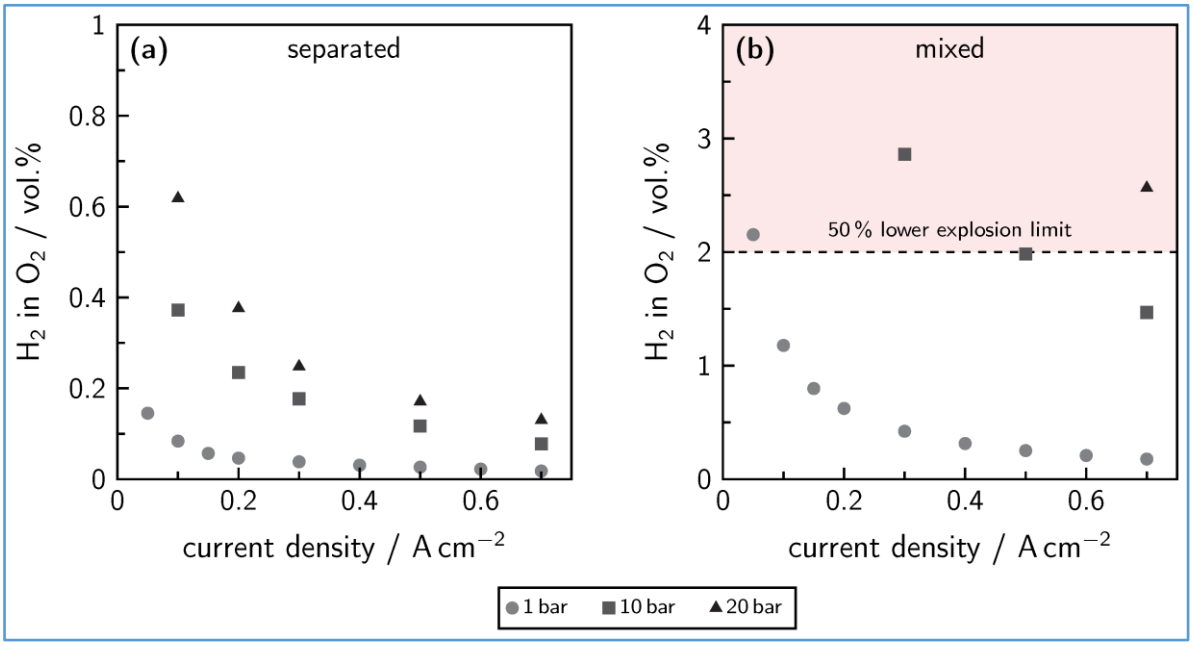

Figure 15 Anodic gas impurity (H2 in O2) in relation to current density at different pressure levels for (a) separated and (b) mixed electrolyte cycles

 Processes 2020, 8(2), 248; https://doi.org/10.3390/pr8020248

i. Oxygen Quality *(TOP)*

The typical oxygen purity is in the range 99.0 to 99.5% Vol. The most relevant impurity is hydrogen crossing the separator. The gas crossover is mainly due to gas dissolution in the electrolyte and diffusion through the separator, and hence depends on pressure, current density and electrolyte circulation configuration, either with separate or mixed cycle. With increasing pressure more hydrogen is dissolved in the electrolyte and therefore more hydrogen can reach the other semi-cell. Increasing current density results in higher hydrogen generation, and considering that current does not affect the amount of gas crossing the separator, higher dilution of the crossing hydrogen. Operation with mixed electrolyte circulation increases the level of contamination.

An example of hydrogen concentration in the oxygen outlet stream by changing pressure, current and electrolyte flow segregation is given in Figure 15 for a 32% concentrated electrolyte at 60°C and 0.35 $L \cdot min^{-1}$ flow rate.

ii. oxygen production rate *(TOP)*

See 5.1.3

iii. electrolyte concentration at anode outlet *(TOP)*

The concentration difference between electrolyte outlet and inlet serves as a test validity criterion and should not exceed +/- 5wt% (see table 15).

iv. electrolyte temperature at anode outlet *(TOP)*

The temperature difference between electrolyte outlet and inlet serves as a test validity criterion and should not exceed +/- 2K (see table 15).

5.2.5 CATHODE CONDITIONS

The related TIPs are identical to those for the anode electrolyte inlet (temperature, quality, pressure) discussed before. An additional TIP at cathode side is

i. Hydrogen outlet pressure *(TIP)*

see 5.2.4 i

TOPs at cathode side are:

ii. Hydrogen quality *(TOP)*

See 5.1.4

iii. hydrogen production rate *(TOP)*

see 5.1.4

5.2.6. SETTINGS of TIPS for AWE REFERENCE OPERATING CONDITIONS

The settings of the TIPs for the Reference Operating Conditions ("reference settings") for alkaline water electrolysis for single cell and short stack are agreed as:

Table 15. Agreed reference settings for TIPs for AWE single cell and short stack testing

	Test input parameters	Unit	Reference Settings
cell / short stack	Cell / stack temperature	°C	65
	conductivity of water used for electrolyte preparation and supply to electrolyser	$\mu S \cdot cm^{-1}$	≤1, ISO 3696 Grade 2 @ 25 °C
ANODE	electrolyte inlet temperature	°C	65
	electrolyte inlet pressure	kPa	100
	electrolyte inlet concentration	wt.%	30
	Min. electrolyte inlet flow rate	$ml \cdot cm^{-2} \cdot min^{-1}$	1
	Oxygen outlet pressure (absolute)	kPa	100
CATHODE	electrolyte inlet temperature	°C	65
	electrolyte inlet pressure	kPa	100
	electrolyte inlet concentration	wt.%	30
	Min. electrolyte inlet flow rate	$ml \cdot cm^{-2} \cdot min^{-1}$	1
	Hydrogen outlet pressure (absolute)	kPa	100

5.2.7 TEST HARDWARE CONFIGURATION AND REQUIREMENTS FOR MEASUREMENT DEVICES OF TIPS AND TOPS

Figure 16 shows a scheme with the location of the instrument measuring points for an alkaline water electrolysis experimental set-up.

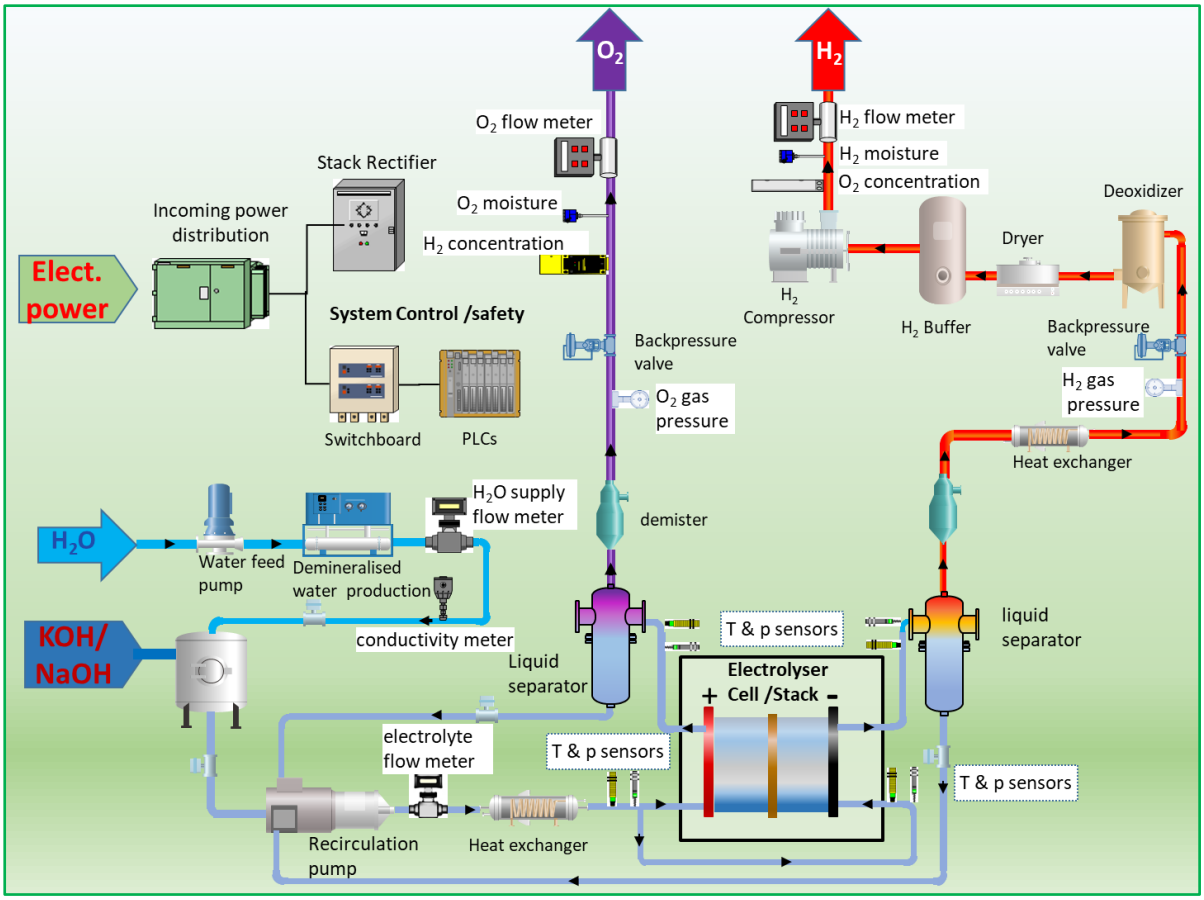

Figure 16. Scheme of AW Electrolyser with the position of monitoring devices

Table 16 summarises the location of sensors or measuring devices (as in the figure above).

The incorporation of additional temperature sensors at appropriate locations in the test rig layout of Figure 16 can provide supplementary information on performance in terms of efficiency of the cell/short stack (see chapter 7). Next to depending on the functional performance of its components and of the cell/short stack itself, efficiency may be affected e.g. by recuperating heat by the introduction of exchangers at different locations, as shown in Figure 16).

Table 16. Sensor type/location for AWE cell/stack testing

INPUT / OUTPUT PARAMETER	TIP/TOP	LOCATION OF SENSOR
Current (or current density)	TIP	Power supply module
Cell/Stack voltage	TOP	Cell Hardware, Current collectors, Voltage terminals
Temperatures		
Cell Temperature	TIP	Close to electrodes, TIP uses anode as reference
Anode inlet	TIP	as close as possible to cell/stack hardware inlet
Anode outlet	TOP	as close as possible to cell/stack hardware outlet
Cathode inlet	TIP	as close as possible to cell/stack hardware inlet
Cathode outlet	TOP	as close as possible to cell/stack hardware outlet
Pressures		
Electrolyte Anode inlet	TIP	as close as possible to cell/stack hardware inlet
Electrolyte Anode outlet	TOP	as close as possible to cell/stack hardware outlet
Electrolyte Cathode inlet	TIP	as close as possible to cell/stack hardware inlet
Electrolyte Cathode outlet	TOP	as close as possible to cell/stack hardware outlet
H_2 outlet	TIP	after liquid and vapour separation
O_2 outlet	TIP	after liquid and vapour separation
Flow rates		
electrolyte recirculation	TIP	recirculation loop
Water make-up	TOP	outlet demineralised/DI water production
Hydrogen	TOP	Mass Flow Meter after water knockout
Oxygen	TOP	Mass Flow Meter after water knockout
Water quality		
Water conductivity	TIP	outlet demineralised/DI production & recirculation loop
Gas safety sensor		
Hydrogen concentration	TOP	H_2 gas sensor in O_2 outlet
Oxygen concentration	TOP	O_2 gas sensor in H_2 outlet

For the generation of valid results from in-situ tests the following conditions have to be met during the full test duration:

- As a minimum all the TIPs and TOPs listed in Table 15 shall be measured
- The measurement accuracy and sampling rate shall meet the specifications listed in Table 14

- The temperature difference between electrolyte outlet and electrolyte inlet shall not exceed +/- 2K.
- The concentration difference between electrolyte outlet and electrolyte inlet shall not exceed +/- 5 wt%.
- Any deviation from the suggested hardware configuration and/or from the location of measuring devices shall be reported

5.3 AEMWE REFERENCE OPERATING CONDITIONS

Because of the similarity between PEMWE and AEMWE, the same set of Reference Operating Conditions as those for PEMWE can be used for AEMWE for both single cells and short stacks.

5.3.1 CELL TEMPERATURE

See 5.1.1

5.3.2 WATER QUALITY

See 5.1.2

5.3.3 ANODE OPERATING CONDITIONS

See 5.1.3

5.3.4 CATHODE OPERATING CONDITIONS

See 5.1.4

5.3.5 SETTINGS of TIPS for AEMWE REFERENCE OPERATING CONDITIONS

The settings of the TIPs for the Reference Operating Conditions ("reference settings") for Anion Exchange Membrane Water Electrolysis for single cell and short stack are agreed as shown in Table 17.

For further testing in alkaline environment it is possible to replace water as electrolyte using a KOH solution with molarity equal to 0.2M or 1 M.

Table 17: agreed reference settings for TIPs for AEMWE single cell and short stack testing

	Test Input Parameters	Unit	Reference Settings
Cell/short stack	cell / stack temperature	°C	50
	Water quality (conductivity) at recirculation loop ***inlet***	$\mu S \cdot cm^{-1}$	≤1.0 ISO 3696 Grade 2 @ 25 ^{0}C
ANODE	water inlet temperature	°C	50
	water inlet pressure (absolute)	kPa	100
	Water quality (conductivity) ***within recirculation loop***	$\mu S \cdot cm^{-1}$	<1.0 ISO 3696 Grade 2 @ 25 ^{0}C
	Minimum Water inlet flowrate	$ml.min^{-1}.cm^{-2}$	1
	Oxygen outlet pressure	kPa	100
CATHODE	**water inlet temperature**	**°C**	**50**
	water inlet pressure (absolute)	**kPa**	**100**
	Water quality	**µS·cm-1**	**<1.0** ISO 3696 Grade 2 @ 25 ^{0}C
	Minimum Water inlet flowrate	$ml.min^{-1}.cm^{-2}$	1.0
	Hydrogen outlet pressure (abs)	kPa	100

5.3.6 TEST HARDWARE CONFIGURATION AND REQUIREMENTS FOR MEASUREMENT DEVICES OF TIPS AND TOPS

Figure 17 shows a scheme with the location of the instrument measuring points for an AEM water electrolysis experimental set-up.

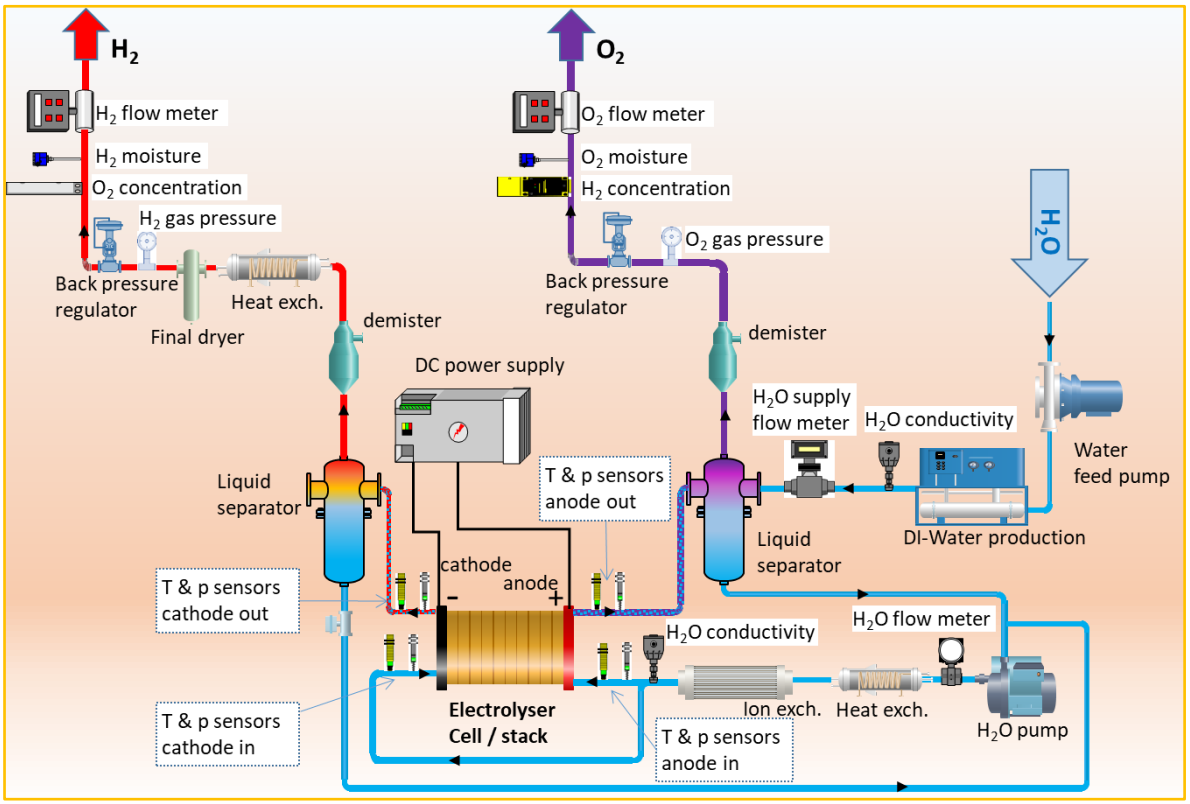

Figure 17. Scheme of AEMW electrolyser with the position of monitoring devices

For the generation of valid results from in-situ tests the following conditions have to be met during the full test duration:

- Considering the similarity with PEMWE the minimum set of TIPs and TOPs listed in Table 13 shall be measured
- The measurement accuracy and sampling rate shall meet the specifications listed in Table 14
- The temperature difference between water outlet and water inlet shall not exceed +/- 2K.
- Any deviation from the suggested hardware configuration and/or from the location of measuring devices shall be reported

The incorporation of additional temperature sensors at appropriate locations in the test rig layout of Figure 17 can provide supplementary information on performance in terms of efficiency of the cell/short stack (see chapter 7). Next to depending on the functional performance of its components and of the cell/short stack itself, efficiency may be affected e.g. by recuperating heat by the introduction of exchangers at different locations, as shown in Figure 17).

6 STRESSOR CONDITIONS FOR SINGLE CELL AND SHORT STACK TESTING

6.1 Approach

In this chapter a methodology is established for examining the relative influence that TIPs deviating from the reference operating conditions (chapter 5) exert on the performance and durability of single cells and short stacks. The methodology is also applied to investigate the effect of a number of other factors which may cause deviation from normal operation. The factors causing such deviation are hereafter called "stressors".

Investigating the effect of the identified stressors on cell and stack performance and durability, requires a systematic approach that consists of two consecutive stages. First the relevant types of stressors affecting behaviour at cell and stack level are identified (section 6.2). Following this identification of relevant stressor types, the second element in the systematic approach to investigate how cells and stacks behave under the identified stressor conditions, consists of quantifying the effects of the considered stressors on cell and short stack performance and durability, by performing in-situ tests. In these tests, different settings from those corresponding to the reference operation conditions are used for the TIPs identified in chapter 5.

6.2 TYPES of STRESSORS for SINGLE CELLS AND SHORT STACKS

Table 18 identifies the types of stressors which are briefly discussed below. The first two stressor types are extensively covered in the following parts of this report, whereas the other four are not further considered.

Table 18: CATEGORIES OF STRESSORS

1	**STRESSORS DUE TO OPERATING CONDITIONS**
2	**STRESSORS DUE TO LOAD CYCLING**
3	**STRESSORS DUE TO MECHANICAL EFFECTS**
4	**STRESSORS DUE TO SEAL LEAKAGE**
5	**STRESSORS DUE TO WATER QUALITY**
6	**STRESSORS DUE TO ENVIRONMENTAL CONDITIONS**

6.2.1 Stressors due to operating conditions

These cover both higher and lower settings of the TIPs considered in chapter 5. Because different TIPs apply for the three considered low-temperature electrolysis technologies,

different sets of operational stressor conditions are used for each technology in sections 6.4 to 6.6 below.

6.2.2 Load cycling

Load cycling is applied in cell and stack testing to simulate the variable operating conditions, including transients associated to start-up and stop sequences that electrolyser systems experience in practice and which affect performance and durability. Durability is evaluated through endurance testing by applying a repetitive load profile and measuring performance degradation rate in terms of voltage increase rate as function of operating hours (see chapter 7). To assess degradation rate a representative dynamic load profile is required. Such load profiles are derived from the Real World Degradation (RWD) profiles that represent a simplification of the load profiles that electrolyser systems are expected to encounter in a number of service applications.

6.2.3 Mechanical stressors

These include a.o. the compression force applied to the cell (in single cell or short stack configuration), which is however fixed at the beginning of the test and not expected to change during in-situ testing; hence it will not be further considered in this report. Mechanical effects may also arise from variations in environmental conditions (pressure, temperature) as well as from acceleration and deceleration forces. Because these variations rather affect the performance and durability at system than at cell and short stack level, they are not considered here. Other mechanical stressors are vibrations induced by Balance of Plant (BoP) components like pumps, PSA, compressors, etc. These effects are also not considered in this document.

6.2.4 Seal leakage

Leakage of seals can cause mechanical degradation of gaskets, particularly in the presence of pressure cycling, which may result in gas leakage. This represents more a safety than a performance issue and is therefore not covered in this report. However, the occurrence of possible leakages should be monitored using a leak test apparatus.

6.2.5 Water quality

The tolerance of cells/stacks to water impurity level is an important factor. However, because of experimental difficulties/limitations to actively control water impurity level (decrease and/or increase of contaminants) in most test bench hardwares, this stressor is considered in this report as optional, when feasible. A commonly used method for characterising water quality is through electrical conductivity measurement which reflects the total amount of ions present, but does not allow differentiating between chemical species. When relevant for the experimental campaign, ion selective sensors (i.e. fluoride, magnesium, calcium, etc.) can be added in the circulation loop for continuous monitoring, or water can be sampled and analysed with other type of chemical analysis for ad hoc monitoring.

6.2.6 Environmental conditions

Environmental conditions are mostly relevant at system level, such as cold start and freeze when the system is exposed to sub-zero temperatures. For single cell and stack applications this stressor is not applicable and is not addressed in this document.

6.3 OPERATING CONDITION STRESSORS for SINGLE CELL AND SHORT STACK TESTING

The reference settings for the TIPs identified in chapter 5 in principle correspond to the centre of the normal operation window. Stressors due to operating conditions relate to operation of the cell or stack at TIP settings falling outside of this operation window.

In principle in-situ tests under operation stressor conditions should enable to determine the effects of stressors associated to a specific TIP separately from the effect caused by other stressors. However, because performance in in-situ tests depends on a number of factors, and is therefore affected by a number of TIPs, such discrimination between the effects of the considered operation stressors may not be possible. For that reason, and for limiting the test effort, operation stressors are identified for a reduced number of TIPs than those considered in chapter 5, by selecting the ones that are more sensitive to process variation and that are adjustable within the majority of laboratory test benches, and for each of these stressors two settings are presented, resp. one higher and one lower than the reference setting.

For each operation stressor, the expected effect of increase or of decrease of its setting compared to the reference settings agreed in chapter 5 is discussed.

Because similarly to the reference settings identified in chapter 5, settings for operating condition stressors differ for the different electrolysis technologies, Effects of operation stressors specific for each technology are discussed separately.

6.4 EFFECTS of OPERATION STRESSORS for PEMWE

6.4.1. PEMWE ANODE STRESSORS

i. CELL TEMPERATURE STRESSOR – WATER TEMPERATURE STRESSOR

Higher operating temperatures generally have a positive effect on performance due to increased reaction kinetics corresponding to higher current densities at the same operating voltage or higher hydrogen production rate at the same efficiency.

Lower operating temperatures generally have a negative effect on performance but may result in a lower degradation rate, provided that the cell/stack is not operated above nominal voltage to compensate for lower reaction kinetics to maintain the hydrogen production rate.

ii. WATER QUALITY STRESSOR

Water quality can have an important immediate or short-term effect (in minutes to hour scale) on performance e.g. through poisoning the electrolyte and/or the electrodes, or by catalysing the formation of products causing membrane degradation. The sensitivity of performance to water quality is usually expressed in terms of increase in ohmic resistance and electrode overpotential.

iii. WATER INLET FLOW RATE STRESSOR

Too low water inlet flowrate may result in insufficient wetting, with risk of creating dry active area hot spots. It may also decrease the removal rate of gas bubbles from the membrane surface, resulting in hotspots or increased overpotential.

When the water inlet flowrate is too high, the increased speed and pressure can accelerate catalyst loss due to dissolution/erosion effects.

iv. OXYGEN OUTLET PRESSURE STRESSOR

Oxygen outlet pressure stressor tests are not considered in this document because of safety considerations.

v. WATER INLET PRESSURE STRESSOR

Water pressure could be relevant for temperature near or above 100 °C due to the effect on the two-phase liquid water/vapour ratio. As the stressor test conditions Table 19 are limited to 80°C, this stressor is not considered.

6.4.2 PEMWE CATHODE STRESSORS

i. WATER TEMPERATURE STRESSOR

When water circulation is implemented at the cathode side, water temperature is assumed to be the same of the anode one.

ii. HYDROGEN OUTLET PRESSURE STRESSOR

Hydrogen pressure affects both hydrogen cross-over and leakage to the exterior and is affected by the electrolyser operation mode, balanced (same pressure applied at anode and cathode side) or differential (different pressure in the two compartments creating additional mechanical stress on the MEA).

From the thermodynamic point of view, increasing hydrogen pressure is expected to increase the cell voltage. Experimental data shows that this effect is not so evident, likely due to the beneficial effect of pressure increase on kinetic and mass transport overpotentials. The kinetic effect may result from improved water circulation into the porous structure of the catalyst layer, while a reduction of vapour contribution in the two-phase flow, reduced viscosity and surface tension for liquid phase may benefit the mass transport

6.4.3 SETTINGS of OPERATION STRESSORS for PEMWE

Table 19 shows the agreed reference, low and high settings for operation stressors for PEMWE single cells and short stacks. As indicated in the table, a total number of 7 tests is proposed for comparing the effect of operation stressors on the performance of PEMWE cells and short stacks with the performance obtained under reference operating conditions..

Table 19. SETTINGS of OPERATION STRESSORS FOR PEMWE SINGLE CELL AND SHORT STACK TESTING

	Parameters	Unit	REFERENCE Setting	Cell Temperature Stressor settings		Hydrogen Pressure Stressor settings	Water quality (conductivity) at the *recirculation loop Stressor setting*		Water inlet flowrate cell/stack (with recirculation) stressor setting	
				Test 1	Test 2	Test 3	Test 4	Test 5	Test 6	Test 7
	Cell / stack temperature	°C	60	40	80	60	60	60	60	60
ANODE	Water inlet temperature	°C	60	40	80	60	60	60	60	60
ANODE	Water quality (conductivity) at the *recirculation loop*[9]	$\mu S \cdot cm^{-1}$	≤1.0	≤1.0	≤1.0	≤1.0	≤0.1	≤5.0	≤1.0	≤1.0
ANODE	Water inlet min. flowrate cell/stack (with recirculation)	$ml.min^{-1} \cdot cm^{-2}$	2.0	2.0	2.0	2.0	2.0	2.0	0.5	2.5
CATHODE	Water inlet temperature	°C	60	40	80	60	60	60	60	60
CATHODE	Hydrogen outlet pressure (absolute)	kPa	100	100	100	3000[10]	100	100	100	100

[9] Optional test to be done only if feasible with test bench

[10] In case of equipment/safety limitation an intermediate pressure step, of 500 kPa should be added as an additional testing point.

6.5 EFFECTS of OPERATION STRESSORS for AWE

For in-situ testing of AWE cells and short stacks, the effects of the operation stressors at anode and cathode are qualitatively similar to those considered for PEMWE.

6.5.1 AWE ANODE STRESSORS

i. CELL TEMPERATURE STRESSOR - ELECTROLYTE TEMPERATURE STRESSOR

For AWE the temperature has a direct effect on the electrolyte conductivity as shown in Figure 14. The higher the temperature the lower is the viscosity, which increases ion mobility and hence conductivity. This conductivity increase at higher temperature has a positive effect on performance because ohmic overvoltage is reduced. In addition, higher operating temperature generally positively affects performance due to increased reaction kinetics.

A negative effect of higher temperature could be on the durability of components in contact with the caustic environment.

ii. WATER QUALITY STRESSOR

Water quality can have an important immediate or short-term effect (in minutes to hour scale) on performance, e.g. through poisoning the electrolyte and/or the electrodes. As previously mentioned, presence of magnesium and calcium cations forming low soluble hydroxides may affect electrolyte performance.

iii. ELECTROLYTE INLET FLOW RATE STRESSOR

Electrolyte inlet flow rate has an important effect on the thermal balance of the electrolysis cell. Additionally, through its effect on gas bubble formation, it affects cell ohmic resistance through two mechanisms: (i) the barrier effect on the electrode surface and (ii) the void fraction in the electrolyte. Higher flowrate has in general a positive effect because it facilitates the removal of bubbles from reacting surfaces and from the electrolyte solution. The inlet flow rate also affects the concentration of the electrolyte at electrolyser output, with higher flowrate resulting in smaller concentration difference.

A negative effect of higher electrolyte inlet flowrate can arise from increased erosion that can contribute to reducing cell durability. A higher inlet flow rate also increases power need, reducing overall efficiency.

iv. OXYGEN OUTLET PRESSURE STRESSOR

Oxygen outlet pressure stressor tests are not considered in this document because of safety considerations.

6.5.2 AWE CATHODE STRESSORS

HYDROGEN OUTLET PRESSURE STRESSOR

Hydrogen pressure affects both hydrogen cross-over and leakage to the exterior.

6.5.3 SETTINGS of OPERATION STRESSORS for AWE

Table 19 shows the agreed reference, low and high settings for operation stressors for AWE single cells and short stacks. As indicated in the table, a total number of 5 tests is proposed for comparing the effect of operation stressors on the performance of AWE cells and short stacks with the performance obtained under reference operating conditions.

Electrolyte concentration is not included in the set of operation stressors because of experimental difficulty associated to varying it in a well-controlled manner, as also applies for the operational stressor on water feed quality.

Table 20. SETTINGS of AWE STRESSORS FOR AWE SINGLE CELL AND SHORT STACK TESTING

	PARAMETERS	UNIT	REFERENCE Setting	Cell Temperature Stressor settings		H2 Pressure Stressor settings	Electrolyte Inlet Flowrate Stressor settings	
				Test 1	Test 2	Test 3	Test 4	Test 5
	Cell/stack temperature	°C	65	30	90	65	65	65
ANODE	electrolyte inlet temperature	°C	65	30	90	60	60	60
ANODE	electrolyte inlet flowrate	$ml \cdot cm^{-2} \cdot min^{-1}$	1	1	1	1	0.25	2
CATHODE	electrolyte inlet temperature	°C	65	30	90	60	60	60
CATHODE	electrolyte inlet flowrate	$ml \cdot cm^{-2} \cdot min^{-1}$	1	1	1	1	0.25	2
CATHODE	Hydrogen outlet pressure	kPa	100	100	100	3000	100	100

6.6 EFFECTS of OPERATION STRESSORS for AEMWE

For in-situ testing of AEMWE cells and short stacks, the effects of the identified operation stressors are qualitatively similar to those considered for PEMWE, but considering the different role of anode and cathode.

6.6.1 SETTINGS of OPERATION STRESSORS for PEMWE

Table 21 shows the agreed reference, low and high settings for operation stressors for AEMWE single cells and short stacks. As indicated in the table, a total number of 7 tests is proposed for comparing the effect of operation stressors on the performance of AEMWE cells and stacks with the performance obtained under reference operating conditions.

Table 21. SETTINGS of STRESSORS FOR AEMWE SINGLE CELL AND SHORT STACK TESTING

	Parameters	Unit	REFERENCE setting	Cell Temperature Stressor settings		Hydrogen Pressure Stressor settings	Water quality (conductivity) at the *recirculation loop* *Stressor setting*		Water inlet flowrate cell/stack (with recirculation) stressor setting	
				Test 1	Test 2	Test 3	Test 4	Test 5	Test 6	Test 7
	cell/stack temperature	°C	50	30	80	50	50	50	50	50
ANODE	Water inlet temperature	°C	50	30	80	50	50	50	50	50
ANODE	Water inlet flowrate (with recirculation)	$ml.min^{-1}.cm^{-2}$	1	1	1	1	1	1	0.5	1.5
CATHODE	Water inlet temperature	°C	50	30	80	50	50	50	50	50
CATHODE	Water quality (conductivity) at the *recirculation loop*[11]	$\mu S \cdot cm^{-1}$	<1	<1	<1	<1	<0.1	<5	<1	<1
CATHODE	Water inlet flowrate (with recirculation)	$ml.min^{-1}.cm^{-2}$	1	1	1	1	1	1	0.5	1.5
CATHODE	Hydrogen outlet pressure (absolute)	kPa	100	100	100	3000[12]	100	100	100	100

[11] Optional test to be done only if feasible with test bench

[12] In case of equipment/safety limitation an intermediate pressure step, of 500 kPa should be added as an additional testing point

7 IN-SITU TESTING OF SINGLE CELLS AND SHORT STACKS

Testing of single cells and short stacks aims at characterising the performance and the durability of their constituent materials and components under experimental conditions that can provide relevant information about their behaviour when incorporated in electrolyser systems. As introduced in chapter 4, such testing requires covering experimental conditions which simulate operation under reference conditions (chapter 5) as well as under stressor conditions (chapter 6), covering both static and dynamic loading conditions (chapter 7). Results of these tests provide information on the performance of the cells and short stacks at a given moment in time.

Durability is a measure of the capability of a single cell/short stack to maintain its performance over a period of time. The measured performance is usually compared that established at BoT.

The sections in this chapter sequentially discuss aspects pertaining to both characteristics, performance and durability.

7.1 PERFORMANCE INDICATORS

The performance indicators for tests under Reference Operating Conditions and Stressor Conditions are presented in Table 22 for the three different low temperature water electrolysis technologies.

Table 22. LTWE Performance indicators

	indicator	
1	**Cell/short stack voltage V measured at current densities j**	• **PEMWE: 1.0 A/cm², 2.0 A/cm², and when feasible, j= 3.0 A/cm² and 6.0 A/cm²** • **AEW: 0.4 A/cm², 0.8 A/cm², 1.0 A/cm²** • **AEMWE: 0.4 A/cm², 0.8 A/cm², 1.0 A/cm²**
2	**Energy efficiency ε at covered current densities j**	• **Eq. 7.2 cell;** • **Eq. 7.3 stack**
3	**Current efficiency η_I at covered current densities j**	• **Eq. 7.6 cell;** • **Eq. 7.7 stack**
4	**Total efficiency η_ω at current densities j**	• **Eq. 7.8 cell;** • **Eq. 7.9 stack**
5	**Hydrogen production efficiency $\eta^{(HHV\ or\ LHV)}$ at covered current densities j**	• **Eq. 7.11**

7.2 EFFICIENCY CALCULATION for SINGLE CELL, SHORT STACK

In literature there is currently a lack of uniformity on the definition and on methods used for evaluating efficiency of single cells and short stacks. A detailed discussion on efficiency metrics and the underlying assumptions is presented in [2]. Following a recap of the different efficiency metrics discussed there, this section presents a harmonised approach for evaluating efficiency at single cell and short stack level.

7.2.1 ENERGY EFFICIENCY (ideal efficiency, thermodynamic approach)

The energy efficiency $\boldsymbol{\varepsilon_{cell}}$ of an electrolysis cell is defined as the ratio of the amount of total energy required for splitting one mole of water under reversible conditions and the actual total amount of energy (electricity and heat) used in the process, i.e. including the energy to overcome irreversibilities.

$$\varepsilon_{cell} = \frac{energy\ requirement\ in\ reversible\ conditions}{energy\ requirement\ in\ irreversible\ conditions} = \frac{W_t\ (J.mol^{-1})}{W_r\ (J.mol^{-1})} \qquad [Eq\ 7.1]$$

The efficiency of a single cell can be expressed as:

$$\boldsymbol{\varepsilon_{cell}} = \frac{\Delta G}{\Delta H} = 1 - T\frac{\Delta S}{\Delta H} = \frac{\boldsymbol{n \cdot F \cdot U_{tn}}}{\boldsymbol{n \cdot F \cdot U_{cell} + Q_{input}}} \qquad [Eq.\ 7.2]$$

where U_{cell} is the measured cell voltage[13] and Q_{input} the heat supplied to the cell by an external source.

For cell voltages exceeding U_{tn}, the electrolysis reaction is exothermic and Q_{input} is zero. For lower operating voltage, electrolysis is endothermic and heat from an external source has to be provided for isothermal cell operation, i.e. $Q_{input}>0$.

For a short stack, energy efficiency is calculated as for a single cell by accounting for the number N of single cells connected in series in the stack.

$$\boldsymbol{\varepsilon_{stack}} = \frac{\boldsymbol{N \cdot n \cdot F \cdot U_{tn}}}{\boldsymbol{N \cdot n \cdot F \cdot U_{cell} + Q_{input\ stack}}} \qquad [Eq.\ 7.3]$$

When reporting the efficiency value calculated according to Eq. 7.2 or 7.3, it should be clearly indicated whether the heat supplied has been measured or not.

7.2.2 CURRENT EFFICIENCY (or Faraday efficiency)

In an electrochemical reaction, current efficiency is based on the fraction of the electric current passing through an electrochemical cell, which accomplishes the chemical reaction.

[13] U_{cell} is composed of the sum of the reversible cell voltage and of the voltage contributions from ohmic resistance, charge transfer and diffusion limitations.

For water electrolysis it is expressed as:

$$\eta_I(T,p,I) = \frac{I-I_{loss}}{I_{DC}} = 1 - \frac{I_{loss}}{I_{DC}} = 1 - \frac{2\cdot F\cdot\left[\dot{n}_{H_2\text{loss}}(T,p,I) + 2\dot{n}_{O_2\text{loss}}(T,p,I)\right]}{I_{DC}}. \quad \text{[Eq. 7.4]}$$

Where $I_{loss} = z \cdot F \cdot \left[\dot{n}_{i_{loss}}(T,p,I)\right]$ [Eq. 7.5]

Where $\dot{n}_{i\ \text{loss}}$ is the molar flowrate of component (i) permeated through the gas separator, z = 2 for H_2 and z = 4 for O_2, I_{DC} is the direct current provided to the cell.

In an ideal cell, $\dot{n}_{H_2{}_{loss}} = \dot{n}_{O_2{}_{loss}} = 0$, leading to $\eta_I(T,p,I) = 1$, independent of operating conditions (T,p,I).
In a real cell, $\dot{n}_{H_2{}_{loss}} \neq \dot{n}_{O_2{}_{loss}} \neq 0$, resulting in $\eta_I(T,p,I) < 1$.

Because loss flow rates are small and impractical to measure, the current efficiency is usually expressed in terms of the flow rates of hydrogen and of oxygen measured at the exit of the cell. When only considering hydrogen production, the current efficiency at single cell level is calculated as:

$$\eta_I^{H_2} = \frac{2\cdot F\cdot \dot{n}_{H_2\,measured}}{I_{DC}} \quad \text{[Eq. 7.6]}$$

For a short stack the current efficiency for hydrogen production only is given by eq. 7.7, with N representing number of cells in the stack:

$$\eta_{Istack}^{H2} = \frac{2\cdot F\cdot \dot{n}_{H_2}}{I_{DC}\cdot N} \quad \text{[Eq. 7.7]}$$

Considering that hydrogen production rate without loss corresponds to current efficiency η_I=1, another interpretation of the current efficiency η_I is that it represents the ratio between the actual hydrogen production rate and the theoretical maximum hydrogen production rate, or the ratio of the actually produced amount of hydrogen and the theoretically maximum possible amount.

7.2.3 TOTAL EFFICIENCY

The total efficiency, η_ω, is defined as the product of energy efficiency and of current efficiency.

For a single cell the total efficiency is given by:

$$\eta_{\omega,cell} = \varepsilon_{cell} \cdot \eta_{I,cell} \quad \text{[Eq. 7.8])}$$

For a short stack the total efficiency is given by:

$$\eta_{\omega,stack} = \varepsilon_{stack} \cdot \eta_{I,stack} \quad \text{[Eq. 7.9]}$$

7.2.4 HYDROGEN PRODUCTION EFFICIENCY

In an alternative energy efficiency definition to that of eq. (7.1), the nominator, namely the energy for reversible reaction conditions, is replaced by the energy content of the reaction products. The denominator does not change and represents the total energy required for the reaction (electricity and heat):

$$efficiency = \frac{energy\ content\ of\ the\ reaction\ products}{total\ energy\ required} \quad \text{[Eq. 7.10]}$$

When only hydrogen is considered as useful reaction product, the nominator only contains the energy content of the hydrogen, i.e. the generated amount of hydrogen multiplied by its specific energy content, either HHV or LHV. Because in practice, the flow rate of the produced hydrogen, $\dot{n}H_2$, is measured, the above equation can be written as:

$$\eta^{(HHV\ or\ LHV)} = \frac{HHV\ or\ LHV}{P_{th}+P_{el}} \cdot \dot{n}_{H_2} \quad \text{[Eq. 7.11]}$$

with P_{th} and P_{el} representing respectively the thermal power and electric power provided. $\eta^{(HHV\ or\ LHV)}$ is known as the (instantaneous) hydrogen production efficiency.

When determining hydrogen production efficiency, specification of the higher or lower heating value is clearly relevant. For operating temperatures above 100 °C, LHV is to be used, as explained earlier. For low-temperature electrolysis, generally HHV is used in efficiency calculations, based on the consideration that irrespective of the use that is made of the hydrogen, it may be possible to exploit the excess heat produced when operating the electrolyser at voltages higher than the thermoneutral voltage. Accordingly, efficiency targets for low temperature electrolysis in the FCH-JU programme are expressed in terms of HHV. [14]

It should be noted that some authors argue that the use of LHV or of HHV in determining efficiency values for low temperature electrolysis should be decided based on the use of the produced hydrogen [15]:

- When the hydrogen is considered as a feedstock for the chemical industry, the higher heating value HHV is used.
- When, on the other hand, the generated hydrogen is used for energy production purposes, the lower heating value LHV is relevant, because it accounts for the energy contained in the produced hydrogen that can effectively be used in subsequent conversion steps to mechanical, electrical or thermal energy. Indeed, in the case of low-temperature electrolysis without use of an external heat source, the excess heat generated when operating at voltages higher than the thermoneutral voltage is mostly not exploited and is lost to the environment. It hence does not make sense to include a heat-related component in the specific energy content of the produced hydrogen, and LHV represents the practically relevant value. This approach is followed in the DoE programme.

[14] For electrolysis, efficiency calculated on the basis of HHV results in a higher value than that based on LHV. The opposite applies for fuel cells.

The above considerations apply to efficiency at single cell or short stack level. Efficiency of electrolysis *at system level* can also be expressed in terms of the electric energy required for producing a normal cubic meter or a kilogram of hydrogen. Using this specific electricity consumption (SEC) to characterize electrolyser performance sidesteps the issue of using HHV or LHV. However, when experimentally determined values of specific electricity consumption are to be related to the theoretically minimum achievable value (or when having to set targets for it), identification of HHV or LHV is again required as comparison basis. For low temperature electrolysis when water is fed at ambient temperature and pressure to the system and all energy input is provided in the form of electricity, the minimum specific electricity consumption on HHV-basis equals 3.54 $kWh \cdot Nm_{H2}^{-3}$, resp. 39.4 kWh/kg_{H2}. When water is supplied as vapour, the values on LHV-basis equal 3.00 $kWh \cdot Nm_{H2}^{-3}$, resp. 33.3 kWh/kg_{H2}. Higher system efficiencies corresponding to specific energy consumption below these values (lower electrical energy input needs) can be attained by providing heat energy to the system. State of the art low temperature systems can reach electrical energy inputs around 50 kWh/kgH2, corresponding to an efficiency on HHV-basis of 79%.

7.3 PERFORMANCE ASSESSMENT: presentation of test results

The set of performance indicators identified in Table 22 are determined through tests performed under reference and under stressor operation conditions. The indicator values or test results obtained for the latter are normalized according to equation 7.12:

$$\text{Normalised performance output} = 1 - \frac{test\ output\ under\ stressor\ conditions}{test\ output\ under\ \text{reference}\ conditions} \qquad \text{[Eq. 7.12]}$$

A normalised performance output equal to zero indicates that the stressor condition applied does not affect performance. Non-zero normalised performance outputs imply that the considered stressor does have an impact performance, with negative normalised outputs corresponding to an increased test output and positive ones to a decreased test output. Whether an increase or a decrease in normalised performance output corresponds to performance enhancement or performance degradation, depends on the indicator considered. However, it should be noted that a positive effect by a stressor on *performance* may have a negative effect on *durability*.

The normalised performance outputs are presented in a spider plot where each of the axes corresponds to a specific performance indicator (Table 22). Figure 18 shows an example for test results obtained on a PEMWE cell, with the ordinate on each axis representing the normalised output for a given PEMWE stressor condition (Table 19). In Figure 18 the blue polygon with ordinate value equal to zero corresponds to PEMWE Reference Operating Conditions (Table 12).

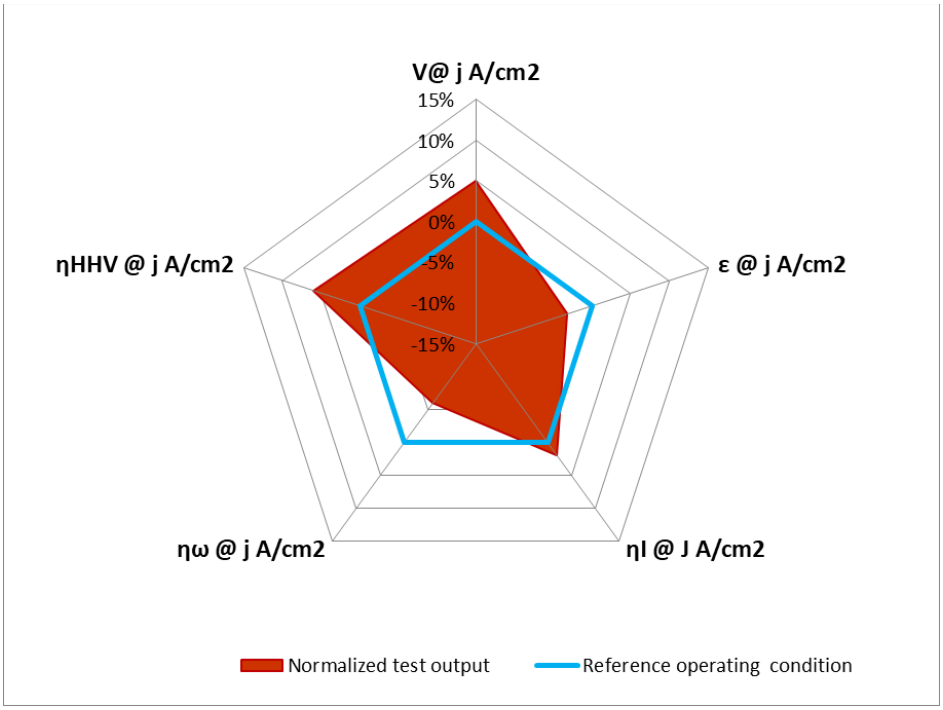

Figure 18. illustration of spider plot representing normalised performance outputs for PEMWE

7.4 DURABILITY ASSESSMENT

Successful operation of an electrolysis device depends not only on its performance but also on its capability to maintain performance over a period of time, known as durability. Such capability is affected by a number of factors, including cell design, manufacturing and assembly procedures, but also by the preceding operating history.

7.4.1 Selection of durability indicator for in-situ testing

Durability [2] is related to the loss of performance of the electrolysis device over a given time period. The life-span of the device is expressed as its total number of hours of operation, irrespective of the actual nature of this operation (e.g. steady state, transient, cyclic, …). As such, durability is a concept that applies at system level.

In order to address durability through tests on single cells or short stacks, there is a need for a parameter that can be derived from performing tests at cell and short stack level. Such a parameter is the degradation rate, defined as the rate at which performance - characterised by one of the performance indicators listed in Table 22 - changes with time from its initial value.

Because a number of indicators can be used to characterise performance of an electrolysis cell or short stack (see 7.1), consideration should be given to which performance indicator among those listed in Table 22 is most suited for assessing durability through degradation rate. The performance indicator most frequently used in practice to assess degradation rate (and hence durability) is cell or short stack voltage (V) at reference operating conditions (T,p,I, see Table 22). Because cell/short stack voltage at reference operating conditions tends to increase as a function of time, the degradation rate represented by voltage rate is positive.

The use of voltage increase rate as durability indicator is explained in the following section.

7.4.2 Voltage increase rate as durability indicator

Voltage increase rate is experimentally determined by monitoring voltage in a number of test blocks interspersed by rest periods. To obtain a meaningful value of voltage increase, the loading profile (steady or dynamic) used in each block should be identical.

Part of the overall voltage increase observed from one test block to the next may be recovered upon shutdown and consecutive restart. Also shutdown and restart may lead to reduced overall voltage increase compared to uninterrupted (steady or dynamic) operation. Both observations suggest that voltage increase is composed of reversible and irreversible contributions, as shown in Figure 19 and Figure 20.

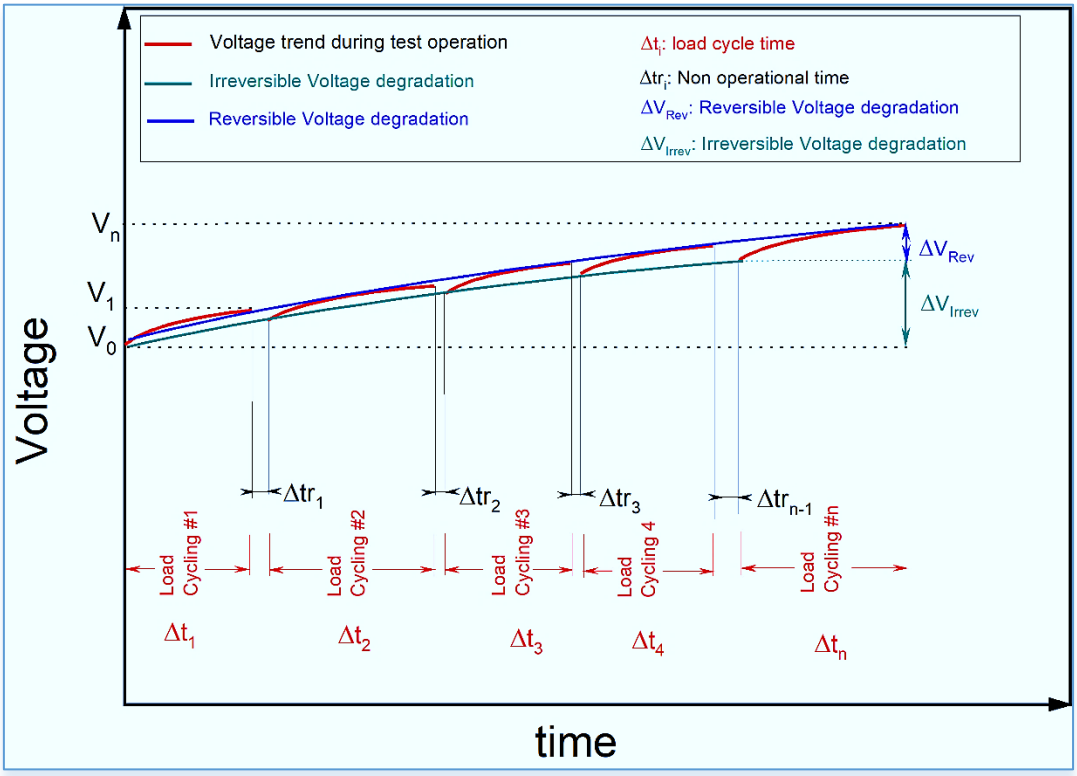

Figure 19. Reversible and irreversible voltage increase during consecutive in-situ test cycles

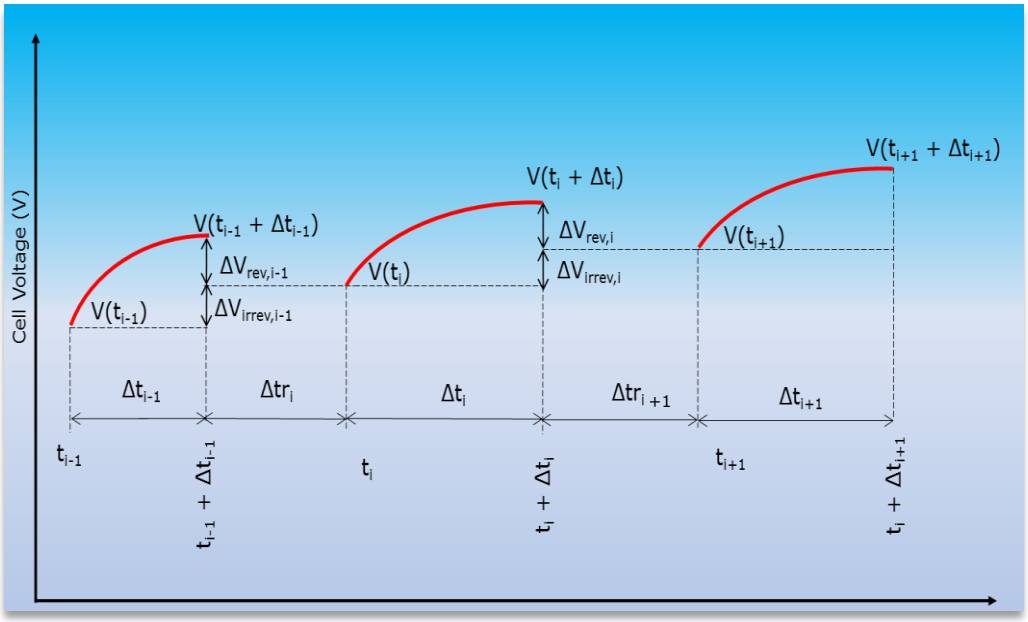

Figure 20. Reversible & irreversible voltage increase, graphical definition –

The reversible voltage increase ΔV_{rev} corresponds to the recoverable part of the overall voltage increase. For a typical test block in which the cell is operated (either in steady state mode or in dynamic operation) for a time Δt_i between a start-up and a shut-down, the reversible voltage increase $\Delta V_{rev,i}$ is the difference between the cell voltage $V(t_{i+1})$ at the start time t_{i+1} of the test block $i+1$ and the voltage $V(t_i + \Delta t_i)$ at the end time $t_i + \Delta t_i$ of the test block i:

$$\Delta V_{rev,i} = V(t_i + \Delta t_i) - V(t_{i+1}) \quad \text{[Eq. 7.13]}$$

The total reversible voltage increase $\Delta V_{rev,1\rightarrow N}$ upon performing N test blocks in total is the sum of all reversible voltage increments:

$$\Delta V_{rev,\,1\rightarrow N} = \sum_{i=1}^{N} \Delta V_{\mathrm{rev,\,I}} \quad \text{[Eq. 7.14]}$$

The total reversible voltage increase rate $\dot{V}_{rev,1\rightarrow N}$ of all N test blocks is the ratio of $\Delta V_{rev,1\rightarrow N}$ to the sum of the duration of all N test blocks:

$$\dot{V}_{rev,1\rightarrow N} = \frac{\Delta V_{rev,1\rightarrow N}}{\sum_{i=1}^{N} \Delta t_i} \quad \text{[Eq. 7.15]}$$

The irreversible voltage increase due to a test block i is defined as the difference between the cell voltage $V(t_i)$ at starting time t_i of the test block i and the voltage $V(t_{i+1})$ at the ending time t_{i+1} of the recovery period Δtr_i (i.e. the voltage at starting time t_{i+1} of test block i+1):

$$\Delta V_{irrev,i} = V(t_{i+1}) - V(t_i) \quad \text{[Eq. 7.16]}$$

The total irreversible voltage increase $\Delta V_{irrev,1\rightarrow N}$ upon performing N test blocks is the sum of all irreversible voltage losses:

$$\Delta V_{irrev,\,1\rightarrow N} = \sum_{i=1}^{N} \Delta V_{\mathrm{irrev,\,I}} \quad \text{[Eq. 7.17]}$$

The total irreversible voltage increase rate $\dot{V}_{irrev,1\rightarrow N}$ of all N test blocks is the ratio of $\Delta V_{irrev,1\rightarrow N}$ to the sum of the duration of all N test blocks:

$$\dot{V}_{irrev,1\rightarrow N} = \frac{\Delta V_{irrev,1\rightarrow N}}{\sum_{i=1}^{N} \Delta t_i} \quad \text{[Eq. 7.18]}$$

The sum of reversible and irreversible voltage increase rate is the overall degradation rate:

$$\dot{V} = \dot{V}_{rev} + \dot{V}_{irrev} \quad \text{[Eq. 7.19]}$$

As implied in eq. 7.15, 7.18 and 7.19, the degradation rate is reported in terms of voltage increase versus time, at a given current density.

7.4.3 Additional durability indicator

Evaluation of degradation rate through voltage increase rate only partially addresses durability because it does not take into account another relevant factor in this respect, namely initial voltage. Indeed, for the same degradation rate at a given current density, starting from a lower initial voltage results in a lower cumulative voltage. This widens the voltage range under which the cell/short stack can operate and may hence extend its life.

A parameter that considers both degradation rate and initial voltage at a given current density j is the stability factor SFj, defined as the inverse product of voltage increase rate, $\dot{V}_j$, and the initial overvoltage (U_{cellj}). The initial overvoltage at BoL is defined as the overvoltage after activation and conditioning:

$$\text{Initial overvoltage,j} = U_{cell,j} = V(j) - U^{tn}$$

$$\mathbf{(SF)_j} = 1 / (\dot{V}_j \cdot U_{cellj}) \qquad \text{[eq.7.20]}$$

7.5 DURABILITY TESTING

7.5.1 Identification of load versus time profiles for durability testing

To assess durability by in-situ testing of single cells and short stacks, the operation history that the electrolyser system experiences in actual service needs to be "translated" into load-versus-time profiles to be imposed in the in-situ tests. Such translation involves a number of sequential steps:

- Identification of operational conditions experienced during actual service
- appropriate simulation of these as operation conditions to be imposed in in-situ tests on cell or short stack
- establishing the degradation rate (corresponding to the selected performance indicator, usually cell/short stack voltage) through in-situ testing
    - by continuous monitoring of the performance indicator during testing to establish its instantaneous degradation rate, or
    - by executing performance tests at BoT and at different stages after interruption of the simulated service conditions, to establish average degradation rates[15]

To simplify execution of in-situ testing for the second step, actual service conditions are usually simulated by imposing two types of time-profiles for the electric power supply, namely operation at steady state and dynamic operation according to pre-defined profiles that are representative of transients and dynamic conditions. These are discussed in 7.5.2 and 7.5.3, respectively.

To enable "translating" service operating conditions into load profiles to be used in in-situ tests, the electric power inputs to an electrolyser system need conversion into inputs of electrical current density. For this purpose, the maximum current density, $j_{max,}$ to be imposed during in-situ testing is proposed as that corresponding to a given voltage on the polarisation curve at the Beginning of Test (BoT), while reaching a (higher) voltage at the same current is proposed as End of Test (EoT) criterion. As an example, for PEMWE the respective cell voltages are proposed as 1.8 V and 2.0 V, respectively[16] (Figure 21). A similar approach, with adapted values for the cell voltages to be decided, is proposed for AWE and AEMWE.

[15] Next to performing in-situ tests, ex-situ testing can provide complementary information on degradation mechanism(s) causing the change in performance induced by the simulated operation conditions

[16] Values proposed and used in Electrohypem project

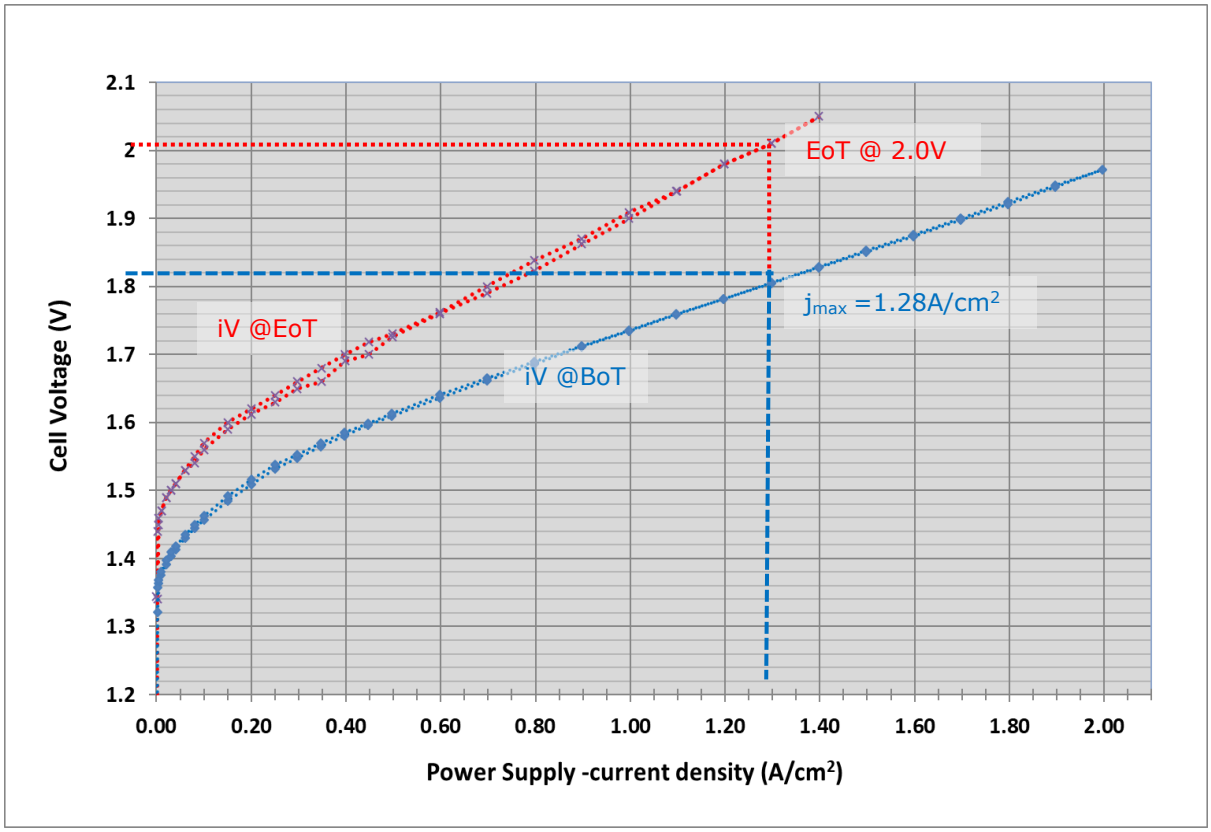

Figure 21. Illustration of determination of j_{max} and of EoT criterion for PEMWE

7.5.2 STEADY STATE LOADING

Degradation rate under steady state loading is identified as the voltage increase rate calculated according to equation 7.19.

The time period considered for determining voltage increase and calculating voltage increase rate should exclude the initial conditioning period, where the cell potential may decrease with time due to artefacts (e.g. change of the oxidation state of the anode catalyst, in-situ membrane purification). It should also exclude time periods during which microstructural instabilities caused by pre-exposure may affect the value and evolution of cell voltage with time. To enable reliable evaluation of a representative voltage increase rate, the time period for its determination should only start when the average value of $\dot{V}=(\Delta V/\Delta t)$ calculated over the preceding two-hour period is equal or greater than zero.

The protocol agreed for assessing degradation rate under steady state loading for PEMWE, AWE and AEMWE is presented in

Table 23.

Table 23. Agreed protocol for assessing steady state degradation rate for in-situ cell and short stack testing of PEMWE, AWE and AEMWE

STEADY STATE DEGRADATION TEST PROTOCOL	
STEP	**DESCRIPTION**
1	Perform activation and conditioning according to cell / stack manufacturer specifications.
2	Set the test input conditions (TIPs) according to reference operating conditions (chapter 5, Table 12,Table 15,Table 17)
3	Perform a BoT polarization curve [7] and record voltage at the corresponding current density j, $V(t_1)$.
4	Operate the cell/short stack at constant TIPs for 1000 hours
5	Perform a polarization curve and record voltage at same j, representative of $V(t_1 + \Delta t_1)$ (or $V(t_i + \Delta t_i)$ *for subsequent iterations)*
6	disconnect the current supply and leave the testing set-up under OCV conditions for 60 minutes maintaining the water recirculation flowrate and test temperature
7	re-apply the TIPs of step 1 and let voltage stabilise for 120 min. If ΔV/Δt calculated over this period is equal or greater than zero, go to next step, otherwise extend the stabilisation period for another 60 min until reaching a positive ΔV/Δt over the preceding 120 min
8	Perform a polarization curve and record voltage at same j, representative of $V(ti)$.
9	Repeat steps 3 to 7. The test ends with step 4 after 3000 hours of steady state operation or when EoT criterion is reached

Test validity criteria are met when measurement accuracy given in Table 14 are fulfilled.

The quality of the result strictly depends on the measurement accuracy of the test parameters concerned.

Depending on the test hardware available, additional relevant information may be obtained from performing EIS or HFR tests[17] in steps 3, 5 and 8. Also performing ex-situ

[17] EIS is used for assessing degradation impact on ohmic resistance, anode and cathode charge transfer resistances, diffusion resistance. If EIS is not available, HFR should be used to determine ohmic resistance and calculate iR free cell voltage.

tests on component materials retrieved from intermittent in-situ tests can provide elements of clarification on the degradation mechanisms.

7.5.3 DYNAMIC LOAD PROFILES

The conventional approach for assessing degradation rate and hence durability under dynamic loading conditions differentiates between system level and cell/short stack level:

- At system level Real World Degradation (RWD) is considered, with a load versus time profile based on actual operating conditions experienced in different electrolysis systems applications.
- At single cell and short stack level, Laboratory World Degradation (LWD) is normally considered, in which the load versus time profile is derived from, yet differs from that experienced in actual service. One factor causing the difference between RWD and LWD is the load that may be induced by BoP components which form part of the system, but are not present at cell/short stack level. Moreover, for reducing the expenditure and experimental effort for in-situ testing, LWD load profiles may be further simplified from those considered under RWD. Hence, LWD load versus time profiles imposed in in-situ testing of cells and stacks serve as simplified simulation in a laboratory environment of actual service loads, excluding those induced by BoP.

However, to avoid the inherent conservatism associated with subjecting cells/short stacks to LWD load profiles that do not include those arising from BoP and are simplified from those of RWD, the approach in this report stipulates that the dynamic load profiles to be applied in laboratory testing of single cells and short stacks are identical to those experienced by the electrolysis system in actual service, i.e. RWD load profiles rather than LWD profiles are imposed.

Hence, the Real World Degradation load profiles which electrolyser systems are expected to be subjected to in a number of service applications presented in chapter 8, are directly applicable to testing of single cells/short stacks.

7.5.4 Protocol for assessing degradation rate (durability) under dynamic loading

The agreed protocol for assessing degradation rate under dynamic loading for PEMWE, AWE and AEMWE is described in Table 24 which is valid for a given imposed load profile, an example of which is shown in Figure 22.

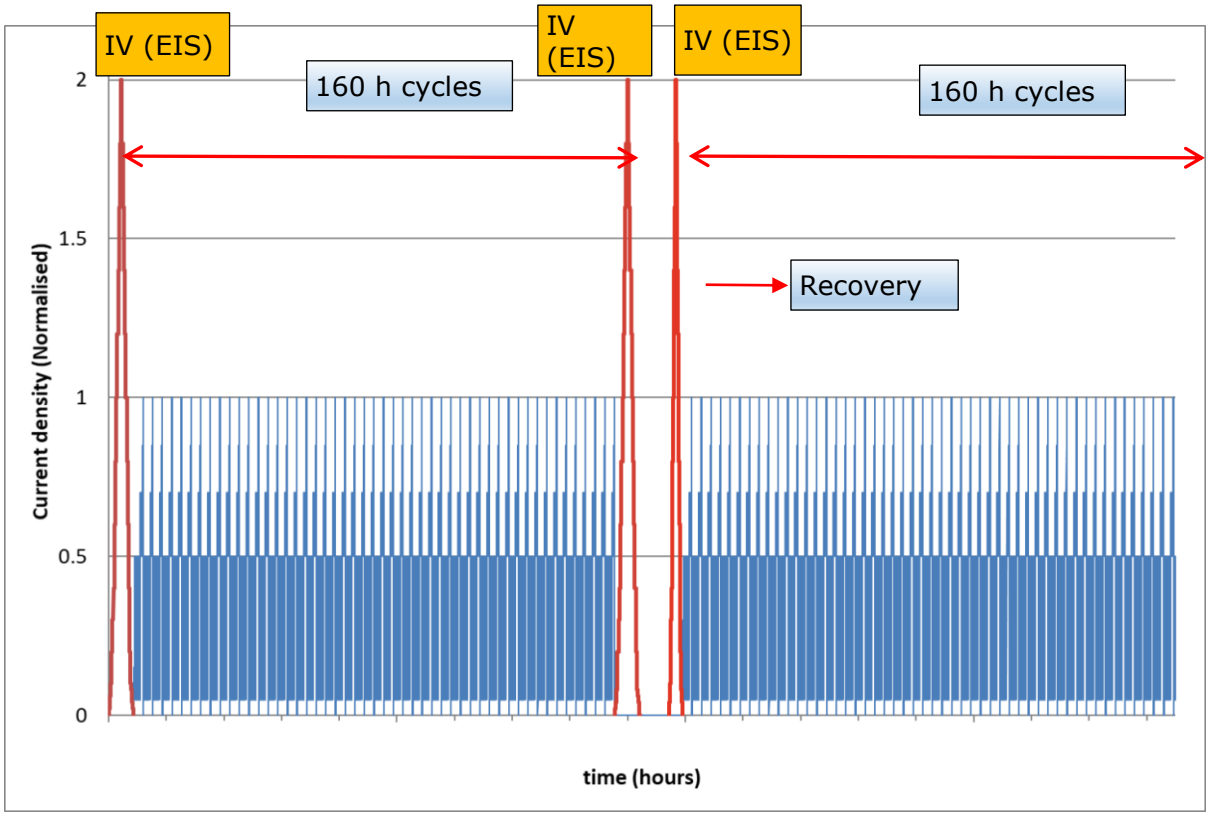

Figure 22. Example of a load profile used in dynamic load degradation tests

Table 24. Agreed dynamic load degradation test protocol for in-situ cell and short stack testing of PEMWE, AWE and AEMWE

DYNAMIC LOAD DEGRADATION TEST PROTOCOL	
1	Perform activation and conditioning according to cell / stack manufacturer specifications.
2	Set the test input conditions (TIPs) according to reference operating conditions (chapter 5, Table 12, Table 15, Table 17).
3	Perform a polarization curve [7] and record voltage at the corresponding j, representative of $V(t_1)$.
4	Operate the cell/short stack at the selected RWD load versus time profile for N cycles equivalent to 160 hours (with N rounded to the closest integer).
5	Perform a polarization curve record voltage at same j, representative of $V(t_1 + \Delta t_1)$ (or $V(t_i + \Delta t_i)$ *for subsequent iterations).*
6	Disconnect current supply and leave under OCV for 60 minutes maintaining the water recirculation flowrate and test temperature.
7	re-apply the TIPs of step 1 and let voltage stabilise for 120 min. If $\Delta V/\Delta t$ calculated over this period is equal or greater than zero, go to next

DYNAMIC LOAD DEGRADATION TEST PROTOCOL	
	step, otherwise extend the stabilisation period for another 60 min until reaching a positive ΔV/Δt over the preceding 120 min
8	Perform a polarization curve and record voltage at same j, representative of *V(ti)*.
9	Repeat steps 4 to 8. The test ends at step 5 after 10 loops for a total of 1600 hours, or earlier upon reaching one of the EoT criteria.

Test validity criteria are met when measurement accuracy given in Table 14 are fulfilled.

The quality of the result strictly depends on the measurement accuracy of the test parameters concerned.

Depending on the test hardware available, additional relevant information may be obtained from performing EIS or HFR tests[18] in steps 3, 5 and 8. Also performing ex-situ tests on component materials retrieved from intermittent in-situ tests can provide elements of clarification on the degradation mechanisms.

An exhaustive durability assessment exercise usually requires execution of this protocol for a number of load profiles considered relevant.

[18] EIS is used for assessing degradation impact on ohmic resistance, anode and cathode charge transfer resistances, diffusion resistance. If EIS is not available, HFR should be used to determine ohmic resistance and calculate iR free cell voltage.

7.6 DURABILITY ASSESSMENT: presentation of results

There are two methods of presenting the results of durability assessment. The first consists of using a normalised spider graph (Figure 23 below) where each axis corresponds to one of the performance indicators listed in Table 22. LTWE Performance indicators The axis ordinate represents the normalised performance determined according to eq. 7.21:

$$\text{Normalised performance} = \frac{Performance\ indicator\ at\ EOT\ @\ j}{Performance\ indicator\ at\ BOT\ @\ j} \qquad \text{[Eq. 7.21]}$$

in which the nominator represents the value for the considered performance indicator observed/calculated according to sections 7.1 and 7.2, after submitting the cell/short stack to a loading profile according to one of the protocols described in 7.5.2 and 7.5.4. The denominator represents the value of the same performance indicator obtained/calculated at BoT.

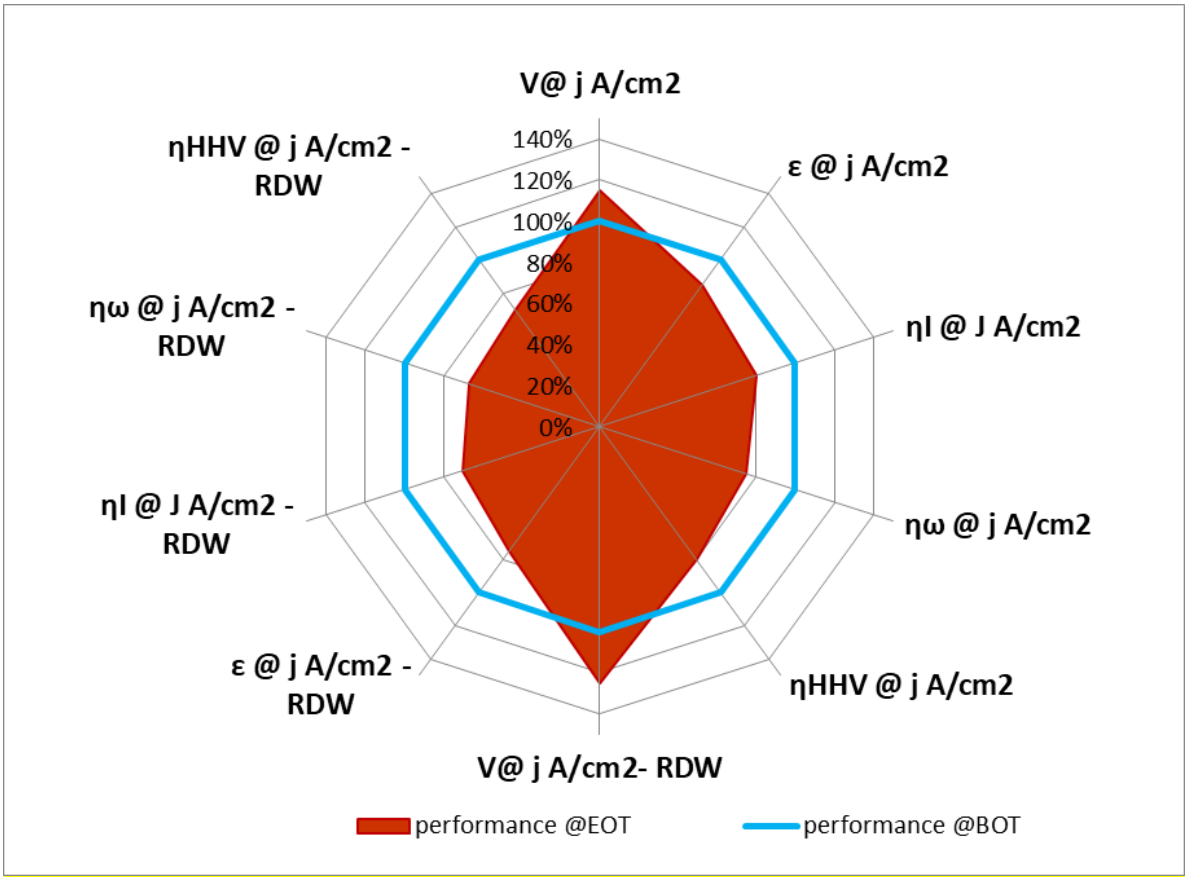

Figure 23. Illustration of durability test results on a PEMWE cell under steady and under a specific RWD load profile. The blue polygon represents PEMWE Reference Operating Conditions (Table 12).

The second way of representing the results of durability tests is through the use of the cell/short stack voltage increase rate as the metric for degradation rate. In this case the indicators listed in **Error! Not a valid bookmark self-reference.** are used, which apply at a given current density at which voltage is measured under either steady state (table 23) or a specific RDW load profile (table 24).

Table 25: Degradation Indicators

INDICATOR	SYMBOL	UNIT	REFERENCE
Total voltage increase rate	$\dot{V}$	µV/h	Eq. 7.19
Reversible voltage increase rate	$\dot{V}_{rev}$	µV/h	Eq. 7.15
Irreversible voltage increase rate	$\dot{V}_{irrev}$	µV/h	Eq. 7.18
Stability factor	SF	$h \cdot V^{-2}$	Eq. 7.20

The results for voltage increase rate can be shown in a bar chart:

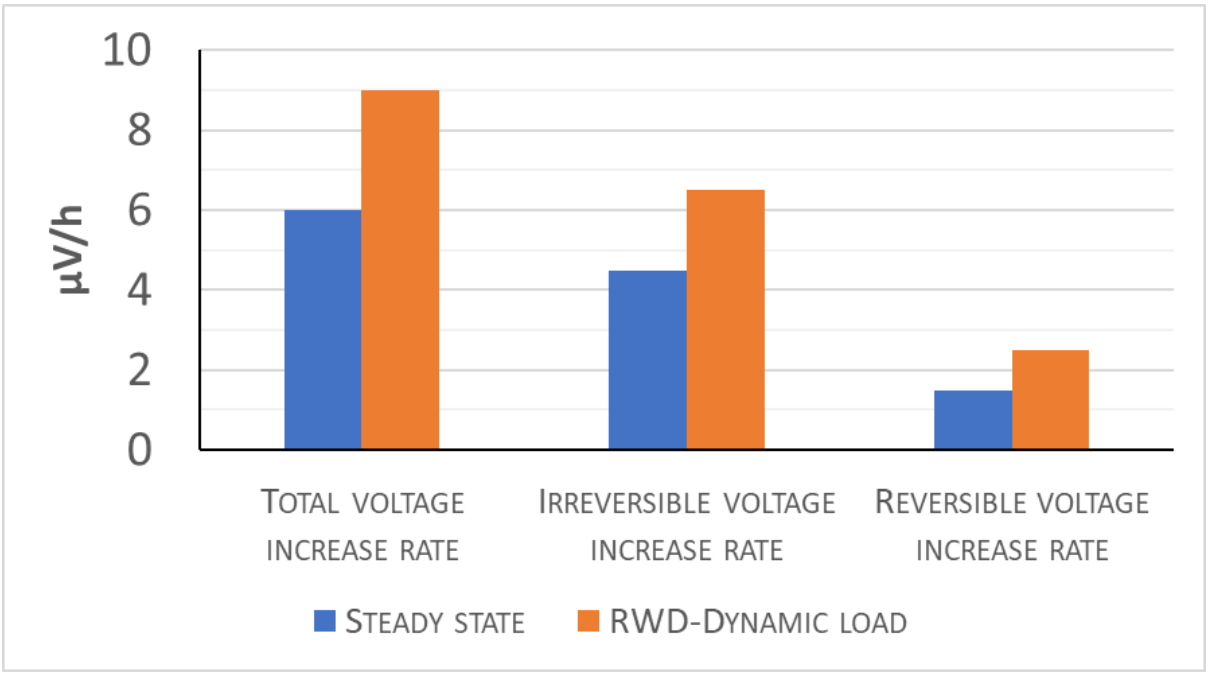

Figure 24: bar chart showing degradation indicators under steady state and under one RWD load profile for PEMWE

7.7 ACCELERATED LIFE and ACCELERATED STRESS TESTING

Considering that the lifetime of an electrolyser system can easily reach many years, it is important when selecting new or improved materials or when assessing durability, to be able to evaluate degradation in a short(er) period of time. "Accelerated testing" is used for that purpose. In such testing, materials and components are subjected to operating conditions outside the normal operation window to trigger similar degradation as expected under actual service conditions but at a faster rate, thus shortening the required testing time.

The approach towards accelerated testing of single cells and short stacks presented in this report differentiates between two types of accelerated tests, each of which serves a specific purpose:

- Accelerated Life Tests (ALT) to be used for investigating the capability of electrolyser component materials to withstand service loads
- Accelerated Stress Test (AST) to assist in fast development of new and improved electrolyser materials

7.7.1 PROTOCOLS FOR ACCELERATED LIFE TESTS (ALT)

To investigate the capability of electrolyser materials to withstand service loads, Accelerated Life Tests aim at mimicking failures under Real World Degradation (RWD) conditions. The ALT protocols are similar to those for dynamic durability tests presented in 7.5.4, and achieve the acceleration by subjecting the materials during in-situ tests to stressor operating conditions (Chapter 6), rather than to reference operating conditions (chapter 5). This requires selection of the appropriate "high" or "low" setting for the stressor triggering performance degradation.

Accelerated Life Tests (ALT) for single cells and short stacks are hence agreed as follows:

- Operating Conditions

  Stressor Operating Conditions for Single Cell and Short Stack Testing for PEMWE, AWE and AEMWE, Table 19, Table 20 and Table 21 respectively for the type of stressor effect that is subject of the evaluation.

- Test Protocol

  Dynamic load degradation test protocol for Single Cell and Short Stack, with RWD load profile from chapter 8, Table 40[19] 8.5.1 FREQUENCY CONTAINMENT RESERVES (FCR) test protocol considered as the most demanding

ALT results are analysed and presented as described in section 7.6.

[19] As for dynamic load degradation testing, the power input settings from RWD profiles at system level have to be translated into current density input settings

7.7.2 PROTOCOLS for ACCELERATED STRESS TESTS

For material development and improvement purpose the ALT approach is not suitable because identification of stressor types and their associated settings for selective degradation of specific materials under conditions representative of actual service, is an as yet unresolved research issue. The absence of scientific consensus on load profiles and stressors able to selectively target degradation of materials for specific cell components hence warrants a different methodology for AST than for ALT.

The approach followed here builds on that adopted for durability testing (see 7.5). The acceleration is realised by increasing the severity of a selected RWD profile. Such increased severity may be achieved by

- using operation stressors
- and/or by increasing (the absolute value of) current ramp rates
- and/or by increasing frequency in the considered RWD profile.

This modified profile is then imposed as dynamic load profile in the durability test. The overall AST protocol consists of including such a profile as step 4 in the dynamic load degradation test protocol of Table 24.

Table 26 presents two load profiles which are considered to represent the most stringent requirements for using electrolysers in a grid balancing application. In future, other load profiles, once validated, can be benchmarked against and possibly update and/or replace this set[20].

Table 26. AST load profil

STEPS	AST load profiles
1	**Flexibility**
2	**Reactivity**

These load profiles are individually described in the sections below. As for dynamic load degradation testing, the power input settings from RWD profiles at system level have to be translated into current density input settings.

7.7.3 FLEXIBILITY load profile

This profile has the scope of combine in a simplified version but increasing the severity of the RWD profiles defined in section 8.5 by imposing higher current ramp rate and by modifying the settings for the stressor operating conditions to simulate applications where the system is expected to experience frequent periods of overload. Two overload

[20] such alternative AST profiles have been proposed within a number of FCH JU projects

cases are considered, stepwise increase to 100% and to 200% of design current density (left axis in Figure 25, resp. Figure 26).

Table 27. FLEXIBILITY LOAD PROFILE

FLEXIBILITY LOAD PROFILE	
Step	**DESCRIPTION**
1	Increase the current setting by 25% using a ramp-up profile with a ramp rate **+N** (A/s) and then maintain constant current for 15 minutes
2	Repeat step 1 up to 100% or 200% of design operating current
3	Decrease the current setting by 25% using a ramp-down profile with a ramp rate of **-N** (A/s) and then maintain constant current for 15 minutes
4	Repeat step 5 until reaching 25% of maximum operating current
Note	Ramp rate **N** is defined as j_{max} ·0.2 of maximum design test current I. This implies that each ramp is executed in a maximum time of 5 seconds, which is faster than the **FCR** test requirement. (see Table 41) I = A· j_{max} is the active area A multiplied by maximum operating current density

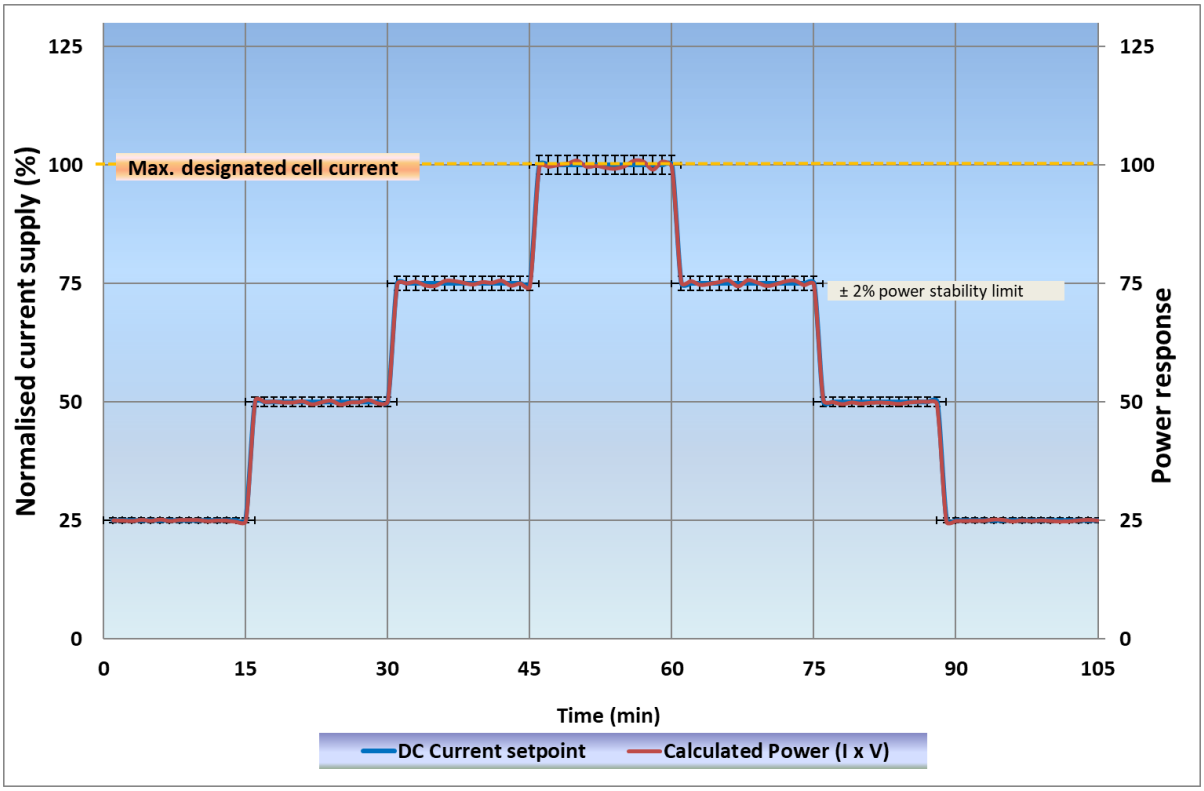

Figure 25. 100% of design current flexibility profile

When using the flexibility profile in AST according to the protocol described in Table 24, the variation of the power at each current setting (i.e. the product of the imposed current and the measured cell/stack voltage, right axis in Figures. 24 and 25) shall be smaller than +/- 2%. The parameters to be determined from ALT using this profile and their derivation for each time the profile is imposed are given in 8.5.1.

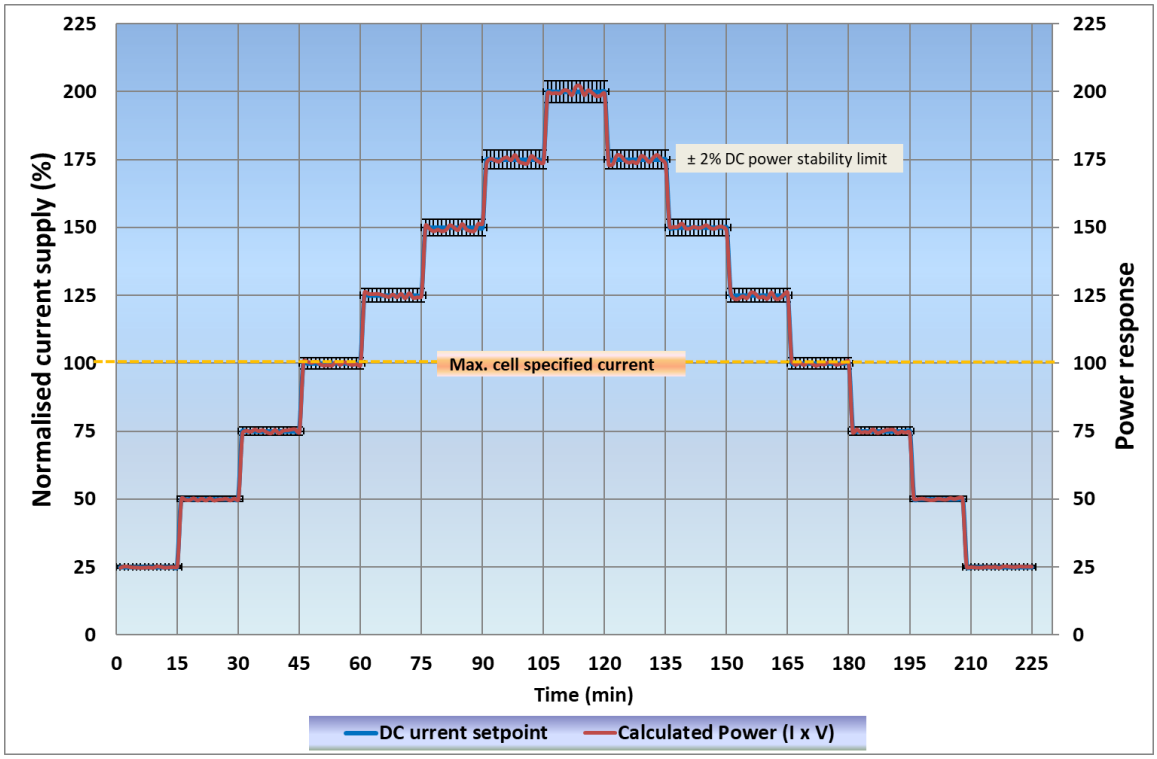

Figure 26. 200% of design current flexibility profile

The results of an AST test with the flexibility load profile are analysed and presented as described in section 7.6.

7.7.4 REACTIVITY LOAD profile

The reactivity load profile is derived from FCR RWD profile (8.5.1), with more severe conditions in terms of ramp rate and of frequency of current change. This is realised by two factors: limiting the constant current step to 60 seconds instead of 15 minutes and using different magnitudes for the step variation, corresponding to 25%, 50%, 75% and 100% of the current range (Figure 27).

Table 28. Reactivity load profile

REACTIVITY LOAD profile	
1	Set the current input to 100% of design operating current
2	perform 7 consecutive current cycles, each of 60 s total duration, with stepwise increasing amplitude of 25% of the rated design operating current at a current ramp rate of ±- N (A/s)
Note	Ramp rate **N** is defined as j_{max}· 0.2 of maximum design test current I. This implies that each ramp is executed in a maximum time of 5 seconds, which is faster than FCR test requirement. (see **Error! Reference source not found.**,

appendix C)
$I = A \cdot j_{max}$ is the active area multiplied by maximum operating current density

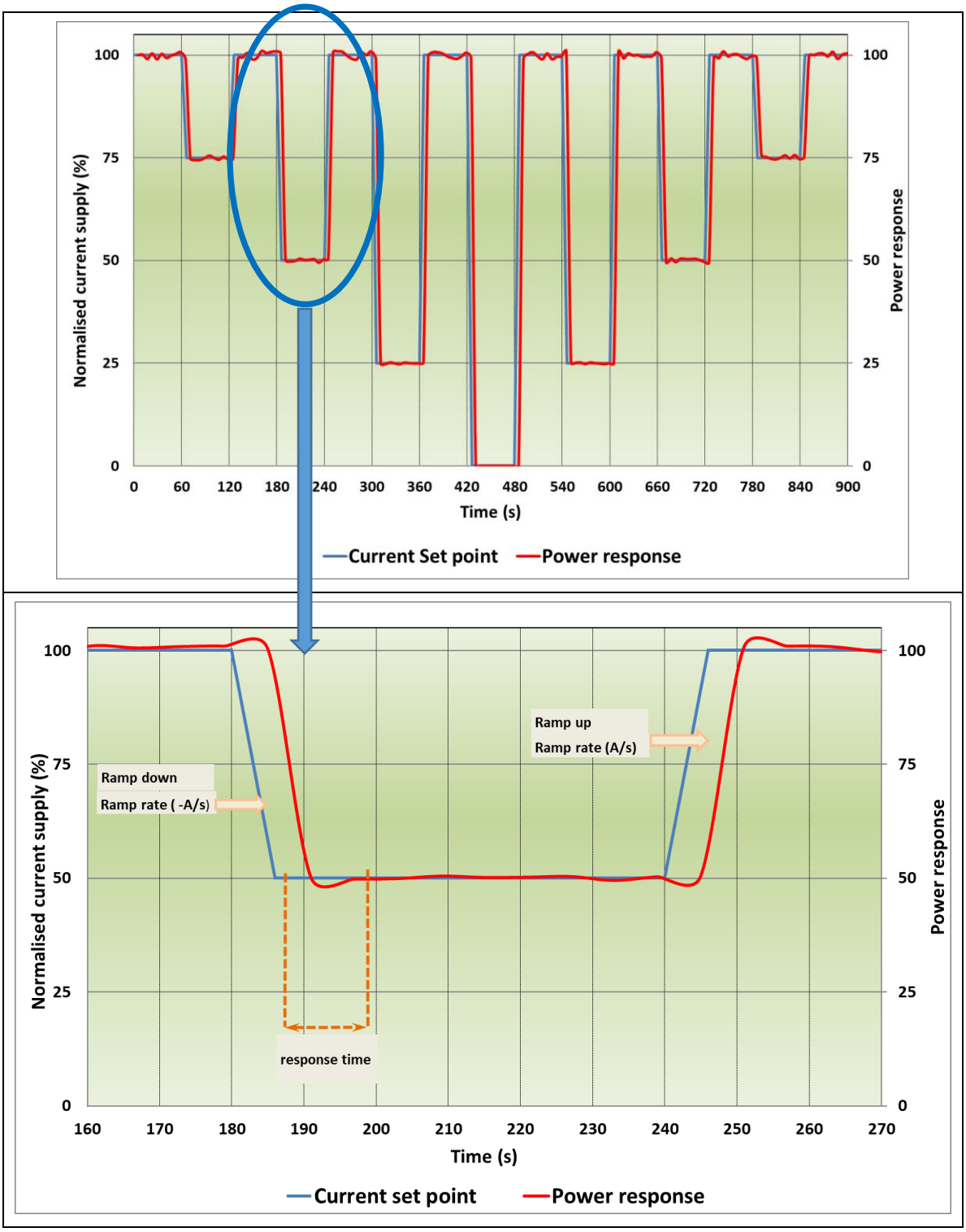

Figure 27. Reactivity profile

When using the reactivity profile in AST according to the protocol described in Table 24, the variation of the power response (i.e. the product of the imposed current and the measured cell/stack voltage, right axis in Figures Figure 25 and Figure 26) shall be smaller than +/- 2%.

The parameters to be determined from ALT using this profile and their derivation for each time the profile is imposed are the power response rate of change (in $\%\cdot s^{-1}$) and response time following the methodology described in section 8.5.1.

The results of an AST test with the reactivity load profile are analysed and presented as described in section 7.6.

8 ELECTROLYSER SYSTEM-LEVEL TESTING

An electrolyser is an energy conversion device which transforms electrical energy into chemical energy (H_2 and O_2). Its operation is bounded by constraints, both downstream (H_2 production demand) and upstream (availability and source of power input).

Downstream applications include production of hydrogen (and/or oxygen) as chemical feedstock for a range of process industries (PtX), generation of hydrogen for long-term (seasonal) storage, or for short-duration storage and subsequent use in transport (PtT) or re-electrification (PtP) (see Figure 2). These applications are characterised by different production volume versus time profiles reflecting the needs of the different customers, but because of economic considerations they are not expected to necessitate large and/or quick deviations from steady state electrolyser operation.

Next to these applications based on the use of hydrogen, the provision of services to the power grid by acting as flexible electrical load (flexible demand) constitutes an increasingly interesting business case. However, in this case the necessity for the electrolyser to cope with transient and dynamic power inputs, decreasing as well as increasing (possibly exceeding maximum nominal power), at different rates and frequencies, is much more challenging for its performance and durability.

Upstream operation bounds are set by the availability of power to the electrolyser. Electrolyser systems operating off-grid that have to rely on variable and intermittent renewable electricity from wind and/or solar, will be exposed to frequent start-ups from and shut-downs to various stand-by modes. Operation under such non-steady conditions poses challenges to performance and durability.

The downstream and upstream operation bounds have in common that they require the electrolyser system to be able to withstand a number of load-versus-time profiles with different levels of severity. This chapter establishes a set of agreed application-relevant load profiles and associated test protocols for assessing performance at system-level. Contrary to testing at cell/short stack level which includes both performance and durability characterisation (see chapter 7), testing at system-level only covers evaluation of performance. However, as explained in section 7.5, the load profiles used in durability tests at cell/short stack level (RWD load profiles) are directly derived from load-versus-time profiles described in this chapter, which are experienced by electrolyser systems in a number of service applications.

The chapter first presents an overall schematic for electrolyser system level testing considering the power sourcing and envisaged applications (section 8.1). This is followed by an overview of grid support services (section 8.2) and how electrolysers can provide these by acting as a flexible electric load (section 8.3). Sections 8.4 and 8.5 subsequently deal with the establishment of agreed test protocols for assessing the capacity of electrolyser systems to meet the load-versus-time requirements imposed by the specific application of providing grid balancing services.

The contents of the chapter is based on and builds upon efforts in the Qualigrids project in which PEMWE and AWE are considered [10].

8.1 SYSTEM TESTING: OVERVIEW

An electrolyser system is an assembly of various subsystems including electrolysis stack, power supply, water conditioning, etc., each of which contains a number of components. The types and specifications of these components play an important role in the specification of the electrolyser system, in its overall performance in terms of efficiency, flexibility, responsiveness, durability, and in its capital expenditure and cost of ownership.

A general description of electrolyser system components is given in the document "EU harmonised terminology for low-temperature water electrolysis for energy-storage applications"[2]. Figure 28 presents a scheme of a PEM water electrolyser with a representation of its relevant components. Similar figures for the system configurations for AWE and AEMWE are included in [2].

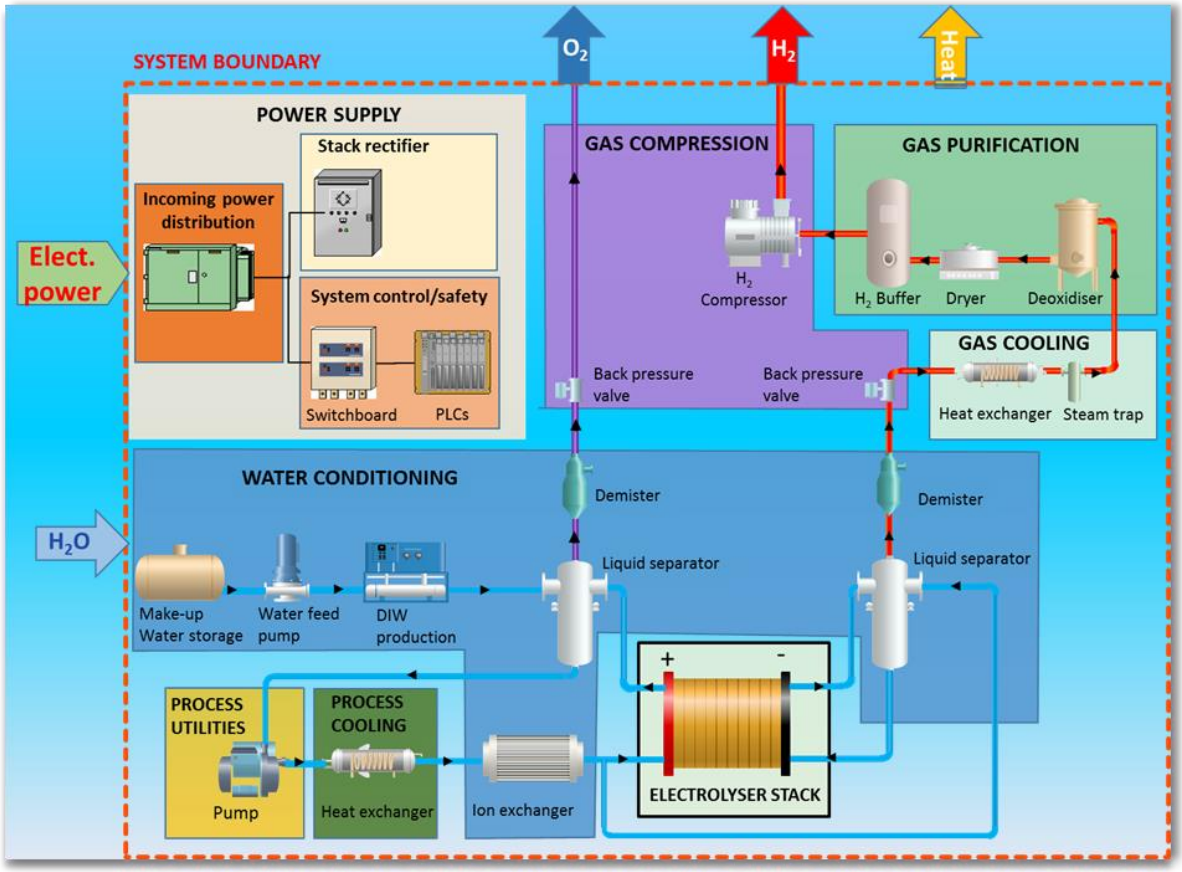

Figure 28. PEM water electrolyser scheme

As a first step in system testing, the various system components are tested because they impact the performance of the overall system. However, it is usually not possible to test individual system components independently. It is hence important for system-level testing to provide an adequate number of measuring instruments to monitor parameters such as electricity and water consumption, fluid flow rate and composition, pressures

and temperatures, etc. at appropriate locations for getting an indication of the contribution of each component to overall system performance.

Subsequent aspects of system-level testing discussed in the following parts of this chapter address the envisaged applications of the electrolyser. This consists of multiple stages, as indicated in Figure 29.

For stationary mode testing the system shall be tested at the reference conditions based on system technology whenever possible, and to the supplier recommended nominal condition applying the methodology described in section 7 to determine the indicators of Table 22 and in section 8.7: Table 48.

For transient mode testing, in the first stage the basic performance characteristics of the system are checked by performing a number of simple "fit-for-purpose" screening tests for system use as a flexible electric load. Such tests, described in section 8.4, can also provide an indication for which specific application a particular system is more suitable. Testing in the second stage aims at assessing performance in the light of the specific application, by incorporating system-level service-representative load-versus-time profiles (section 8.5). The present report is limited to system-level testing aspects related to the use of electrolysers in conventional grid-connected applications (grey boxes in Figure 29). In future, applications for renewable electricity (distributed generation, remote off-grid) may be included (green boxes in Figure 29).

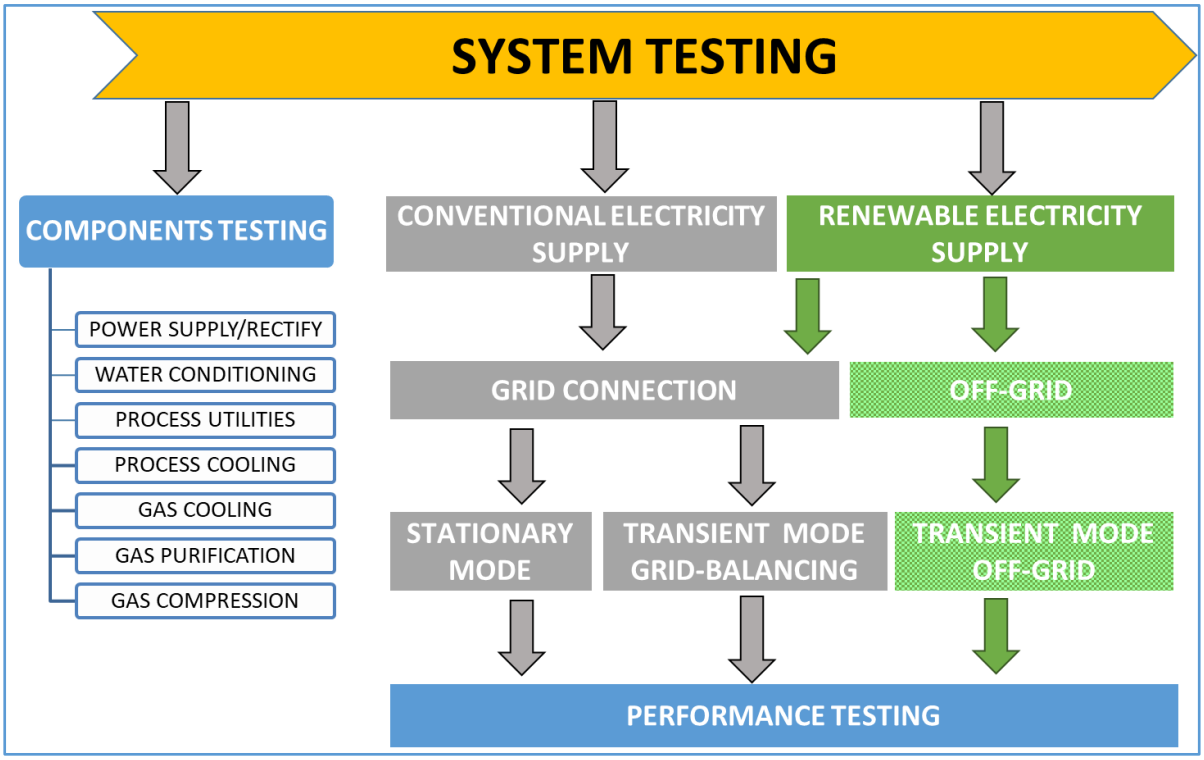

Figure 29. System testing scheme

8.2 Overview of grid services

Electricity grid services refer to a range of services needed to maintain a reliable and balanced electrical power system. Grid services are used to address imbalances between supply and demand, maintain a proper flow and direction of electricity, and help the system recover after a power system event. Conventionally, grid services are provided to the grid operators by big generation units and large scale industrial loads, either as an obligation or through a service market. Small/medium scale units are usually excluded by grid operators because grid services have specific requirements on capacity, ramping, duration, location and auxiliary units for measurement, communication and control etc.

Grid services at the transmission level ("ancillary services") include frequency response (to maintain system frequency with automatic/manual active power reserves), voltage control (by reactive power support), capacity and congestion management (i.e. strategic reserves aimed at increasing security of supply by organizing adequate long-term peak and non-peak capacity), and redundancy support (providing emergency power, black start capability and island capability)[21].

Increasing penetration of intermittent renewables and of distributed energy resources intensifies the demand for grid services to manage enhanced variability and uncertainty of generation at different voltage levels and to avoid or delay network reinforcement[22]. At the same time, the importance of using different technologies, such as electrolysers, to provide grid service is increasingly recognized and facilitated by improved market designs and regulations.

8.2.1 grid balancing services to address network frequency deviations

Because of the impossibility to store electricity, it is necessary to balance power generation and consumption at all times in the network. Any non-balance is manifested through a change in frequency of the alternating current: frequency increases when active power generation exceeds active power consumption and decreases in the opposite case.

The currently applicable EU Regulatory Framework on the provision of grid balancing services required to be deployed upon a frequency disturbance event, is summarised in Appendix C. This section introduces the concepts which are relevant for electrolyser systems contributing in the provision of grid balance services.

When a frequency imbalance occurs, a series of actions involving three frequency control processes and related active power reserves are sequentially deployed, either automatically and/or manually, at varying time scales to return frequency to the nominal 50 Hz (see table 29).

[21] The electricity distribution grid also needs a number of support functions for its safe and reliable operation. These resemble to a large degree those at transmission level, but are targeted to local issues at medium/low voltage levels. Therefore, frequency support is presently not needed at distribution level.

[22] This may require ancillary grid services at distribution level in future

Table 29. types of RESERVES for grid balancing[23]

Frequency Containment Reserve (FCR), (EU)2017/1485 art. 142, FCRs are automatically triggered within 15-30 s from a disturbance to prevent further frequency deviation and maintain frequency within a range centered around 50Hz[24]
Frequency Restoration Reserve (FRR), (EU)2017/1485 art. 143, FRRs take over from the activated FCR and are deployed automatically (aFRR, fast ramping) or manually (mFRR, slower ramping) to bring the frequency back to 50 Hz
Replacement Reserve (RR), (EU)2017/1485 art. 144. RRs progressively restore the activated FRRs to be prepared for a further system imbalance and/or support the FRR activation

Regulation (EU)2017/1485 stipulates that each TSO is responsible for establishing a pre-qualification process to assess a service provider's capability against the technical requirements for the intended services FCR, FRR and RR. These requirements are briefly described below.[25]

8.2.2 pre-qualification

The terms FCR, a/mFRR and RR which represent the fundamental principles for frequency control, are harmonized in the EU. However, due to structural differences among countries, actual implementation of frequency control and formulation of the corresponding requirements varies.

A service provider wanting to offer grid balancing services has to provide evidence of meeting a number of pre-qualification requirements. These include successfully passing acceptance criteria in dedicated tests established by the relevant transmission system operator (TSO). In such tests, the capability of meeting the performance required by the TSO in terms of capacity, speed of action, ability of ramping, and ability of offering a reliable dynamic/non-dynamic response over the designated service period is evaluated.

[23] Terminology still sometimes used classifies frequency reserves as Primary (FCR), Secondary (aFRR) and Tertiary Reserves (mFRR fast tertiary, RR slow tertiary)

[24] Different frequency bandwidths in different synchronous areas

[25] In addition to prequalification requirements for grid balancing, grid operators also set technical requirements for limiting other network disturbances. These include electromagnetic compatibility requirements, avoidance of rapid voltage changes, harmonics, phase unbalances, reactive power compensation, ….

Load profiles by the TSOs[26] include both step signals and continuous signals, either practically measured (historical/real-time) or developed through simulations. Step signals are used to test performance characteristics such as accuracy, response delay, speed of response, ramping performance, etc., thereby offering an impression of the unit's technical performance. Continuous signals are used to test the unit's response within a longer time period. Currently, the total duration of pre-qualification tests varies from a few minutes up to two hours. Durability testing, as applied a cell/short stack level (see 7.5), to assess the long term performance and degradation of a service providing unit are not requested by grid operators during pre-qualification.

Assessment criteria for each performance characteristic are normally expressed in terms of permissible response ranges.

Because load-versus-time profiles included in the pre-qualification requirements of TSOs in the different member states are different for the three frequency control processes, it is useful to harmonise them into a single set of representative load profiles to be used for pre-qualification purposes[27].

8.3 electrolysers for grid balancing support

The European Network of TSOs for the electricity grid (ENTSO-E) acknowledges that a range of technologies can serve grid balancing, such as power generators, batteries, flow batteries, electrolysers, etc. Which of these technologies is eligible depends on the conditions applicable in national reserve markets.

Because of their capacity to be connected/disconnected/regulated when requested to do so by grid operators, electrolysers can in principle act as flexible electrical loads (flexible demand) and thereby offer a variety of grid balancing services, provided that operation is technically and economically feasible. Because grid balancing is as a minimum in the MW range, at present only AWE and PEMWE technologies can deliver grid balancing services[28].

To qualify for providing grid balancing services, electrolysers must have an appropriate range of operational capacity and of dynamic characteristics. The most relevant dynamic characteristics are load flexibility and response time (reactivity) under fast load changes (up/down). Load flexibility refers to the capability of being operated under a broad range of load. The response time under fast load changes depends on the electrolyser status, namely in operation, at ambient conditions, or stand-by conditions (See 8.4).

Because of the aforementioned difference in pre-qualification requirements in Europe from service to service and from country to country, evaluating the suitability of an electrolyser system to offer grid balancing services would greatly benefit from an agreement on a set of representative load-versus-time profiles to assess electrolyser system load flexibility and response times. This is the objective of the QualyGridS project, and a selection of the harmonised set of load profiles developed in this project is summarised and presented in the subsequent sections of this report.

[26] Regulation (EU)2017/1485 prescribes the minimum features that a pre-qualification load-versus-time must possess. (see appendix C)

[27] This is also in line with the recommendation to promote introduction of standard products to enhance competition between providers of balancing services (Network code on Electricity Balancing Article 31.6)

[28] Water electrolysers in the kW range also have potential when many units are aggregated for providing balancing services.

8.4 fit-for-purpose testing

This set of tests aims at checking whether the electrolyser system is fit-for-purpose for use as flexible electric load and for which grid balancing service(s) it might in principle be suitable. The characteristics addressed are available power range and duration required for transients, as shown in Figure 46 of appendix C. Based on the outcome of these "screening" tests, the testing protocols relevant for the specific grid service (section 8.x) can then be applied in the next step (section 8.5).

The set of agreed screening tests is listed in Table 30 and the different protocols taken from [10, deliverable 2.4] are reported below. Some wording in protocols titles and tables has been adapted for the use in this document

Table 30. FIT-for-Purpose test PROTOCOLS [10] QualyGridS

PROTOCOLS	
IDENTIFICATION OF SYSTEM POWER (SP) RANGE[29]	8.4.1
DETERMINATION OF MINIMUM-MAXIMUM SP DYNAMICS (RESPONSE TIME)	8.4.2
DETERMINATION OF NOMINAL TO MAXIMUM SP DYNAMICS (RESPONSE TIME)	8.4.3
RESPONSE TIME FROM NOMINAL SYSTEM POWER TO STAND BY[30]	8.4.4
TIME AT MAXIMUM SYSTEM POWER[31]	8.4.5
COLD START TIME TO NOMINAL POWER	8.4.6
START-UP TIME FROM STANDBY MODE	8.4.7
POWER DOWN TO STANDBY TIME	8.4.8

8.4.1 IDENTIFICATION OF SYSTEM POWER RANGE

This protocol aims at defining the minimum and maximum power for the system. The maximum power corresponds to generating the highest possible continuous output of hydrogen. The minimum power corresponds to the lowest continuous hydrogen output. The protocol is described in Table 31 and the test profile is schematically shown in Figure 30

[29] Identified as "Protocol for identification of the power range available for grid services" in [10]

[30] Identified as "Protocol for determination of power down to standby time" in [10]

[31] Identified as "Protocol for Determination of Duration of Maximum Power" in [10]

Table 31. SYSTEM POWER RANGE TEST PROTOCOL, [10]

STEP	DESCRIPTION
1	Start system
2	Set system power for maximum possible continuous H_2 production output (Comment: for most systems this state will be the Nominal Operational Mode [2], for systems with overload capability it might be higher than nominal power)
3	Wait for power to stabilize *
4	Note the power $P_1=P_{max}$ system
5	Keep the state for 2 hours with power variation below $\pm 2\% \cdot P_{max}$ system
6	Set system at 0% H_2 production output (or minimal continuously attainable output), respectively minimum rectifier power input
7	Wait for power to stabilize*
8	Note the power $P2=P_{min}$ system
9	Keep the state for 2 hours with power variation below $\pm 5\% \cdot P_{min}$ system
10	End of test
	The system power is considered stable if the average power of two consecutive intervals of 60 seconds does not differ by more than (±2%· P max system)

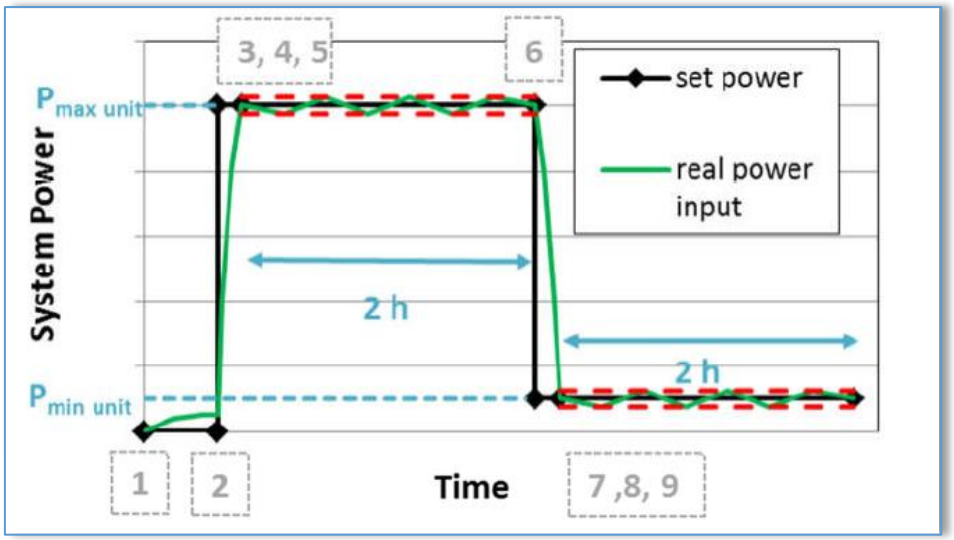

Figure 30. example of system Power range test profile, [10]

- P_{max} system is defined as the average electrical power input in step 5.
- P_{min} system is defined as the average electrical power input in step 8.

8.4.2 DETERMINATION OF MINIMUM-MAXIMUM SP DYNAMICS (RESPONSE TIME)

This protocol aims at identifying the times required for the system to switch from minimum to maximum power and vice-versa. The protocol is described in Table 32 and the test profile is schematically shown in Figure 31.

Table 32. MIN-MAX DYNAMICS (RESPONSE TIME) TEST PROTOCOL, [10]

STEP	DESCRIPTION
1	Set system power at Pmin system for 15 min
2	Set system power P_{max} system
3	Wait for rectifier power to stabilize to ±0.05·(P_{max} system - P_{min} system)
4	Hold at P_{max} system for 15 min
5	Set system power at 0% H_2 production output (or minimal continuously attainable output) as defined as P_{min} system
6	Wait for rectifier power to stabilize to ±0.05·(P_{max} system - P_{min} system)
7	maintain system power at Pmin system for 15 min

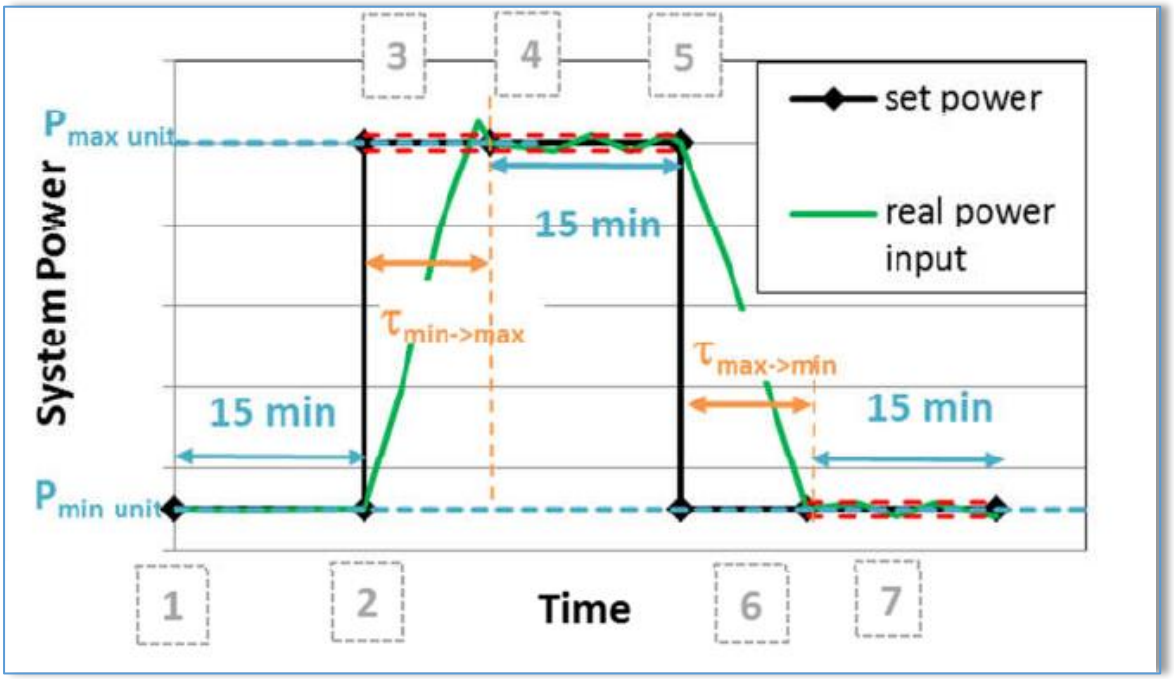

Figure 31. Response times Min-Max test profile, [10]

- The Response Time Minimum Power to Maximum Power $\tau_{min->max}$ is defined as the time from beginning of step 2 to end of step 3.
- The Response Time Maximum Power to Minimum Power $\tau_{max->min}$ is defined as the time from beginning of step 5 to end of step 6.

8.4.3 DETERMINATION OF NOMINAL TO MAXIMUM SP DYNAMICS (RESPONSE TIME)

This protocol is only relevant for systems which can be operated continuously for at least 15 minutes above nominal power. The protocol is described in Table 33 and the test profile is schematically shown in Figure 32.

Table 33. NOMINAL TO MAXIMUM SP DYNAMICS (RESPONSE TIME) TEST PROTOCOL, [10]

STEP	DESCRIPTION
1	Set system operation at nominal power for 15 min
2	Set system power to P_{max} system
3	Wait for rectifier power to stabilize to ±0.05·(P_{max} system - P_{min} system)
4	Hold at P_{max} system for 15 min
5	Set system at nominal system power
6	Wait for ~~rectifier~~ power to stabilize to ±0.05·(P_{max} system - P_{min} system)
7	maintain system at nominal power for 15 min

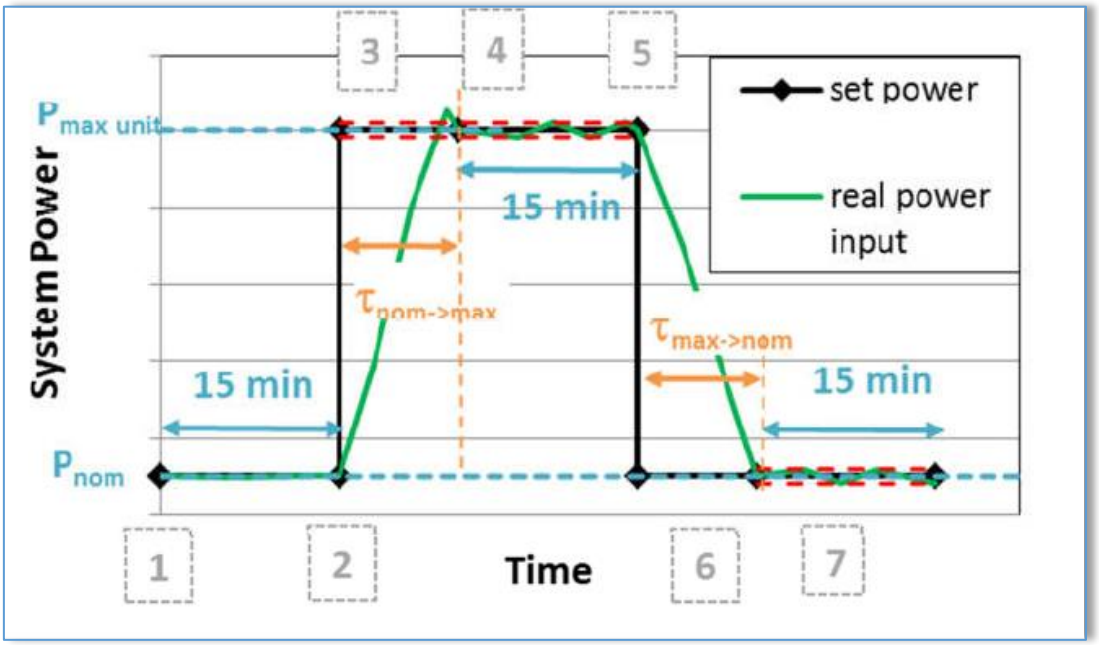

Figure 32. Example of Nominal-Maximum dynamics identification test profile, [10]

- The Response Time nominal Power to Maximum Power $\tau_{nom->max}$ is defined as the time from beginning of step 2 to end of step 3.
- The Response Time Maximum Power to Nominal Power $\tau_{max->nom}$ is defined as the time from beginning of step 5 to end of step 6.

8.4.4 RESPONSE TIME FROM NOMINAL POWER TO STAND BY

This protocol aims at identifying the time required for the system to switch from nominal power to (one of) the stand-by condition(s) identified by the manufacturer. The protocol is described in Table 34.

Table 34. RESPONSE TIME FROM NOMINAL POWER TO STAND BY TEST PROTOCOL, [10]

STEP	DESCRIPTION
1	Set system operation at NOMINAL power for 2 hours
2	Set system power at Pmin system
3	When 0% H_2 production or minimum continuously attainable output is reached switch the system to standby state as defined by the manufacturer
4	Wait for standby state to be reached

Time from nominal to standby state: $\tau_{down\_to\_standby}$=Time from start of Step 2 to end of Step 3.

The test should be repeated for each of the standby modes identified by the manufacturer.

8.4.5 TIME AT MAXIMUM SYSTEM POWER

This protocol is only relevant for systems which can be operated continuously for at least 15 minutes above nominal power. The protocol is described in Table 35 and the test profile is schematically shown in Figure 33.

Table 35. TIME AT MAXIMUM SYSTEM POWER TEST PROTOCOL, [10]

STEP	DESCRIPTION
1	Set system operation at nominal power for 15 min
2	Set system power to P_{max} system
3	Wait for rectifier power to stabilize to ±0.05·(P_{max} system - P_{min} system)
4	Hold at P_{max} system for 4 hours or until system specifications require power reduction
5	Set system at nominal system power
6	Wait for rectifier power to stabilize to ±0.05·(P_{max} system - P_{min} system)
7	Operate at nominal power for 15 min

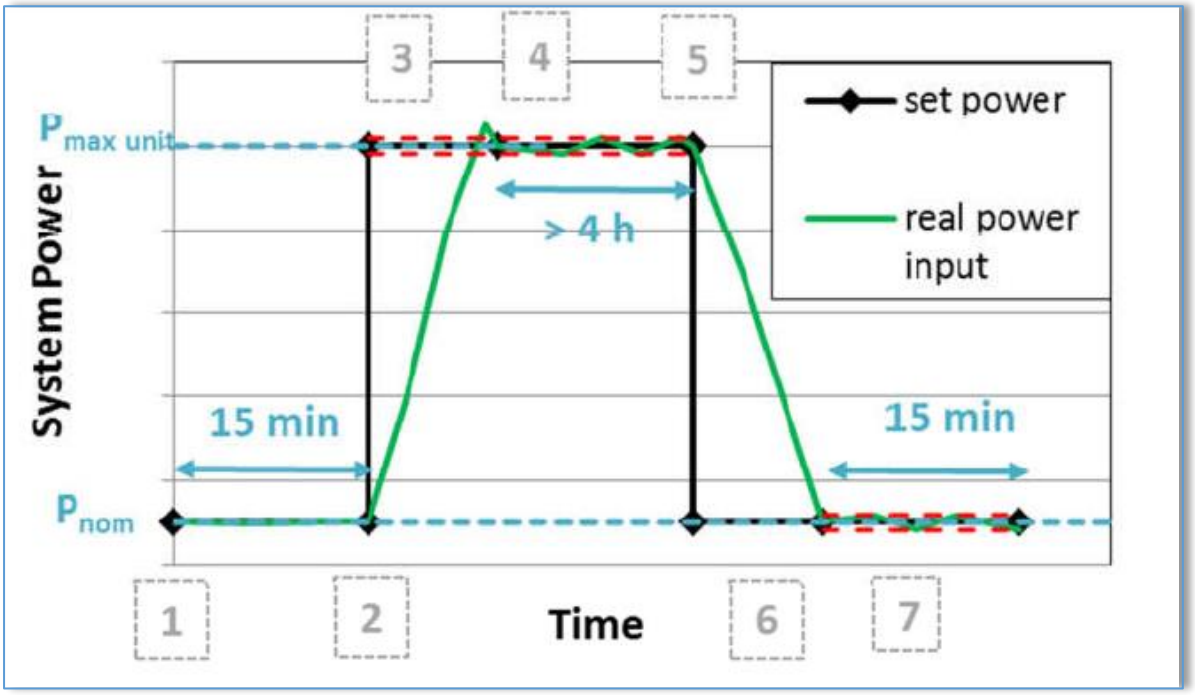

Figure 33. Example of time at maximum power test profile

The duration time of maximum power τmax for which the system can remain in maximum power is determined by the duration of step 4.

8.4.6 COLD START TIME TO NOMINAL POWER TEST PROTOCOL

At the beginning of this test the system should have been in Cold Standby State for at least 2 hours.

Table 36. COLD START TIME TO NOMINAL POWER TEST PROTOCOL, [10]

STEP	DESCRIPTION
1	Trigger the "start" button on the system
2	Wait for end of start-up protocol to reach nominal power
3	Wait for rectifier input power constant by +- 5% in a 15 min interval

Cold Start Time to Nominal Power: τ_{cold} = Time from start of Step 1 to end of Step 3 minus 15 min.
In case the nominal power is not reached within 30 minutes, the test can be interrupted since performing the following grid services from standby state will not be possible for this system.

8.4.7 START-UP TIME FROM STANDBY MODE TEST PROTOCOL

At the beginning of this test the system should have been in standby state for at least 2 hours. For systems that have different types of standby modes the start-up time from standby mode should be determined for each of these states.

Table 37. START-UP TIME FROM STANDBY MODE TEST PROTOCOL, [10]

STEP	DESCRIPTION
1	Set the power of the system power control to nominal power
2	Wait for rectifier input power constant by +- 5% in a 15 min interval

Start-up time from Standby State to Nominal Electrical Power Input: $\tau_{start,standby}$= Time from start of Step 1 to end of Step 2 minus 15 min.
Average Electrical Power Input of the system in Standby State is $P_{standby}$

8.4.8 POWER DOWN TO STANDBY TIME TEST PROTOCOL

At the beginning of this test the system should have been at nominal power for at least 2 hours.

Table 38. POWER DOWN TO STANDBY TIME TEST PROTOCOL, [10]

STEP	DESCRIPTION
1	Set system at 0% H2 production output (or minimal continuously attainable output) as defined as Pmin system state
2	When 0% H2 production or minimum continuously attainable output is reached switch the system to standby state as defined by the manufacturer
3	Wait for standby state to be reached

Time from nominal to standby state: $\tau_{down\_to\_standby}$ = Time from start of Step 1 to end of Step 3.
If different types of standby mode are available for this electrolyser, the test should be repeated for each of the standby modes.

8.4.9 FIT FOR PURPOSE TEST RESULTS AND VALIDITY CRITERIA

The result of the fit for purpose test can be summarised as follow:

1- The available power range for grid services depending on the selected lower power state is:

Power Range ΔP = $P_{max\ system}$ -$P_{min\ system}$ or

$P_{max\ system}$ - $P_{standby}$ or

$P_{max\ system}$ - $P_{cold\text{-}standby}$

Minimum partial load operation = $P_{min\ system}$ / $P_{max\ system}$ %

2- The dynamics for increasing power depends on the selected lower and upper power state:

Time to power up τ_{up} = $\tau_{cold} + \tau_{nom->max}$ or

$\tau_{start,standby} + \tau_{nom->max}$ or

$\tau_{min->max}$

3- The dynamics for decreasing power depends on the selected lower and upper power state:

Time to power down τ_{down} = $\tau_{max->min}$

$\tau_{down\_to\_standby} + \tau_{max->nom}$ or

$\tau_{down\_to\_cold} + \tau_{max->nom}$

minimum part load to full load is calculated as rate of load change (%) per second using $\tau_{min->max}$

full load to minimum part load is calculated as rate of load change (%) per second using $\tau_{max->min}$

8.4.9.1 DATA MEASUREMENT

- The recommended data sampling rate is 1 per second.
- Values for three or more measurements of the test input and output parameters shall be within the range of ±5% of their average.

8.5 LOAD PROFILES for grid balancing

As indicated in section 8.2.2, the actual implementation of frequency control and of the formulation of the corresponding requirements vary from country to country. In particular, load-versus-time profiles included in the pre-qualification requirements of TSOs in the different member states are different for the three grid balancing services identified in Regulation EU(2017)1485 (Table 29). It is therefore useful to harmonise the different load profiles into a single set of representative load profiles to be used for pre-qualification purposes of electrolysers. This is the main objective of the Qualigrids project which has formulated the set of 7 load profiles listed in Table 39, corresponding to the frequency control processes for grid balancing listed in Table 29. The set of harmonised load profiles is summarised and presented in this section.

Table 39. load profiles for grid balancing

	LOAD PROFILES FOR GRID BALANCING	SECTION
1	**FREQUENCY CONTAINMENT RESERVE FCR**	**8.5.1**
	***AUTOMATED* FREQUENCY RESTORATION RESERVE aFRR**	**8.5.2**
2	➢ **aFRR Negative Control Power**	**8.5.2.1**
3	➢ **aFRR Positive Control Power**	**8.5.2.2**
	***MANUAL* FREQUENCY RESTORATION RESERVE mFRR**	**8.5.3**
4	➢ **mFRR Negative Control Power**	**8.5.3.1**
5	➢ **mFRR Positive Control Power**	**8.5.3.2**
	REPLACEMENT RESERVES RR	**8.5.4**
6	➢ **RR Negative (Upward) Control Power**	**8.5.4.1**
7	➢ **RR Positive (Downward) Control Power**	**8.5.4.2**

The load profiles used by TSOs for pre-qualification purposes represent those in the intended grid balance application and have been referred to as system-level RWD load profiles (see section 7.7). Hence the harmonised load profiles established by Qualigrid also represent system-level RWD. Individual load profiles from this set are therefore used for assessing degradation rate or durability under dynamic conditions in in-situ tests at cell/short stack level (see 7.7).

It is to be noted that the set of 7 harmonised load profiles simulating requirements for grid balancing services does not prevail over and does not intend to substitute the regulatory requirements regarding pre-qualification in different member states. Consequently, electrolyser system compliance with these load profiles described below does not imply meeting the pre-qualification requirements by TSOs.

8.5.1 FREQUENCY CONTAINMENT RESERVES (FCR) test protocol

The agreed load profile, depicted in Figure 34, aims at determining the electrolyser system response to positive and negative power steps, by assessing the characteristic duration times identified in FCR prequalification load profiles. The associated agreed test protocol is described in Table 40. The parameters Pup, Plow and Pmed are determined as described in 8.4.1 as P_{max}, P_{min}, but they can be limited for grid servicing to a smaller power system interval. For this reason, in this section the terms P_{up}, P_{low} and P_{med} will be used. P_{med} is defined as $0.5(P_{low}+P_{up})$. The same apply for all test protocols given in table 39

Table 40. agreed FCR test protocol

STEP	TEST TIME (S)	DESCRIPTION
1	0	Set the power set point to P_{med}. Measure the system electrical power input and the rectifier electrical power input vs. time.
2	3600	Set the power set point to P_{up}. Measure the system electrical power input and the rectifier electrical power input vs. time.
3	4530	Set the power set point to P_{med}. Measure the system electrical power input and the rectifier electrical power input vs. time.
4	5460	Set the power set point to P_{up}. Measure the system electrical power input and the rectifier electrical power input vs. time.
5	6390	Set the power set point to P_{med}. Measure the system electrical power input and the rectifier electrical power input vs. time.
6	7320	Set the power set point to P_{low}. Measure the system electrical power input and the rectifier electrical power input vs. time.
7	8250	Set the power set point to P_{med}. Measure the system electrical power input and the rectifier electrical power input vs. time.
8	9180	Set the power set point to P_{low}. Measure the system electrical power input and the rectifier electrical power input vs. time.
9	10110	Set the power set point to P_{med}. Measure the system electrical power input and the rectifier electrical power input vs. time.
10	10240	End of test.

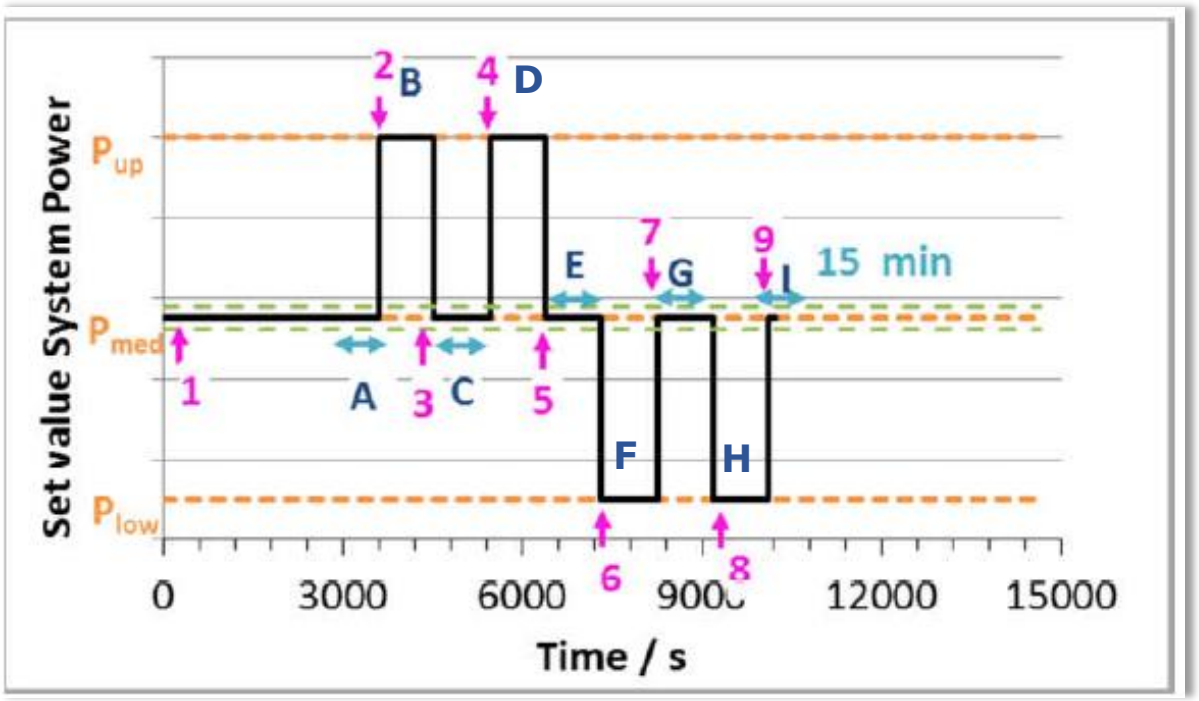

Figure 34. FCR PROFILE, illustration of phases A-I for stability evaluation, allowed range for system power during these phases (marked with green dashed line) and steps 1-8. [10]

The parameters to establish are related to the upward and downward ramps:

- **Ramps up duration (t_m; t_{full}):** upward ramps (2 and 4 (Figure 34)) are characterised by two characteristic times (Figure 35) which have to be determined for each of the ramps.

  t_m is the time from the start of the power increase to reach 50% of the value of the imposed step response, i.e. system power reaching $(0.5 \cdot (P_{up}-P_{med}))$.

  t_{full} is the time from the start of the power increase to stabilise system power at P_{up}: In the following 15 min the system power must remain between P_{up} and $(P_{up} \pm 0.05 \cdot (P_{up}- P_{med}))$.

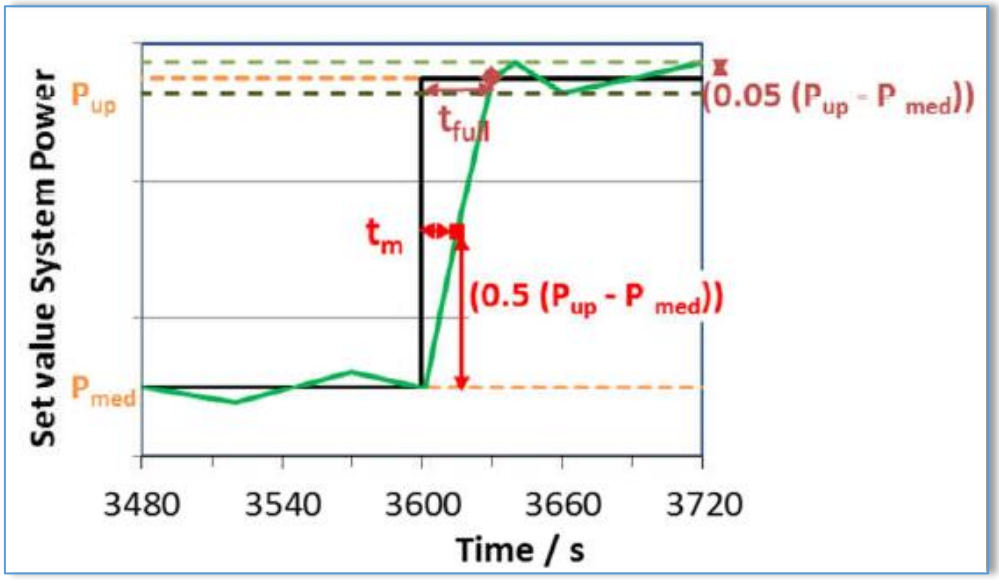

Figure 35. FCR PROFILE: illustration evaluation of ramps up. Black full line: power set points, green full line example of real system power, [10]

- **Ramps down duration (t_m; t_{full})**: downward ramps 6 and 8 (Figure 34) are characterised by two characteristic times (Figure 36) which have to be determined for each of the ramps:

  t_m is the time from the start of the power decrease to reach 50% of the value of the set step response, i.e. system power reaching $(0.5 \cdot (P_{med} - P_{low}))$.

  t_{full} is the time from the start of the power decrease to stabilise system power at P_{low}: In the following 15 min the system power must remain between P_{low} and $(P_{low} \pm 0.05 \cdot (P_{up} - P_{med}))$.

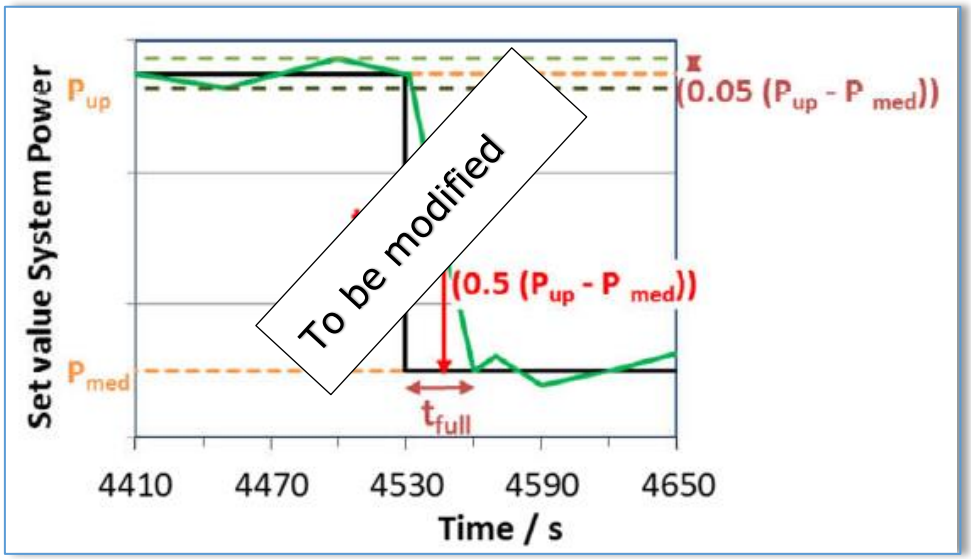

Figure 36. FCR PROFILE: Illustration evaluation of ramps down. Black full line: power set points, green full line example of real system power

Data analysis

- **Initial response time (t_{init}):** For steps 2, 4, 6 and 8 the time between the change of the power setpoint and the start of the system response is to be determined. For an upward ramp this is the time between the step request signal and the moment when the system power monotonically increases and has the value $>P_{med}$. For a downward ramp this is the time between the step request signal and the moment when the system power monotonically decreases and has the value $<P_{med}$.

KPI Initial response time: Maximum of t_{init} for ramps 2, 4, 6 and 8. Required value: 1.5 sec

During all phases of constant power setpoint, power fluctuations must be limited to maximum 0.05·(Pmed-Plow):

- Power setting at P_{med}: The maximum deviation from P_{med} during phases A, C, E, G and I (see Figure 34) shall be documented in the 15 min period before the respective imposed power step changes (2, 4, 6, 8) and before the end of test
- Power setting at P_{up}: The maximum deviation from P_{up} during phases B and D (see Figure 34) shall be documented in the 15 min period following the first 30 s after the respective imposed power step changes 2 and 4
- Power setting at P_{low}: The maximum deviation from P_{low} during phases F and H (see Figure 34) shall be documented in the 15 min period following the first 30 s after the respective imposed power step changes 6 and 8

The agreed performance targets for the FCR test are listed in Table 41.

Table 41. FCR performance targets

Indicator	Symbol	Target
Ramp duration	t_m	≤15 s
	t_{full}	≤ 30 s
Initial response time	t_{init}	≤ 1.5 s
Power stability		≤ 0.05 · (P_{med} - P_{low})

8.5.2 AUTOMATED FREQUENCY RESTORATION RESERVES (aFRR) TESTING PROTOCOL

This protocol aims at determining the electrolyser system response to power steps by assessing the characteristic duration times identified in aFRR prequalification load profiles. The protocol consists of two parts, with fast and medium ramp rates upwards and downwards, enabling separate evaluation of the services of negative and positive control power, respectively.

8.5.2.1 aFRR NEGATIVE CONTROL POWER (electrolyser power increase upon request)

The agreed load profile is depicted in Figure 37 and the associated agreed test protocol is described in Table 42.

Table 42. aFRR Upward ramp protocol from lower power level

STEP	DESCRIPTION
1	Set system at P_{up}
2	Wait for system power to stabilize*
3	Operate at this level for 1 hour
4	At $t=t_1$, initiate power ramp of power (-25% (P_{up} - P_{low})) in 800 seconds
5	$t=t_1+800$ seconds: end of the ramp
6	Keep set power for 5 minutes
7	Set system at P_{up} (the time the system needs to return to P_{up} is not Evaluated)
8	Wait for system power to stabilize *
9	At $t=t_2$, initiate power ramp of power (-50% (P_{up} - P_{low})) in 800 seconds
10	$t=t_2+800$ seconds: end of the ramp
11	Keep set power for 5 minutes
12	Set system at P_{up} (the time the system needs to return to P_{up} is not evaluated)
13	Wait for system power to stabilize *
14	At $t=t_3$, initiate power ramp of power (-75% (P_{up} - P_{low})) in 800 seconds
15	$t=t_3+800$ seconds: end of the ramp
16	Keep set power for 5 minutes
17	Set system at P_{up} (the time the system needs to return to P_{up} is not evaluated)
18	Wait for system power to stabilize *
19	At $t=t_4$, initiate power ramp of power (-100% (P_{up} - Pl_{ow})) in 800 seconds
20	$t=t_4+800$ seconds: end of the ramp
21	Keep set power for 15 minutes
22	At $t=t_5$, initiate power ramp of power (+100% (P_{up} - P_{low})) in 800 seconds
23	$t=t_5+800$ seconds: end of the ramp
24	Keep set power for 15 minutes

STEP	DESCRIPTION
25	At $t=t_6$, initiate power ramp of power (-100% (P_{up} - P_{low})) in 800 seconds
26	$t=t_6$+800 seconds: end of the ramp
27	Keep set power for 15 minutes
28	At $t=t_7$, initiate power ramp of power (+100% (P_{up} - P_{low})) in 800 seconds
29	$t=t_7$+800 seconds: end of the ramp
30	Keep set power for 15 minutes
31	at=t_8, initiate power ramp of power (-25% (P_{up} - P_{low})) in 133 seconds
32	$t=t_8$+133 seconds: end of the ramp
33	Keep set power for 5 minutes
34	Set system at P_{up} (the time the system needs to return to P_{up} is not evaluated)
35	Wait for system power to stabilize*
36	At $t=t_9$, initiate power ramp of power (-50% (P_{up} - P_{low})) in 133 seconds
37	$t=t_9$+133 seconds: end of the ramp
38	Keep set power for 5 minutes
39	Set system at P_{up} (the time the system needs to return to P_{up} is not evaluated)
40	Wait for system power to stabilize*
41	At $t=t_{10}$, initiate power ramp of power (-75% (P_{up} - P_{low})) in 133 seconds
42	$t=t_{10}$+133 seconds: end of the ramp
43	Keep set power for 5 minutes
44	Set system at P_{up} (the time the system needs to return to P_{up} is not evaluated)
45	Wait for system power to stabilize*
46	At $t=t_{11}$, initiate power ramp of power (-100% (P_{up} - P_{low})) in 300 seconds
47	$t=t_{11}$+300 seconds: end of the ramp
48	Keep set power for 15 minutes
49	At $t=t_{12}$, initiate power ramp of power (+100% (P_{up} - P_{low})) in 300 seconds
50	$t=t_{12}$+300 seconds: end of the ramp
51	Keep set power for 15 minutes
52	At $t=t_{13}$, initiate power ramp of power (-100% (P_{up} - P_{low})) in 300 seconds
53	$t=t_{13}$+300 seconds: end of the ramp
54	Keep set power for 15 minutes
55	At $t=t_{14}$, initiate power ramp of power (+100% (P_{up} - P_{low})) in 300 seconds
56	$t=t_{14}$+300 seconds: end of the ramp
57	Wait for system power to stabilize*
58	At $t=t_{15}$, initiate power ramp of power (-100% (P_{up} - P_{low})) in 300 seconds

STEP	DESCRIPTION
59	$t=t_{15}+133$ seconds: end of the ramp
60	Keep set power for 15 minutes
61	At $t=t_{16}$, initiate power ramp of power (+100% (P_{up} - P_{low})) in 133 seconds
62	Keep set power for 5 minutes
63	End of test

*The system power is considered stable if the average power of two consecutive intervals of 60 seconds does not differ by more than (±0.05 · (Pup-Plow))

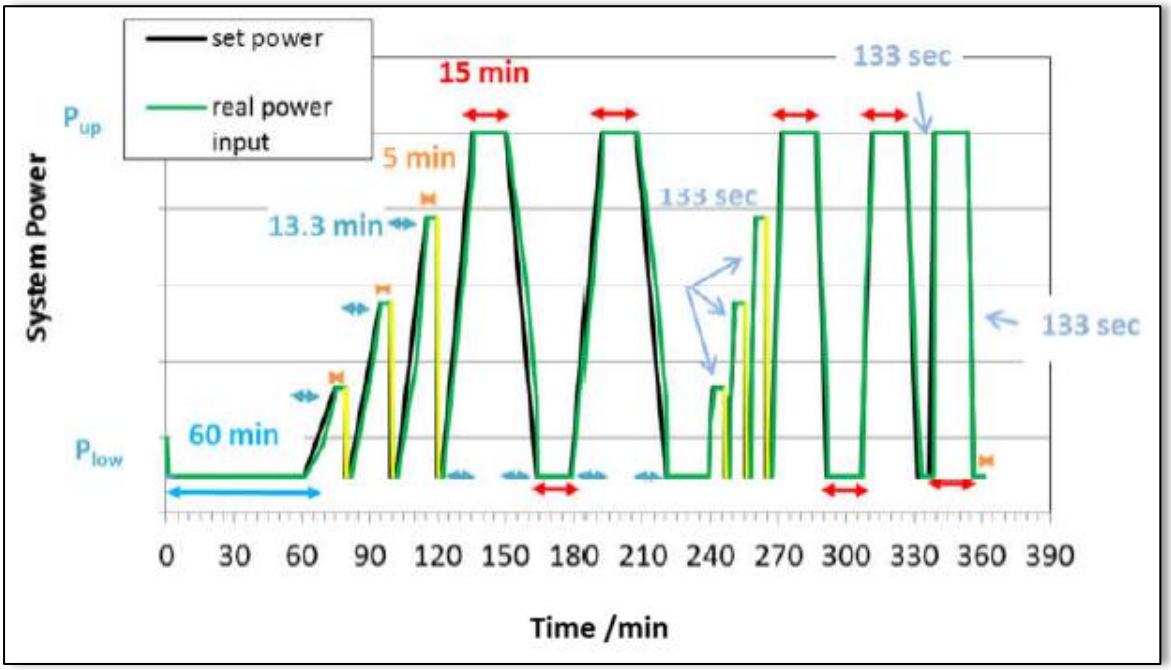

Figure 37. aFRR PROFILE WITH NEGATIVE CONTROL POWER,[10]

8.5.2.2 aFRR POSITIVE CONTROL POWER (electrolyser power decrease upon request)

The agreed load profile is depicted in Figure 38 and the associated agreed test protocol is described in Table 43.

Table 43. aFRR downward ramp protocol from upper power level

STEP	DESCRIPTION
1	Set system at P_{low}
2	Wait for system power to stabilize*
3	Operate at this level for 1 hour
4	At $t=t_1$, initiate power ramp of power (25% (P_{up} - P_{low})) in 800 seconds
5	$t=t_1+800$ seconds: end of the ramp

STEP	DESCRIPTION
6	Keep set power for 5 minutes
7	Set system at P_{low} (the time the system needs to return to P_{low} is not Evaluated)
8	Wait for system power to stabilize *
9	At t=t_2, initiate power ramp of power (50% (P_{up} - P_{low})) in 800 seconds
10	t=t_2+800 seconds: end of the ramp
11	Keep set power for 5 minutes
12	Set system at P_{low} (the time the system needs to return to P_{low} is not evaluated)
13	Wait for system power to stabilize *
14	At t=t_3, initiate power ramp of power (75% (P_{up} - P_{low})) in 800 seconds
15	t=t_3+800 seconds: end of the ramp
16	Keep set power for 5 minutes
17	Set system at P_{low} (the time the system needs to return to P_{low} is not evaluated)
18	Wait for system power to stabilize *
19	At t=t_4, initiate power ramp of power (100% (P_{up} - P_{low})) in 800 seconds
20	t=t_4+800 seconds: end of the ramp
21	Keep set power for 15 minutes
22	At t=t5, initiate power ramp of power (-100% (P_{up} - P_{low})) in 800 seconds
23	t=t_5+800 seconds: end of the ramp
24	Keep set power for 15 minutes
25	At t=t_6, initiate power ramp of power (+100% (P_{up} - P_{low})) in 800 seconds
26	t=t_6+800 seconds: end of the ramp
27	Keep set power for 15 minutes
28	At t=t_7, initiate power ramp of power (-100% (P_{up} - P_{low})) in 800 seconds
29	t=t_7+800 seconds: end of the ramp
30	Keep set power for 15 minutes
31	at=t_8, initiate power ramp of power (25% (P_{up} - P_{low})) in 133 seconds
32	t=t_8+133 seconds: end of the ramp
33	Keep set power for 5 minutes
34	Set system at P_{low} (the time the system needs to return to P_{low} is not evaluated)
35	Wait for system power to stabilize*
36	At t=t_9, initiate power ramp of power (50% (P_{up} - P_{low})) in 133 seconds
37	t=t_9+133 seconds: end of the ramp
38	Keep set power for 5 minutes
39	Set system at P_{low} (the time the system needs to return to P_{low} is not evaluated)
40	Wait for system power to stabilize*
41	At t=t_{10}, initiate power ramp of power (75% (P_{up} - P_{low})) in 133 seconds
42	t=t_{10}+133 seconds: end of the ramp

STEP	DESCRIPTION
43	Keep set power for 5 minutes
44	Set system at P_{low} (the time the system needs to return to P_{low} is not evaluated)
45	Wait for system power to stabilize*
46	At $t=t_{11}$, initiate power ramp of power (100% (P_{up} - P_{low})) in 300 seconds
47	$t=t_{11}$+300 seconds: end of the ramp
48	Keep set power for 15 minutes
49	At $t=t_{12}$, initiate power ramp of power (-100% (P_{up} - P_{low})) in 300 seconds
50	$t=t_{12}$+300 seconds: end of the ramp
51	Keep set power for 15 minutes
52	At $t=t_{13}$, initiate power ramp of power (+100% (P_{up} - P_{low})) in 300 seconds
53	$t=t_{13}$+300 seconds: end of the ramp
54	Keep set power for 15 minutes
55	At $t=t_{14}$, initiate power ramp of power (-100% (P_{up} - P_{low})) in 300 seconds
56	$t=t_{14}$+300 seconds: end of the ramp
57	Wait for system power to stabilize*
58	At $t=t_{15}$, initiate power ramp of power (+100% (P_{up} - P_{low})) in 300 seconds
59	$t=t_{15}$+133 seconds: end of the ramp
60	Keep set power for 15 minutes
61	At $t=t_{16}$, initiate power ramp of power (-100% (P_{up} - P_{low})) in 133 seconds
62	Keep set power for 5 minutes
63	End of test

*The system power is considered stable if the average power of two consecutive intervals of 60 seconds does not differ by more than (±0.05 · (P_{up}-P_{low}))

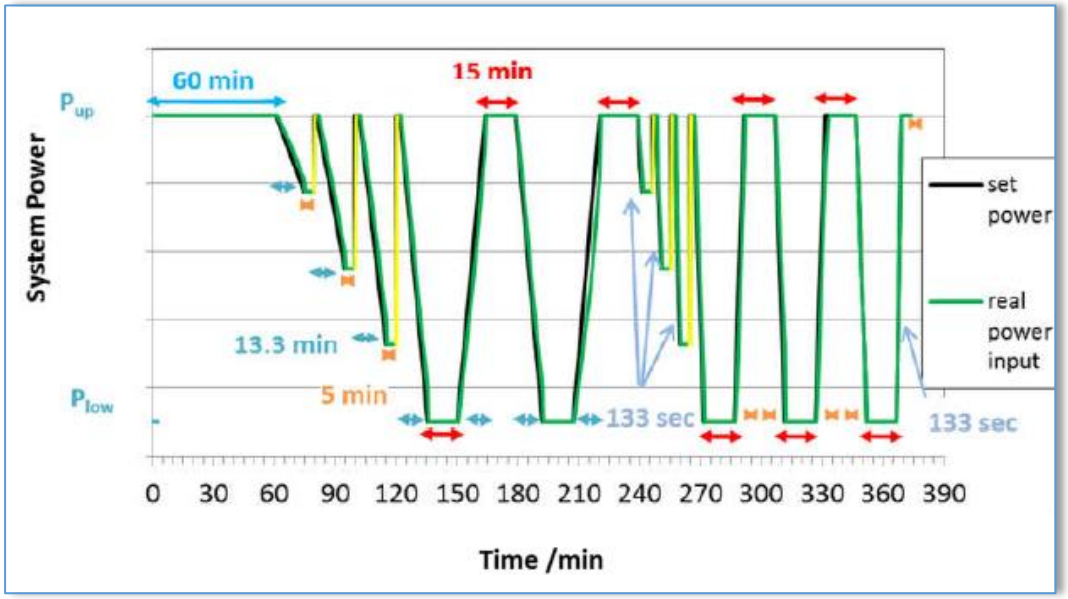

Figure 38. aFRR PROFILE WITH POSITIVE CONTROL POWER, [10]

Data evaluation and validation

The following conditions and limit as depicted in Figure 39 must be met:

- The power difference $\Delta P=2P_r$ measured at the end of the ramp must correspond to the target.
- During the periods of constant power request the real system power must be in the range ($\pm 0.05 \cdot (P_{up}-P_{low})$) around the requested power.
- The actual power of the system must remain 95% of the time in the bracket [$P_{tol} - \varepsilon_v$; $P_c + \varepsilon_v$] in case of a positive ramp, and [$P_c - \varepsilon_v$; $P_{tol} + \varepsilon_v$] for a negative ramp, with:
  - P_0: initial power level of the system at the beginning of the ramp
  - Pr: power value at the half the ramp power amplitude
  - N: parameter going from 0 at t=0 to +1 at the end of the ramp in case of ramp up, and 0 to -1 in case of negative ramp
  - $P_c=P_0 + N \cdot Pr$
  - $P_{tol}=P_c \cdot$ (t-20 second): set power at t-20 seconds
  - ε_v : 1% of the target ΔP

Analysis of the test results: the time and amount of deviation from the requested ranges are the subject of this evaluation.

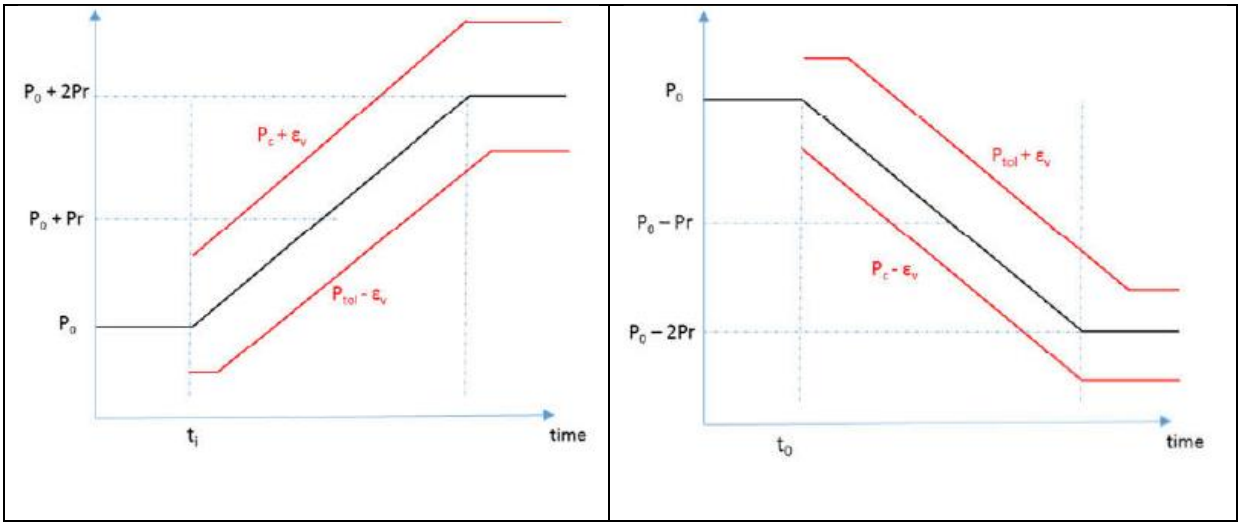

Figure 39. Positive and negative ramp acceptance limits

8.5.3 MANUAL FREQUENCY RESTORATION RESERVES (mFRR) TESTING PROTOCOL

This protocol aims at determining the electrolyser system response to power steps by assessing the characteristic duration times identified in mFRR prequalification load profiles. The protocol consists of two parts, with fast and medium ramp rates upwards and downwards, enabling separate evaluation of the services of negative and positive control power, respectively.

As the aFRR profile the mFRR profile contains ramps between a power level P_{low} and a power level P_{up} as well as fractions of the range. The ramp rates in mFRR are lower than for aFRR.

8.5.3.1 mFRR NEGATIVE CONTROL POWER (electrolyser power increase upon request)

The agreed load profile is depicted in Figure 40 and the associated agreed test protocol is described in Table 44.

Table 44. mFRR upward ramp protocol from lower power level

STEP	DESCRIPTION
1	Set system at P_{low}
2	Wait for system power to stabilize*
3	Operate at this level for 1 hour
4	At $t=t_1$, initiate power ramp of power (25% (P_{up} - P_{low})) in 15 minutes
5	$t=t_1+900$ seconds: end of the ramp
6	Keep set power for 5 minutes
7	Set system at P_{low} (the time the system needs to return to P_{low} is not Evaluated)
8	Wait for system power to stabilize *
9	At $t=t_2$, initiate power ramp of power (50% (P_{up} - P_{low})) in 15 minutes
10	$t=t_2+900$ seconds: end of the ramp
11	Keep set power for 5 minutes
12	Set system at P_{low} (the time the system needs to return to P_{low} is not evaluated)
13	Wait for system power to stabilize *
14	At $t=t_3$, initiate power ramp of power (75% (P_{up} - P_{low})) in 15 minutes
15	$t=t_3+900$ seconds: end of the ramp
16	Keep set power for 5 minutes
17	Set system at P_{low} (the time the system needs to return to P_{low} is not evaluated)
18	Wait for system power to stabilize *
19	At $t=t_4$, initiate power ramp of power (100% (P_{up} - P_{low})) in 15 minutes
20	$t=t_4+900$ seconds: end of the ramp

STEP	DESCRIPTION
21	Keep set power for 15 minutes
22	At t=t5, initiate power ramp of power (-100% (P_{up} - P_{low})) in 15 minutes
23	t=t_5+900 seconds: end of the ramp
24	Keep set power for 15 minutes
25	At t=t_6, initiate power ramp of power (+100% (P_{up} - P_{low})) in 15 minutes
26	t=t_6+900 seconds: end of the ramp
27	Keep set power for 60 minutes
28	At t=t_7, initiate power ramp of power (-100% (P_{up} - P_{low})) in 15 minutes
29	t=t_7+900 seconds: end of the ramp
30	Wait for system power to stabilize*
31	End of test

*The system power is considered stable if the average power of two consecutive intervals of 60 seconds does not differ by more than (±0.05 (Pup-Plow))

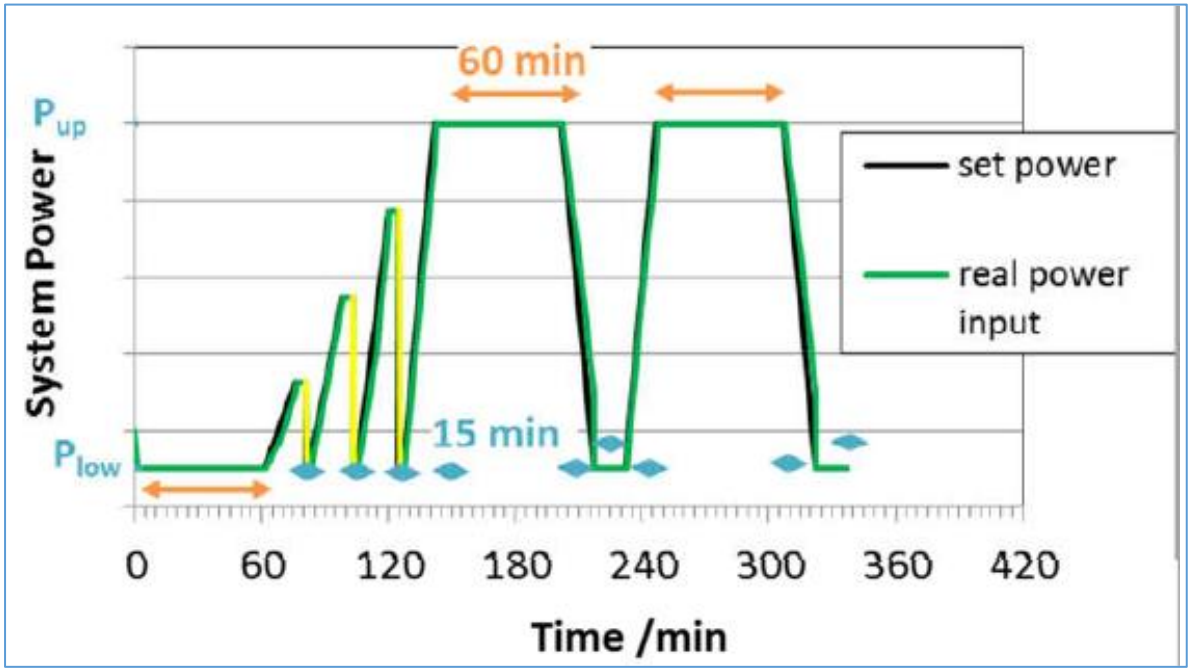

Figure 40. mFRR PROFILE WITH NEGATIVE CONTROL POWER,[10]

8.5.3.2 mFRR POSITIVE CONTROL POWER (electrolyser power decrease upon request)

The agreed load profile is depicted in Figure 41and the associated agreed test protocol is described in Table 45.

Table 45. mFRR downward ramp protocol from upper power level

STEP	DESCRIPTION
1	Set system at P_{low}
2	Wait for system power to stabilize*
3	Operate at this level for 1 hour
4	At $t=t_1$, initiate power ramp of power (-25% (P_{up} - P_{low})) in 15 minutes
5	$t=t_1$+900 seconds: end of the ramp
6	Keep set power for 5 minutes
7	Set system at P_{low} (the time the system needs to return to P_{low} is not Evaluated)
8	Wait for system power to stabilize *
9	At $t=t_2$, initiate power ramp of power (-50% (P_{up} - P_{low})) in 15 minutes
10	$t=t_2$+900 seconds: end of the ramp
11	Keep set power for 5 minutes
12	Set system at P_{low} (the time the system needs to return to P_{low} is not evaluated)
13	Wait for system power to stabilize *
14	At $t=t_3$, initiate power ramp of power (-75% (P_{up} - P_{low})) in 15 minutes
15	$t=t_3$+900 seconds: end of the ramp
16	Keep set power for 5 minutes
17	Set system at P_{low} (the time the system needs to return to P_{low} is not evaluated)
18	Wait for system power to stabilize *
19	At $t=t_4$, initiate power ramp of power (-100% (P_{up} - P_{low})) in 15 minutes
20	$t=t_4$+900 seconds: end of the ramp
21	Keep set power for 15 minutes
22	At t=t5, initiate power ramp of power (+100% (P_{up} - P_{low})) in 15 minutes
23	$t=t_5$+900 seconds: end of the ramp
24	Keep set power for 15 minutes
25	At $t=t_6$, initiate power ramp of power (-100% (P_{up} - P_{low})) in 15 minutes
26	$t=t_6$+900 seconds: end of the ramp
27	Keep set power for 60 minutes
28	At $t=t_7$, initiate power ramp of power (+100% (P_{up} - P_{low})) in 15 minutes
29	$t=t_7$+900 seconds: end of the ramp
30	Wait for system power to stabilize*
31	End of test

*The system power is considered stable if the average power of two consecutive intervals of 60 seconds does not differ by more than (±0.05 · (Pup-Plow))

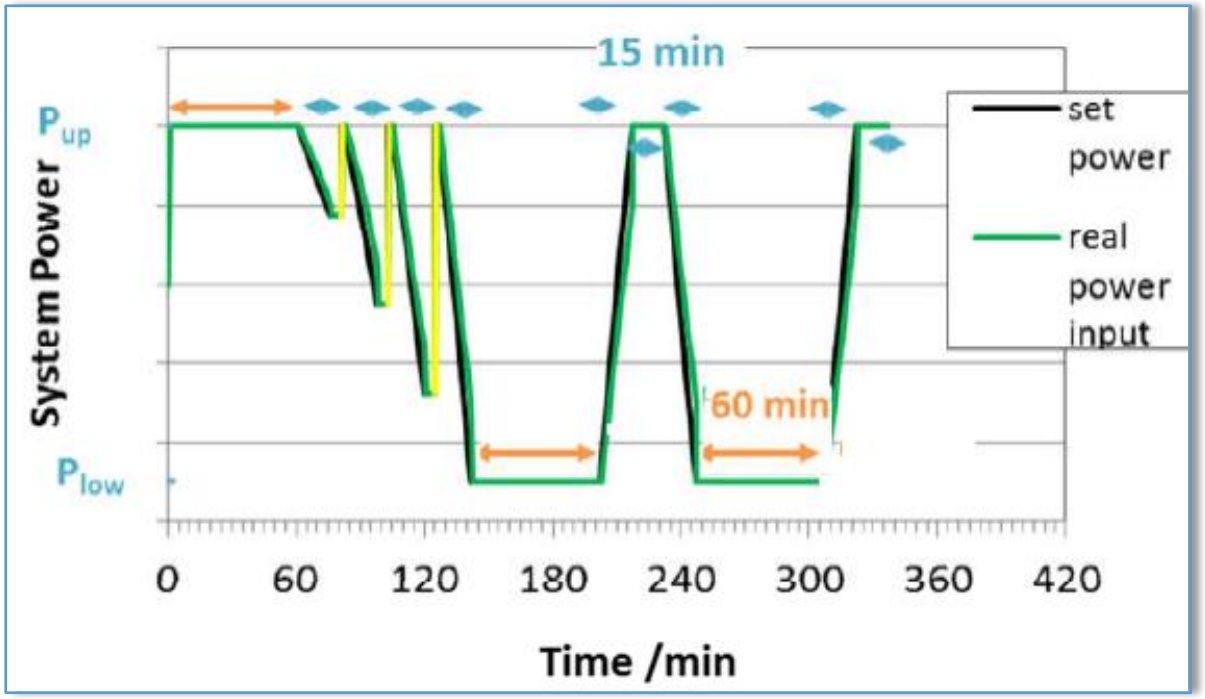

Figure 41. mFRR PROFILE WITH POSITIVE CONTROL POWER,[10]

Data evaluation and validation

The following conditions and limit as depicted in Figure 42must be met:

- The power difference $\Delta P=2P_r$ measured at the end of the ramp must correspond to the target.
- During the periods of constant power request the real system power must be in the range (± 0.05 (P_{up}-P_{low})) around the requested power.
- The actual power of the system must remain 95% of the time in the bracket [P_{tol} - ε_v; P_c+ ε_v] in case of a positive ramp, and [P_c- ε_v; P_{tol} +ε_v] for a negative ramp, with:
  - P_0: initial power level of the system at the beginning of the ramp
  - Pr: power value at the half the ramp power amplitude
  - N: parameter going from 0 at t=0 to +1 in the end of the ramp in case of positive ramp, and 0 to -1 in case of negative ramp
  - $P_c=P_0 + N \cdot Pr$
  - $P_{tol}=P_c \cdot$ (t-20 second): set power at t-20 seconds
  - ε_v : 1% of the target ΔP

Analysis of test results: the time and amount of deviation from the requested ranges are the subject of this evaluation.

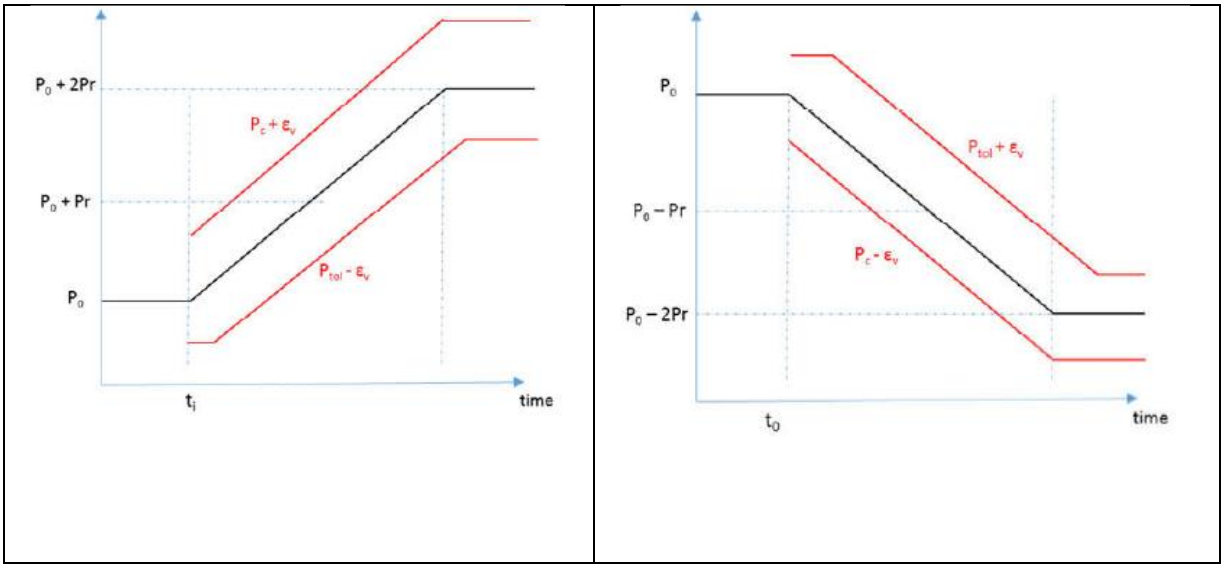

Figure 42. Positive and negative ramp acceptance limits

8.5.4 REPLACEMENT RESERVES (RR) TESTING PROTOCOL

This protocol aims at checking the agreement between consumption based on setpoint and real consumption over time intervals of selected duration. The services of positive and negative control power are considered separately.

8.5.4.1 RR NEGATIVE CONTROL POWER (electrolyser power increase upon request)

The agreed load profile is depicted in Figure 43 and the associated agreed test protocol is described in Table 46.

Table 46: RR upward power conformity protocol from lower power level

STEP	DESCRIPTION
1	Set system at P_{low}
2	Wait for system power to stabilize*
3	Operate at this level for 1 hour
4	At $t=t_1$, set system power to P_{low}+25% (P_{up} - P_{low})
5	Wait until $t=t_1$+15 minutes
6	Keep set power for 5 minutes
7	Set system at P_{low}
8	Wait for system power to stabilize *
9	At $t=t_2$, set system power to P_{low}+50% (P_{up} - P_{low})
10	Wait until $t=t_2$+15 minutes
11	Keep set power for 5 minutes
12	Set system at P_{low}
13	Wait for system power to stabilize *
14	At $t=t_3$, set system power to P_{low}+75% (P_{up} - P_{low})
15	Wait until $t=t_3$+15 minutes
16	Keep set power for 5 minutes
17	Set system at P_{low}
18	Wait for system power to stabilize *
19	At $t=t_4$, set system power to P_{up}
20	Wait until $t=t_4$+15 minutes
21	Keep set power for 60 minutes
22	At $t=t_5$, set system power to P_{low}
23	Wait until $t=t_5$+15 minutes
24	Keep set power for 15 minutes
25	At $t=t_6$, set system power to P_{up}
26	Wait until $t=t_6$+15 minutes
27	Keep set power for 60 minutes
28	At $t=t_7$ set power to P_{low}

STEP	DESCRIPTION
29	Wait until t=t_7+15 minutes
30	Wait for system power to stabilize*
31	End of test

*The system power is considered stable if the average power of two consecutive intervals of 60 seconds does not differ by more than (±0.05 · (P_{up}-P_{low}))

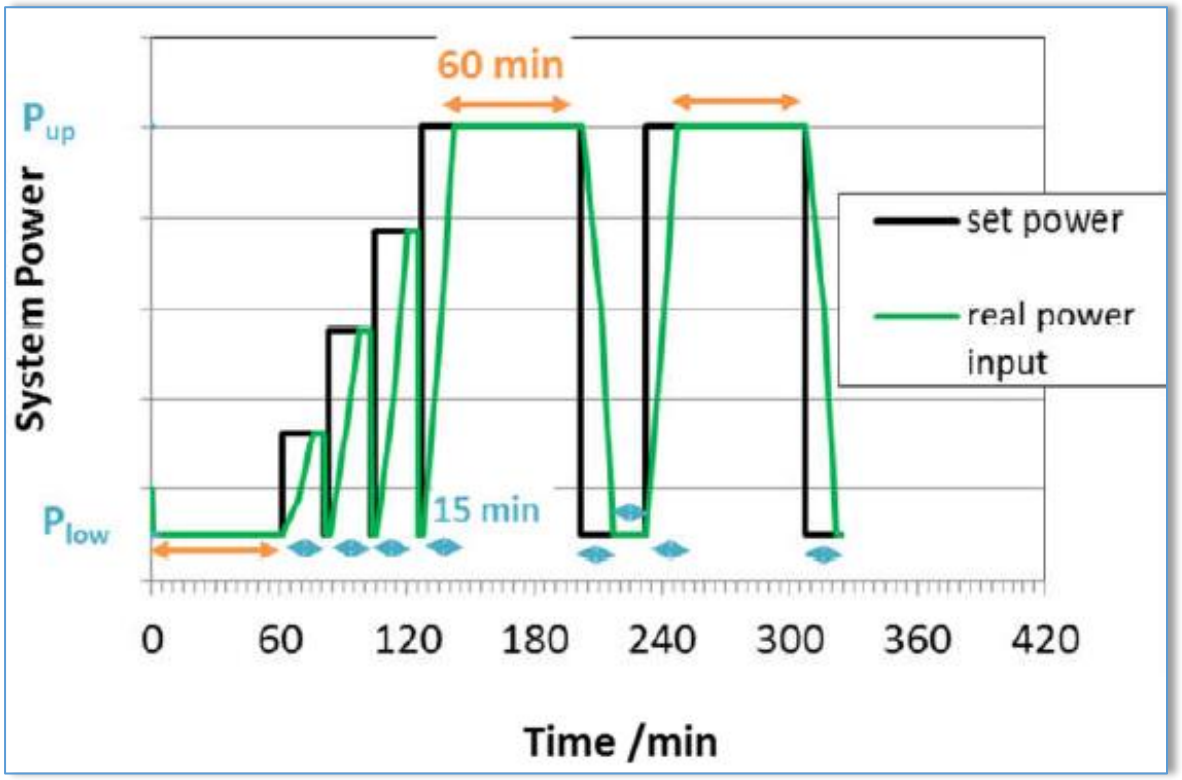

Figure 43: RR PROFILE WITH UPWARD CONTROL POWER,[10]

8.5.4.2 RR POSITIVE CONTROL POWER (electrolyser power decrease upon request)

The agreed load profile is depicted in Figure 44 and the associated agreed test protocol is described in Table 47.

Table 47: RR downward power conformity protocol from lower power level

STEP	DESCRIPTION
1	Set system at P_{UP}
2	Wait for system power to stabilize*
3	Operate at this level for 1 hour
4	At $t=t_1$, set system power to P_{up}-25% (P_{up} - P_{low})
5	Wait until $t=t_1$+15 minutes
6	Keep set power for 5 minutes
7	Set system at P_{up}
8	Wait for system power to stabilize *
9	At $t=t_2$, set system power to P_{up}-50% (P_{up} - P_{low})
10	Wait until $t=t_2$+15 minutes
11	Keep set power for 5 minutes
12	Set system at P_{up}
13	Wait for system power to stabilize *
14	At $t=t_3$, set system power to P_{up}-75% (P_{up} - P_{low})
15	Wait until $t=t_3$+15 minutes
16	Keep set power for 5 minutes
17	Set system at P_{up}
18	Wait for system power to stabilize *
19	At $t=t_4$, set system power to P_{low}
20	Wait until $t=t_4$+15 minutes
21	Keep set power for 60 minutes
22	At $t=t_5$, set system power to P_{up}
23	Wait until $t=t_5$+15 minutes
24	Keep set power for 15 minutes
25	At $t=t_6$, set system power to P_{low}
26	Wait until $t=t_6$+15 minutes
27	Keep set power for 60 minutes
28	At $t=t_7$ set power to P_{up}
29	Wait until $t=t_7$+15 minutes
30	Wait for system power to stabilize*
31	End of test

*The system power is considered stable if the average power of two consecutive intervals of 60 seconds does not differ by more than (±0.05 · (Pup-Plow))

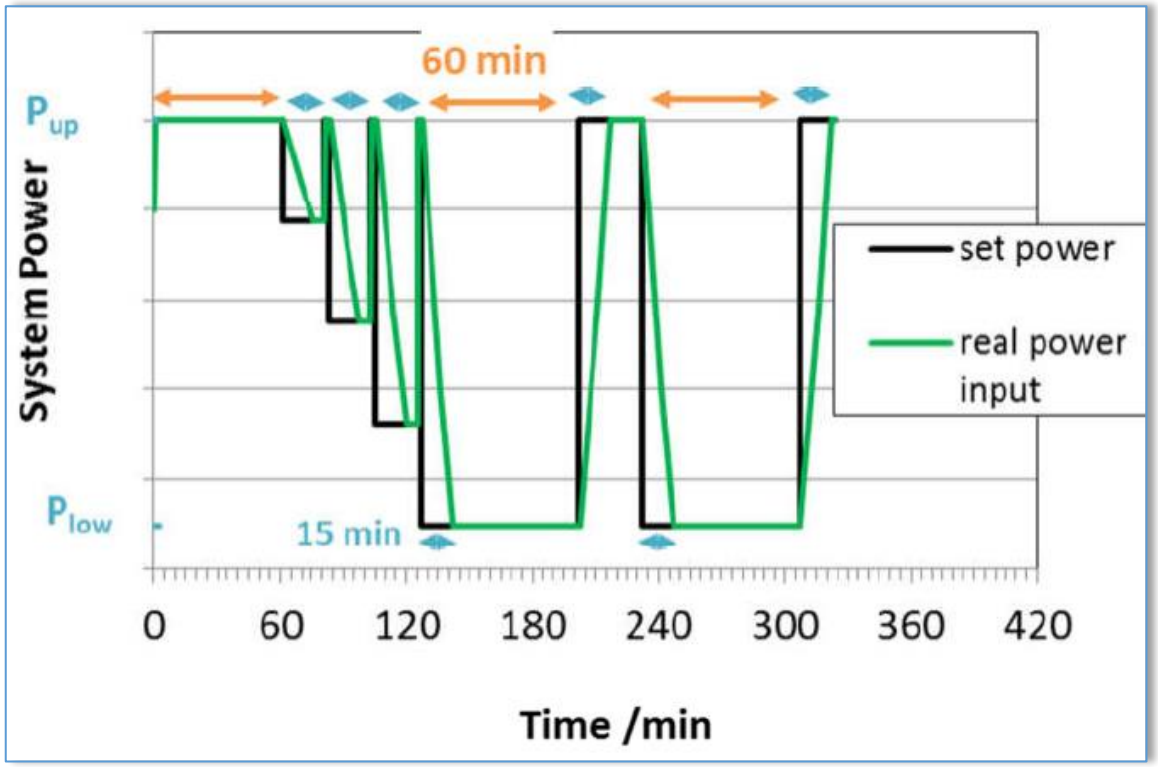

Figure 44: RR PROFILE WITH DOWNWARD CONTROL POWER,[10]

Acceptance criteria

For each step response, the test is considered successful when the measured power is equal to the target power. The target power must be reached after no more than 900 seconds.

8.6 EFFICIENCY at SYSTEM LEVEL

To determine efficiency at system level, the energy consumption of ancillary equipment has to be accounted for. The latter heavily depends on the system boundaries. Within these boundaries, the total energy input to be considered consists of the sum of the electricity and of heat provided to the electrolyser itself and to the BoP components.

Similarly as for the approach described in 7.2.4 at cell level, efficiency at system level is defined as the ratio between the flow rate of the produced hydrogen, $\dot{n}_{H_2}$, multiplied by its energy content, and the total thermal and electric power supplied to the system:

$$\eta^{(HHV\ or\ LHV)} = \frac{HHV\ or\ LHV}{P_{el}+P_{th}} \cdot \dot{n}_{H_2} \qquad \text{[Eq. 8.1]}$$

As described in 7.2.4, the selection of HHV or of LHV matters and should therefore be explicitly mentioned when providing efficiency values.

HHV or LHV are expressed in J mol^{-1}, via some unit conversion the value can be expressed in kWh kg-1, in this case the HHV value is equivalent to 39.4 kWh kg^{-1}. It represents the minimum amount of energy needed to produce 1kg of hydrogen.

The Specfic Energy Consumption (SEC) is the electrolyzer system total energy suppied, in kWh, to produce 1 kg of hydrogen

Rather than in terms of hydrogen production rate, some authors prefer expressing system efficiency in terms of voltage ratio corrected by an AC/DC conversion coefficient:

$$\varepsilon_{system} = \frac{N \cdot U_{tn}(T,p)}{U_{stack}} \left(\frac{\eta_{\frac{AC}{DC}}}{1+\xi} \right) \qquad \text{[eq. 8.2]}$$

with N the number of cells, U_{tn} the thermoneutral voltage, U the electrolyser stack voltage, $\eta_{AC/DC}$ the efficiency of the AC/DC converter and ξ the ratio between parasitic power accounting for energy consumption by auxiliary equipment and net power consumed by the electrolyser.

When additionally considering current efficiency to account for hydrogen losses in the electrolyser (see 7.2.2), the system efficiency is expressed as:

$$\varepsilon_{system} = \frac{N \cdot U_{tn}(T,p)}{U_{stack}} \cdot \frac{2 \cdot F \cdot \dot{n}_{H_2}}{I_{DC} \cdot N} \cdot \left(\frac{\eta_{\frac{AC}{DC}}}{1+\xi} \right) \qquad \text{[eq. 8.3]}$$

8.7 SYSTEM: DATA ANALYSIS FOR PERFORMANCE

System Performance is assessed on the base of the criteria depicted in the following table.

Table 48. System Performance Criteria

	CRITERIA	unit	Ref.
1	System (stack) Voltage	V	
2	System (stack) Current	A	
3	Current density	$A \cdot cm^{-2}$	
4	hydrogen production rate	$Kg \cdot h^{-1}$	
5	System outlet hydrogen pressure	MPa	
6	Hydrogen Quality	%	
7	System Efficiency as $\eta^{(HHV\ or\ LHV)}$	%	Eq 8.1
8	System Efficiency as ε_{system}	%	Eq. 8.2
9	System Efficiency as ε_{system}	%	Eq. 8.3
10	Specific energy consumption (SEC)	$kWh \cdot kg^{-1}$	8.6
11	Response time (t_{init})	s	Table 41
12	Minimum partial load operation	%	8.4.9
13	start-up time (cold) to nominal power load	s	8.4.6
14	minimum part load to full load rate	$\%\cdot s^{-1}$	8.4.9
15	full load to minimum part load rate	$\%\cdot s^{-1}$	8.4.9

Determination of the system performance indicators at different moments in time between BoL and EoL can provide an indication of the change of performance of the electrolysis system. This change of system performance with time is often referred to as "system durability". This approach of assessing durability at system level is directly comparable to the first method described for cell/short stack level in section 7.6 and a spider graph similar to the one given in Figure 23 can be used.

SYMBOLS

Table 49: Definition of Symbols

Symbol	Unit	Description
A	m^2, cm^2	Active area of the cell
C	C	Electric charge, Coulomb
Cp	$J \cdot g^{-1} \cdot K^{-1}$	Heat capacity under standard conditions (Cp_{H2O} = 4.186 $Jg^{-1}K^{-1}$)
E	V	Electrical potential
F	$C \cdot mol^{-1}$	Faraday's constant (F = 96485.3328959 C mol^{-1})
G	$J \cdot mol^{-1}$	Gibbs free energy
H	$J \cdot mol^{-1}$	Molar enthalpy
j	$A \cdot m^{-2}$, $A \cdot cm^{-2}$	Current density (j = I / A)
I	A	Electrical current
I_{max}	A	Maximum electrical current
J	J	Energy unit (Joules)
m	g	mass
M	$g \cdot mol^{-1}$	Molar mass
N		Number of objects
$\dot{n}$	$mol \cdot s^{-1}$	Molar flow rate
p	Pa, bar, atm	Pressure
p^{θ}	Pa, bar	Reference pressure
p^{A}	Pa, bar	Anodic pressure
p^{C}	Pa, bar	Cathodic pressure
P	W	Power
Q	$J \cdot mol^{-1}$	Heat
R	$J \cdot mol^{-1} \cdot k^{-1}$	Universal gas constant (R = 8.31446 J mol^{-1} K^{-1})
S	$J \cdot mol^{-1} \cdot k^{-1}$	Entropy
t	s, h	Time (second, hour)
T	K, °C	Temperature
$T_{x, y}$	K, °C	Temperature of cell fluid *x* at cell location *y* (inlet = in or outlet = out)
T_{env}	K, °C	Ambient temperature
T_{ehs}	K, °C	Temperature of an external heat source
T_c	K, °C	Cell temperature
U	V	Electrical potential
U_{tn}	V	Thermoneutral potential (U_{tn}= 1.48V at SATP conditions)
V	V	Voltage

Symbol	Unit	Description
$\dot{V}$	$\mu V \cdot h^{-1}$	Voltage degradation
V_{irrev}	V	Irreversible voltage loss
V_{rev}	V	Reversible voltage loss
V_{tn}	V	Thermoneutral voltage
W	$J \cdot mol^{-1}$	Work, electrical energy needed to transform 1 mole of reactant
z		Number of electron exchanged in red-ox reaction
Greek symbols		
α		Charge transfer coefficient, dimensionless
δ		Quantity variation (differential)
Δ		Quantity variation (finite)
ε		Energy efficiency, dimensionless
ζ		Exergy yield, dimensionless
η_I		Current efficiency, dimensionless
η_ω		Total efficiency, dimensionless
η^{HHV}		Hydrogen production efficiency
ξ		Ratio between parasitic power and net power consumed by the electrolyser due to the energy consumption by the auxiliaries, dimensionless
λ		Flow coefficient
τ		Response time rate

REFERENCES and BIBLIOGRAPHY

[1] FUEL CELLS AND HYDROGEN JOINT UNDERTAKING (FCH JU); https://www.fch.europa.eu/projects/knowledge-management

[2] Tsotridis G. and Pilenga A., EU harmonised terminology for low-temperature water electrolysis for energy-storage applications, EUR 29300 EN, Publications Office of the European Union, Luxembourg, 2018, ISBN 978-92-79-90387-8, doi:10.2760/138987, JRC112082

[3] Lettenmeier, P., Wang, R., Abouatallah, R. et al. Low-Cost and Durable Bipolar Plates for Proton Exchange Membrane Electrolyzers. Sci Rep 7, 44035 (2017) doi:10.1038/srep44035

[4] J. Electrochem. Soc.-2019-El-Sayed-F458-64

[5] A. Villagra, P. Millet, An analysis of PEM water electrolysis cells operating at elevated current densities, Int. J. Hydrogen Energy, 44(20) (2019) 9708-9717. DOI: https://doi.org/10.1016/j.ijhydene.2018.11.179

[6] http://conference.ing.unipi.it/ichs2005/Papers/120001.pdf

[7] Malkow, T., Pilenga, A., Tsotridis, G. and De Marco, G., EU harmonised polarisation curve test method for low-temperature water electrolysis, EUR 29182 EN, Publications Office of the European Union, Luxembourg, 2018, ISBN 978-92-79-81992-6, doi:10.2760/324006, JRC104045.

[8] Malkow, T., De Marco, G., Tsotridis, G., EU harmonised cyclic voltammetry test method for low-temperature water electrolysis single cells, EUR 29285 EN, Publications Office of the European Union, Luxembourg, 2018, ISBN 978-92-79-89871-6, doi:10.2760/140687, JRC111151

[9] T. Malkow, A. Pilenga, G. Tsotridis, EU harmonised test procedure: electrochemical impedance spectroscopy for water electrolysis cells, EUR 29267 EN, Publications Office of the European Union, Luxembourg, 2018, ISBN 978-92-79-88739-0, doi:10.2760/8984, JRC107053

[10] Deliverable report "Testing protocols for electrolyser qualification " D2.4 v.1 (30.08.2019) – Project FCHJU 735485 – QualyGridS

[11] ENTSO-E Network Code on Load-Frequency Control and Reserves (28.06.2013)

[12] ENTSO-E Supporting Document for the Network Code on Load-Frequency Control and Reserves (28.06.2013)

[13] Deliverable report "Standardized qualifying tests of electrolysers for grid services Electrical grid service catalogue for water electrolyser" D1.1 (27.1.2017) Project FCHJU 735485 – QualyGridS http://www.qualygrids.eu/

[14] Deliverable report "Protocols for characterisation of active components" D2.1 Project FCHJU 300081 Electrohypem

[15] P. Lettenmeier, Efficiency – Electrolysis, January 2019, Article No. SICM-T10001-00-7400

Novel project website https://www.sintef.no/projectweb/novel/publications/
C. Rozain, P. Millet, Electrochimica Acta 131 (2014) 160-167

A. S. Aricò, V. Baglio, N. Briguglio, G. Maggio and S. Siracusano "Proton Exchange Membrane Water Electrolysis" in "Fuel Cells : Data, Facts and Figures" D. Stolten,R. C. Samsun and N. Garland Editors, 2016 Wiley-VCH Verlag GmbH & Co. KGaA.

A. S. Aricò, S. Siracusano, N. Briguglio, V. Baglio, A. Di Blasi, V. Antonucci, "Polymer electrolyte membrane water electrolysis: status of technologies and potential applications in combination with renewable power sources" Journal of Applied Electrochemistry, 2013, 43, 107-118.

C. Lamy, P. Millet "A critical review on the definitions used to calculate the energy efficiency coefficients of water electrolysis cells working under near ambient temperature conditions", Journal of Power Sources, 447 (2020) 227350; https://doi.org/10.1016/j.jpowsour.2019.227350

I. Vincent, D. Bessarabov;" Low cost hydrogen production by anion exchange membrane electrolysis: A review" Renewable and Sustainable Energy Reviews 81 (2018) 1690–1704; http://dx.doi.org/10.1016/j.rser.2017.05.258

Ganley, J. C. (2009)."High temperature and pressure alkaline electrolysis" International Journal of Hydrogen Energy, 34(9), 3604–3611

Varcoe J R, Slade R C T and How Yee E L (2006) "An Alkaline Polymer Electrochemical Interface: A breakthrough in application of alkaline anion-exchange membranes in fuel cells", Chem. Commun., 1428

R.L. LeRoy, C.T. Bowen, D.J. Leroy "The Thermodynamics of Aqueous Water Electrolysis", J. Electrochem. Soc., 127 (1980) 1954

R. Hanke-Rauschenbach, B. Bensmann, P. Millet "Compendium of Hydrogen Energy", Volume 1: Hydrogen Production and Purification, , Chapter 7: Hydrogen production using high-pressure electrolyzers, Woodhead, 2015

Allidieres L et al., "On the ability of pem water electrolysers to provide power grid services", International Journal of Hydrogen Energy, https://doi.org/10.1016/j.ijhydene.2018.11.186

(Supporting Document on Technical Requirements for Frequency Containment Reserve Provision in the Nordic Synchronous Area, 2017), ENTSO-E AISBL

D. Bessarabov, H. Wand, H. Li, N. Zhao "PEM water Electrolysis for hydrogen production: Principles and Applications", , CRC Press (2015)

S. Bessarabov, P. Millet, "PEM water electrolysis", Elsevier, 2016

S. Siracusano, V. Baglio, N. Van Dijk, L. Merlo, A. S. Aricò, Appl Energy (2016), http://dx.doi.org/10.1016/j.apenergy.2016.09.011

Electricity balancing: COMMISSION REGULATION (EU) 2017/2195 of 23 November 2017 https://www.entsoe.eu/network_codes/eb/

Emergency and restoration: COMMISSION REGULATION (EU) 2017/2196 of 24 November 2017 https://www.entsoe.eu/network_codes/er/

Establishing a guideline on electricity transmission system operation: Commission Regulation (EU) 2017/1485 of 2 August 2017

https://www.cobaltinstitute.org/critical-raw-material.html

'Test protocol for accelerated in situ degradation of alkaline water electrolysis under dynamic operation conditions', presentation 15.03.2018, EHEC 2018

F.N. Büchi, 'Cell Performance Determining Parameters in High Pressure Water Electrolysis'. http://dx.doi.org/10.1016/j.electacta.2016.06.120

K.W. Harrison, R. Remick, and G.D. Martin, A. Hoskin "Hydrogen Production: Fundamentals and Cas Study Summaries"

https://www.nrel.gov/docs/fy10osti/47302.pdf

T.G. Douglas, A.Cruden, D. Infield "Development of an ambient temperature alkaline electrolyser for dynamic operation with renewable energy sources" , international journal of hydrogen energy 38 (2013) 723 -739, http://dx.doi.org/10.1016/j.ijhydene.2012.10.071

LIST OF ABBREVIATIONS AND DEFINITIONS

AC	Alternating current
AES	Atomic emission spectroscopy
AFM	Atomic force microscopy
Avg	Average
BET	Brunauer-Emmett-Teller surface area measurement
BoP	Balance of Plans
BoT	Beginning of Test
BoL	Beginning of Life
CV	Cyclic Voltammetry
DC	Direct current
DMA	Dynamic Mechanical Analysis
ECSA	Electrochemical Surface Area
EDX	Energy dispersive X-ray spectroscopy
EoT	End of Test
EoL	End of Life
EW	Equivalent weight
EXAFS	Extended X-ray absorption fine structure
FEG SEM-EDX	Field Emission Gun-Scanning Electron Microscopes Energy Dispersive X-Ray Analysis
FCH-JU	Fuel Cell and Hydrogen Joint Undertaking
FTIR	Fourier transformed infrared analysis
IEC	ion-exchange capacity
KPIs	Key Performance Indicators
HEL	High Explosive Limit, expressed in %
HER	Hydrogen Evolution Reaction
HFR	High Frequency Resistance
HHV	High Heating Value, expressed in $J \cdot mol^{-1}$
HW	Hardware
IEC	International Electrotechnical Commission
LHV	Low Heating Value, expressed in $J \cdot mol^{-1}$
LEL	Low Explosive Limit, expressed in %
MEA	Membrane Electrode Assembly
Micro-CT	X-ray micro computed tomography
NHE	Normal Hydrogen Electrode

OCV	Open circuit voltage
OER	Oxygen Evolution Reaction
PEM	Proton Exchange Membrane
PGM	Platinum Group Metals
RDE	Rotating disk electrode
RES	Renewable Energy Sources
RH	Relative Humidity
SATP	Standard Ambient Temperature and Pressure conditions (T =298.15K and p = 10^5 Pa)
SEM	Scanning electron microscopy
SIMS	Secondary ion mass spectroscopy
SF	Stability Factor expressed in $h \cdot V^{-2}$
SP	System power
St_d	Standard deviation
St_{err}	Standard error
tn	Thermo neutral
TEM	Transmission Electron Microscope
Tg	Glass Transition Temperature
TGA-DSC	Thermogravimetric-Differential Scanning Calorimetry
TSO	Transmission System Operator
UEL	Upper Explosion Limit
Ufw	Water Utilization factor
XANES	X-ray absorption near-edge structure
XPS	X-ray photoelectron spectroscopy
XRD	X-ray diffraction
XRF	X-ray fluorescence

List of figures

9 APPENDIX A. EX-SITU ANALYSIS ADDITIONAL INFORMATION

Ex-situ physico-chemical analysis pre- and post-operation by XRD, XRF, TEM, and SEM-EDX is to be carried out to elucidate structural, chemical, surface and morphology changes in the catalysts.

physico-chemical analyses are carried out by:

- X-ray diffraction (XRD) to determine structural and crystallite size changes: catalysts are scraped from the catalyst coated membrane assembly and corresponding powders are distributed over an amorphous sample holder.
  Crystalline phases are identified vs. the JPDS cards; crystallite size changes are determined from the peak broadening using the Levenberg–Marquardt algorithm for peak fitting and the Debye–Scherrer equation for quantification.

Crystallite size is reported as d_{XRD} / nm.

- X-ray fluorescence (XRF) is carried out to determine chemical modifications e.g. in the IrRuox composition (elemental analysis). The catalyst can be analysed after it is scraped from the CCM.

Chemical formulas are reported as "at. %" content of the elements

- Transmission electron microscopy (TEM) is carried out to determine any change in the mean particle size and particle size distribution (e.g. due to Ostwald ripening effects such as dissolution and reprecipitation): catalysts are scraped from the catalyst coated membrane assembly and powders are dispersed in isopropanol in ultrasounds. A few drops are deposited on Cu grid sample holders and analysed. At least 200 particles are counted in different regions.

Crystallite size is reported as d_{TEM} / nm.

- Scanning electron microscopy and energy dispersive analysis (FEG SEM-EDX) is carried out on the MEA without any further treatment to investigate morphological changes and chemical modifications e.g. inclusion of catalyst particles in the membrane, Ostwald ripening effects (dissolution and re-precipitation), membrane thinning, catalytic layer thinning, particle agglomeration etc.

10 APPENDIX B. EXAMPLES OF EX-SITU TEST PROCEDURES

This appendix presents the testing procedures for **PEMWE membrane** from deliverable 2.1 Electrohypem [14]

REF	TESTS
B1	Measurement of Membrane Ion Exchange Capacity and Equivalent Weight
B2	Membrane Hydrolytic Stability Test
B3	Membrane Chemical Stability Fenton's test
B4	In-Plane Conductivity and/or Through Plane
B5	Measurement of Membrane Thickness and Uniformity
B6	Water Uptake and Linear Expansion
B7	Membrane Permeability to Hydrogen Gas
B8	Thermo-Gravimetric Testing
B9	Tensile testing

B1: MEASUREMENT OF MEMBRANE ION-EXCHANGE CAPACITY AND EQUIVALENT WEIGHT

Summary

A base titration is used to obtain the number of equivalent moles of sulfonic acid groups within the polymer and the results used to calculate the ion-exchange capacity and equivalent weight of the membrane.

MEMBRANE CONDITIONING	**1**	Treat samples with 0.1M sulphuric acid for 1 hr, at 30 °C.
	2	Rinse the samples thoroughly with water and then soak in water for 1 hr, at 30 °C.
	3	Dry the samples in a vacuum oven for 4 hrs, at 50 °C.
TEST CONDITIONS		Approximately 0.5 g of dried sample is required for the test.
	1	Weigh the dried sample and record the mass to 4 decimal points.
	2	Place the sample into 100 ml of 0.01M potassium hydrogen carbonate (aq) solution and leave to soak for 16 hrs, at room temperature.
	3	Titrate the potassium hydrogen carbonate soak solution against 0.01M hydrochloric acid and record the volume of hydrochloric acid required to neutralize the potassium hydrogen carbonate soak solution.
	4	Based on at least three runs, determine the average volume of hydrochloric acid required to neutralize the potassium hydrogen carbonate soak solution.
	5	Calculate the concentration of the potassium hydrogen carbonate soak solution following contact with the membrane.
	6	Calculate the difference between the concentrations of the potassium hydrogen carbonate solution before and after contact with the membrane, to obtain the equivalent number of moles of sulfonic acid groups in the membrane
	7	Using the number of moles of sulfonic acid groups in the membrane and the mass of the dry membrane, calculate the ion exchange capacity and equivalent weight of the membrane

B2: MEMBRANE HYDROLYTIC STABILITY TEST

Summary

A section of the membrane is held in water at 95°C for 24 hours and the mass loss is determined from a comparison of dry mass before and after the test. The IEC of the specimen is then measured and compared to the standard value for the membrane.

MEMBRANE HYDROLYTIC TABILITY TEST		
Membrane Conditioning		Measurements are performed with **membrane conditioned at 23^{0}C, 50%RH**.
Specimen size		4cm x 4cm
Test Conditions		Immersed 24hr in 50ml Type 1 (ASTM D1193-91 Type II Standard) water. Water at 95^{0}C
		Dried in a vacuum oven at 50^{0}C for 4hr.
		Membrane mass measured before and after
Number of repeats		5

METRIC	FREQUENCY	TARGET
Mass Loss	After 24 hours	No target for monitoring
IEC change	After 24 hours	No target for monitoring

B3: MEMBRANE CHEMICAL STABILITY – FENTON'S TEST

Summary

This test provides an indication of the oxidative chemical stability of the membrane. A section of the membrane is held in an aqueous solution of 3% H_2O_2 and 4ppm Fe^{2+} at 80^0C for 2 hours and the mass loss is determined from a comparison of dry mass before and after the test.

MEMBRANE HYDROLYTIC TABILITY TEST		
Membrane Conditioning		Hydrate membrane according to standard hydration procedure, take sample from central area, dry gently under vacuum (500 ^{0}C for 4hrs) and measure the mass
Specimen size		4cm x 4cm
Concentration of Hydrogen peroxide		3% by weight
Concentration of Fe^{2+}		4ppm by weight
Test Conditions-Volume		50ml
Test Conditions-Temperature		80^0C
Test Conditions-Time		2 hrs
Test Conditions		Wash the membrane throughout in Type 1 water (ASTM D1193-91 Type II Standard), before drying the membrane under vacuum at 500 ^{0}C for 4 hrs. Measure the mass.
Mass loss formula		Mass loss (%) = { ($mass_{initial}$ – $mass_{after}$) / mass } x 100
Number of repeats		3

METRIC	CONDITIONS	TARGET
Mass Loss	Average of readings of mass loss to 4	No target for monitoring

B4: MEASUREMENT OF IN-PLANE CONDUCTIVITY

Summary

Using a four-electrode conductivity clamp (e.g. the Bekk Tech BT-110 Conductivity Clamp) in-plane conductivity can be determined by applying a specific current across a linear strip of membrane and measuring the resulting voltage. Four electrodes are used in order to separate voltage drop due to ion transport from that due to any electrochemical reactions.

MEASUREMENT OF IN PLANE CONDUCTIVITY		
Pre-Conditioning		Membrane must be hydrated prior the measurement and the conductivity clamp immersed in a beaker of Type 1 (ASTM D1193-91 Type II Standard) water.
Measurement technique		Four- electrode chronopotentiometry
Membrane sample size		At least 20mm long and less than 17mm wide
Water temperature		Controlled and recorded
Current		Appropriate current such that the voltage is between 0.01 and 1.0V
Technique	**1**	To test whether the electrodes are making good electrical contact with the membrane and to determine the appropriate current:
	2	Apply a linear voltage sweep across the two outer electrodes
	3	Then in the four-electrode mode, apply the predetermined appropriate current for one minute to outer contacts or until a constant voltage is achieved, whichever is longer
	4	Measure voltage difference across inner electrodes
	5	Using the applied current and resulting voltage, the resistance of the sample of membrane can be calculated R = V/I
	6	From the resistance of the membrane sample and the known dimension of the sample, resistivity and conductivity can also be calculated

B5: MEASUREMENT OF MEMBRANE THICKNESS AND UNIFORMITY

Summary

The thickness of a membrane specimen in dry, humidified or hydrated state is the arithmetic mean of the values obtained from at least three dimension measurements (see table for recommended number of measurements) taken at different points across a membrane specimen, using a calibrated micrometer screw gauge capable of measurement to the nearest 2.5 µm The uniformity of a membrane specimen is indicated by the maximum and minimum of the range of the dimension measurements.

MEASUREMENT OF MEMBRANE THICKNESS AND UNIFORMITY		
Membrane Conditioning	1	Dry state: 23 °C ±2 ˚C, 50% relative humidity
	2	Humidified state: As appropriate Should be recorded
	3	Hydrated state: As appropriate Should be recorded
Test Method	1	Prepare and condition each specimen as appropriate.
	2	Close the micrometer on an area of the specimen that has a similar dimension to the one to be measured, but is not one of the measurement positions.
	3	Observe this reading, and then open the micrometer approximately 100 µm beyond the expected reading and move the specimen to the measurement position.
	4	Close the micrometer at such a rate that the scale divisions may be counted easily as they pass the reference mark. This rate is approximately 50 µm/s.
	5	Continue the closing motion until contact with the specimen surface is just made as evidenced by the initial development of frictional resistance to movement of the micrometer screw. If using a micrometer fitted with a calibrated ratchet or friction thimble, continue the closing motion until the ratchet clicks three times or the friction thimble slips. Observe the indicated dimension.
	6	If required, correct the observed indicated dimension using a calibration chart and record the corrected dimension value.
	7	Move the specimen to another measurement position and repeat steps 2 - 6.
	8	Make and record at least three-dimension measurements on each specimen (see table below for recommended measurements). **The arithmetic mean of all dimension values is the thickness of the specimen**

Specimen Dimensions (cm)	Specimen Area (cm^2)	Recommended Number Of Measurements
5 x 5	25	5
10 x 10	100	9
15 x 15	225	16
20 x 20	400	25

FUNCTIONAL PROPERTIES	FREQUENCY	TARGET
Membrane Thickness (µm)	As required	No target for monitoring
Membrane Uniformity (µm)	As required	+/-10% of the mean thickness

B6: WATER UPTAKE and LINEAR EXPANSION

Summary

The hydration of membranes could be characterised by comparing the weight and size of dry samples with that of hydrated samples. From these measurements, water uptake and dimensional change can be calculated.

WATER UPATKE and LINEAR EXPANSION		
Pre-Conditioning		The membrane should be dried in an oven to constant weight.
Measurement technique		A balance capable of measuring to 0.0001g Calipers capable of measuring 0.01mm
Membrane sample size		Approximately 20mm x 10mm.
Hydration temperature		30^0C, 60^0C and 90^0C
Technique	**1**	A minimum of three samples should be used for each test.
	2	The size and weight of pre-conditioned samples are determined
	3	The samples are then place in containers of deionised water and placed in an oven at the appropriate temperature for 24 hours
	4	After 24 hrs, the samples are removed from the oven and measurements of length and weight are taken
Analysis	**5**	% Water Update = { (hydrated mass – dry mass) / dry mass } x 100
	6	% Linear Expansion = { (hydration length – dry length) / dry length } x 100

FUNCTIONAL PROPERTIES	FREQUENCY	TARGET
Water Uptake	**As required**	**No target for monitoring**
Linear Expansion	**As required**	**No target for monitoring**

B7: MEMBRANE PERMEABILITY TO HYDROGEN GAS

Summary

The hydrogen crossover rate through the membrane is assessed via an electrochemical method at relevant temperatures and pressures. The membrane is assembled in a standard test cell with hydrogen flowing on one side of the membrane and water on the other side. A potentiostat is used to sweep the potential. The current resulting from the oxidation of molecular hydrogen is measured and used to calculate the hydrogen crossover rate.

MEMBRANE PERMEABILITY to HYDROGEN GAS		
Membrane Conditioning		Hydrate according to standard method
Temperature		Set as required, must be recorded and reported
Pressure		Set as required, must be recorded and reported
Voltage Range		100mV to 400mV
Scan Rate		2mV/s
Test Method	**1**	Assemble the cell with potentiostat to control voltage and measure current. The anode acts as the reference and counter electrode and the cathode acts as the working electrode.
	2	Set the temperature and pressure as required
	3	Flow 100% of humidified hydrogen on anode (equiv. of 1.5 stoichiometry at 1A/cm2) and de-aerated water on cathode (5ml/min) to keep the membrane hydrated
	4	Sweep cathode potential from rest potential from 100mV to 400mV against anode at 2mV/s
	6	Report crossover at 300mV

FUNCTIONAL PROPERTIES	FREQUENCY	TARGET
Hydrogen crossover current	**As required**	**<1.0 A/cm²**
Hydrogen crossover rate	**As required**	**<0.07 ml/min/cm² hydrogen**

B8- THERMO-GRAVIMETRIC TESTING

Summary

This test gives an indication of the chemical and thermal stability of the membrane

Thermogravimetric/DSC Testing		
Membrane Conditioning		Hydrate according to standard hydratation procedure
Equipment		TA Instruments Q2000 DSC, Q500 TGA or similar
Atmosphere		Nitrogen / Air
Temperature range		25°C to 900°C
Heating ramp		2°C/min
Logging Frequency		1Hz
Number of repeats		3

FUNCTIONAL PROPERTIES	temperature	TARGET
Start of Thermal decomposition		**No target for monitoring**

Thermogravimetric/DSC Testing		
Membrane Conditioning		Hydrate according to standard hydratation procedure
Equipment		TA Instruments Q800 DMA or similar
Atmosphere		Air
Temperature range		25°C to 400°C
Heating ramp		2°C/min
Logging Frequency		1Hz

Number of repeats		3

FUNCTIONAL PROPERTIES	temperature	TARGET
Glass Transition Temperature Tg		**No target for monitoring**

B9: Tensile Testing

Summary

This test gives an indication of the mechanical properties of the membrane and it is based on ASTM D882 - 09 Tensile Properties of Thin Plastic Sheeting. As the machine does not have an environmental chamber, the test will be performed submerged in a water bath.

MEMBRANE HYDROLYTIC TABILITY TEST		
Membrane Conditioning		Hydrate membrane according to standard hydration procedure
Equipment		Instron 3344 or similar
Stamp size		Dumbell shaped stamp similar to Type IV in ASTM D638 - 10. Width of narrow section = 6mm Length of narrow section = 33mm Gauge length = 25mm Distance between the tabs = 65mm Length overall = 115mm Radius of fillet = 14mm Outer radius = 25mm
Initial Grip Separation		60 mm
Initial Strain Rate		0.5mm/mm.min
Rate of Grip Separation		30mm/min (Rate of Grip Separation = Initial Strain Rate x Initial Grip Separation)
Load cell		Suitable for material tested
Water bath temperature		23°C ± 1°C
Number of repeats		5 (in each direction if the sample is anisotropic)

METRIC	FREQUENCY	TARGET
UTS (MPa to 3 significant figures)	As required	No target for monitoring
Elongation at break (% to 2 significant figures)	As required	No target for monitoring
Young's Modulus (MPa to	As required	No target for monitoring

3 significant figures)		

11 APPENDIX C. EU REGULATORY FRAMEWORK for equipment providing grid balancing services

The following legislative documents which touch upon the provision of grid balancing services as part of frequency control measures, are relevant for this report:

- Directive (EU) 2019/944, Directive on common rules for internal market for electricity
- Regulation (EU) 2019/943, Regulation on the internal market for electricity
- Commission Regulation (EU) 2017/1485: Establishing a guideline on electricity transmission system operation
- Commission Regulation (EU) 2017/2195:" establishing a guideline on electricity balancing"
- Network Code on Load-Frequency Control and reserves [12] developed by the European Commission, the Agency for the Cooperation of Energy Regulators (ACER), the European Network of Transmission System Operators for Electricity (ENTSO-E) and market participants
- ENTSO-E, "Supporting Document for the Network Code on Load-Frequency Control and Reserves", 2013, accessed Aug. 2017 http://www.acer.europa.eu/Official_documents/Acts_of_the_Agency/Annexes/ENTSO-E%E2%80%99s%20supporting%20document%20to%20the%20submitted%20Network%20Code%20on%20Load-Frequency%20Control%20and%20Reserves.pdf

LOAD FREQUENCY CONTROL PROCESS

art 139.1 of Commission Regulation (EU) 2017/1485, points out that "*All TSOs of each synchronous area shall specify the load-frequency-control structure for the synchronous area [….]. Each TSO shall be responsible for implementing the load-frequency-control structure of its synchronous area and operating in accordance with it*".

The parameters defining the Frequency Quality art. 19 [11] are illustrated in Figure 45. The figure shows a disturbance event that generates a system imbalance reflected by a frequency change, the different action activation limits and the deployment over time of the different types of reserves, FCR, FRR, and RR. Regulatory requirements on frequency correction actions include frequency ranges as well as time durations in which the respective ranges should be reached. Limits on range and duration are therefore included in the pre-qualification requirements by the TSOs.

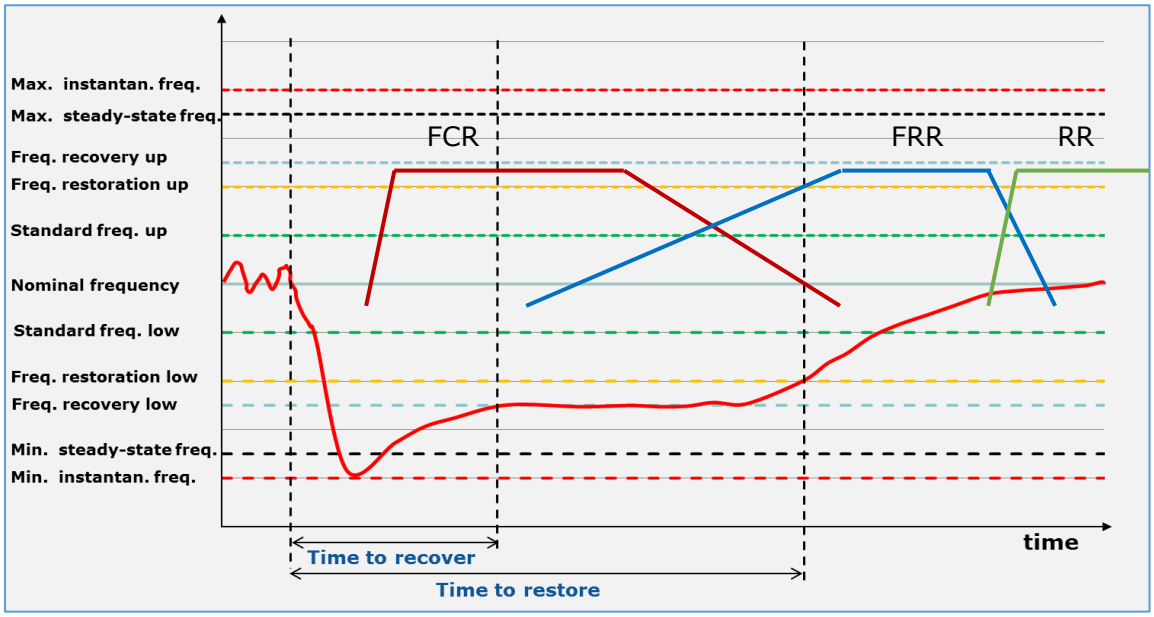

Figure 45. Frequency control parameters and cascade actions following a disturbance event

The Network Code Electricity Balancing article 29.5 [11] provides common requirements for equipment to be used for frequency control service. These include capacity, speed of action, ability of ramping, and ability of offering a reliable dynamic/non-dynamic response over designated service periods. Figure 46 shows a generic profile applicable to the operation of the three types of frequency control reserves FCR, FRR and RR. Whereas the figure shows reserve activation through a positive ramp, negative ramp activation may also be needed.

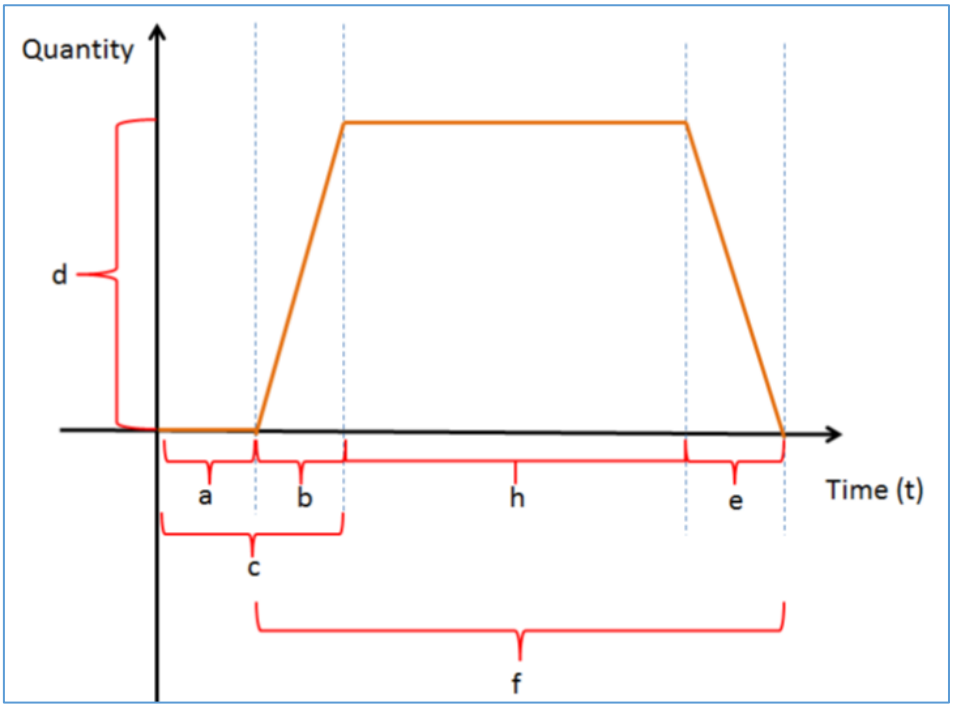

Figure 46: Standard description of any balancing equipment, [Source:13]: (a) preparation period; (b) ramping period; (c) = (a)+(b) full activation time; (d) minimum and maximum quantity; (e) deactivation period; (f) = (b)+(h)+(e) full delivery period; (h) minimum and maximum duration of delivery period

GETTING IN TOUCH WITH THE EU

In person

All over the European Union there are hundreds of Europe Direct information centres. You can find the address of the centre nearest you at: https://europa.eu/european-union/contact_en

On the phone or by email

Europe Direct is a service that answers your questions about the European Union. You can contact this service:

- by freephone: 00 800 6 7 8 9 10 11 (certain operators may charge for these calls),

- at the following standard number: +32 22999696, or

- by electronic mail via: https://europa.eu/european-union/contact_en

FINDING INFORMATION ABOUT THE EU

Online

Information about the European Union in all the official languages of the EU is available on the Europa website at: https://europa.eu/european-union/index_en

EU publications
You can download or order free and priced EU publications from EU Bookshop at: https://publications.europa.eu/en/publications. Multiple copies of free publications may be obtained by contacting Europe Direct or your local information centre (see https://europa.eu/european-union/contact_en).

XX-NA-XXXXX-EN-N

The European Commission's science and knowledge service

Joint Research Centre

JRC Mission

As the science and knowledge service of the European Commission, the Joint Research Centre's mission is to support EU policies with independent evidence throughout the whole policy cycle.

EU Science Hub
ec.europa.eu/jrc

@EU_ScienceHub

EU Science Hub - Joint Research Centre

EU Science, Research and Innovation

EU Science Hub

Publications Office of the European Union

doi:XX.XXXX/XXXXXX

ISBN XXX-XX-XX-XXXXX-X